

AN ABSTRACT OF THE THESIS OF

Julian Yu-liang Yen for the degree of Doctor of Philosophy

in Nuclear Engineering presented on July 12, 1982

Title: Extension of Fuel Burnup in Light Water Reactors

by Using a Strict In-Out Refueling Scheme

Abstract approved: _____

Redacted for Privacy

Dr. Bernard I. Spinrad /

To utilize energy resources as efficiently as possible has become a necessity today. The purpose of this study is to see how this can be done by extending burnup in a light water reactor. Specifically, an in-out refueling scheme might extract the maximum energy from nuclear fuel during its residence in the reactor.

In principle, a reactor loading with minimum neutron leakage and minimum parasitic absorption will best utilize the neutrons. For this, having more fissions near the center of the reactor will reduce leakage, and parasitic absorption by control elements could be reduced by having smaller reactivity changes between reloads.

An in-out refueling scheme, i.e., loading the fresh fuel into the center of the reactor, moving the older fuel outward and removing the oldest fuel from the edge, could best utilize the reactivity of fresh fuel. This is because neutron importance is highest in the center. Placing control preferentially near the center then requires relatively less absorption in control elements to achieve a given degree of reactor control. The non-uniform flux distribution, with peaking at the center, will save neutrons because the fuel assemblies of the lowest neutron production capability are located at the edge of the reactor, and leakage from these fuels is neither very large nor very important.

To simulate the in-out operation of the reactor in this study, two computer codes have been established. One is a one-dimensional code utilizing two group diffusion equations in an iteration scheme, and the other is a two-dimensional code using spatial flux synthesis.

Studies have been made of the effects of the in-out refueling scheme on reactor cycle length, fuel burnup level, power peaking factor and other reactor characteristics.

Results show that an in-out refueling scheme could have a fuel burnup benefit over the conventional (out-in) refueling scheme. The benefit can be up to 13 percent or more, depending on the frequency of refueling, the fuel design and the reactor size, compared with out-in refueling under the same circumstances.

The in-out refueling scheme with short cycle length gets part of its benefit from frequent refueling. However, frequent refueling tends to expose the fuels at the center of the core to very high power peak-

ing. Peaking is a function of batch size (the smaller the batch size the higher the peak), and is closely related to the initial reactivity of the fuel, as well as to the method of fuel management. High power peaking can be alleviated by confining the reactivity-controlling absorber to the center of the reactor. Moreover, with this type of control the cycle length and discharge burnup become larger, for a given replacement batch size, than for a case in which control is applied over the whole core.

Enrichment certainly could elongate the cycle length and so the discharge burnup, but the gain of burnup per enrichment increment decreases with enrichment level.

Lattice design could also have some effects on the discharge burnup. More moderation of neutrons in a looser lattice increases the initial reactivity of the fuel, although it speeds up the rate of reactivity loss per flux-time. The low conversion of the fertile material in the fuel of a loose lattice does not apparently have as much influence on the discharge burnup as the initial reactivity does.

Extension of Fuel Burnup in Light Water Reactors
by Using a Strict In-Out Refueling Scheme

by

Julian Yu-liang Yen

A THESIS

submitted to

Oregon State University

in partial fulfillment of

the requirements for the

degree of

Doctor of Philosophy

June 1983

APPROVED:

Redacted for Privacy

Professor of Nuclear Engineering
in charge of major

Redacted for Privacy

Head of Department of Nuclear Engineering

Redacted for Privacy

Dean of Graduate School

Date thesis is presented July 12, 1982

Typed by Becky Cook and Donna Lee Norvell-Race for Julian Yu-liang Yen

ACKNOWLEDGMENT

Like any other project, this dissertation merged many efforts, time and help from my colleagues and friends.

I sincerely express my thanks to those decent people at Oregon State University who have lent their assistance generously and enthusiastically to the completion of this paper, especially to the faculty in the Nuclear Engineering Department and in the Milne Computer Center.

I honestly admit that it would have been impossible for me to finish this work without help and encouragement from Dr. C. H. Wang, Dr. B. I. Spinrad, Dr. A. H. Robinson, and Dr. F. T. Lindstrom. Drs. Wang and Spinrad's invaluable support have won the continuous sponsorship of my work by Taiwan Power Company. Dr. Robinson and Dr. Lindstrom shared their specialty and helped overcome the many difficulties encountered in the course of this work.

I particularly want to thank Dr. Spinrad, my advisor, for his patience and the advice he has given me over the years. His mastery of the subject and his penetrating analytical power have kept my work continually going on the right track. He not only guided me in my academic work, but also in my attitude toward my profession and human relationships. My feelings for him go well beyond respect and love.

I also greatly appreciate Taiwan Power Company for sponsoring this work. My superior, Mr. P. C. Liu, Director of the Atomic

Power Department, should be credited for supporting the accomplishment of this work.

I owe my family and my wife, Sheue-Yun, very much and I thank them from the bottom of my heart for their understanding and sacrifice.

TABLE OF CONTENTS

Chapter

1	INTRODUCTION	1
2	THEORETICAL BASIS	5
	2.1 The Fuel Group Constants and the LEOPARD Code	5
	2.2 The Theoretical Basis for In-Out Refueling	12
	2.3 The Maximum Discharge Burnup and the Self-sustained Lifetime	17
3	ONE-DIMENSION TWO-GROUP MODEL	26
	3.1 Description of the Algorithm	26
	3.2 The Difference Equations	28
	3.2 a Neutron fluxes	28
	3.2 b Adjoint fluxes	31
	3.3 The Boundary Conditions	32
	3.4 The Criticality Calculation	34
	3.4 a The critical fluxes	34
	3.4 b The critical boron concentration search	35
	3.4 c The critical flux verification	38
	3.5 Individual Bundle Burnup Calculation	45
	3.5 a Burnup algorithm	45
	3.5 b Approximations made in burnup calculation	49
	3.6 Equilibrium Cycle Discharge Burnup	51
	3.7 Extension of the Cycle Length by Coastdown Operation	61

Chapter		Page
4	TWO-DIMENSION TWO-GROUP MODEL	65
	4.1 Description of the Algorithm	65
	4.2 Boundary Conditions	71
	4.3 The Criticality Calculation	72
	4.4 Individual Element Burnup and Bundle Average Burnup	77
	4.5 Equilibrium Cycle Discharge Burnup	79
5	CASE STUDIES	83
	5.1 Effect of Flux Peaking Control	83
	5.2 Effect of Bundle Lattice Design and Enrichment	85
	5.3 Effect of Batch Size	88
	5.4 Effect of Cooldown Operation	89
	5.5 Effect of Reactor Size on Fuel Discharge Burnup	89
6	RESULTS AND DISCUSSIONS	94
	6.1 The Discharge Burnup Advantage	95
	6.2 Batch Size and Maximum Cycle Length	100
	6.3 Enrichment Effects on the Discharge Burnup	102
	6.4 Effect of Bundle Lattice Design on Discharge Burnup	104
	6.5 The Peaking Factor	104
	6.6 Central Zone Reactivity Control	109
	6.7 Effects of Cooldown Operation on the Discharge Burnup	111
7	CONCLUSION	131
	BIBLIOGRAPHY	136
	APPENDICES	
	Appendix A. Tables of Group Constants	138
	Appendix B. One-Dimension Code	155
	Appendix C. Two-Dimension Code	180

LIST OF FIGURES

Figure	Page
2.1 Nuclear Reaction Balance Diagram of U-238 Chain	8
2.2 k_{∞} vs. Burnup for Taiwan Power Company and Battelle Calculations	10
2.3 k_{∞} vs. Burnup for Different Type of Fuels	11
2.4 Fuel Freshness and Obsolescence vs. Burnup	14
2.5 BOC and EOC Burnup Distribution for Different Refueling Frequencies	18
2.6 a Neutron Balance Relation for Reactor of Zero Leakage in Continuous Refueling	21
2.6 b Neutron Balance Relation for Finite Reactor in Continuous Refueling	22
2.7 Neutron Balance Relation for Flat Flux	24
3.1 Sketch of the Reactor and Its Parameters	27
3.2 a BOC and EOC Flux Distributions of 3-Zone Cycle for Oconee Fuel in In-Out Refueling Scheme by our 1-D code.	39
3.2 b BOC and EOC Flux Distributions of 3-Zone Cycle for Oconee Fuel in In-Out Refueling Scheme by AHRCHB code.	39 a
3.3 a BOC and EOC Flux Distributions of 3-Zone Cycle for Oconee Fuel in Out-In Refueling Scheme by our 1-D code.	40
3.3 b BOC and EOC Flux Distributions of 3-Zone Cycle for Oconee Fuel in Out-In Refueling Scheme by AHRCHB code.	40 a
3.4 a BOC and EOC Flux Distributions of 6-Zone Cycle for Oconee Fuel in In-Out Refueling Scheme by our 1-D code.	41
3.4 b BOC and EOC Flux Distributions of 6-Zone Cycle for Oconee Fuel in In-Out Refueling Scheme by AHRCHB code.	41 a

Figure

Page

3.5 a	BOC and EOC Flux Distributions of 6-Zone Cycle for Oconee Fuel in Out-In Refueling Scheme by our 1-D code.	42
3.5 b	BOC and EOC Flux Distributions of 6-Zone Cycle for Oconee Fuel in Out-In Refueling Scheme by AHRCHED code.	42 a
3.6 a	BOC and EOC Flux Distributions of 9-Zone Cycle for Oconee Fuel in In-Out Refueling Scheme by our 1-D code.	43
3.6 b	BOC and EOC Flux Distributions of 9-Zone Cycle for Oconee Fuel in In-Out Refueling Scheme by AHRCHED code.	43 a
3.7	BOC and EOC Flux Distributions of 9-zone Cycle for Oconee Fuel in Out-In Refueling Scheme by our 1-D code.	44
3.7	BOC and EOC Flux Distributions of 9-zone Cycle for Oconee Fuel in Out-In Refueling Scheme by AHRCHED code.	44 a
5.1	Sketch of the Fuel Bundle and Its Parameters	87
6.1	Comparison of Discharge Burnups of In-Out and Out-In Refueling Schemes in 1-D and 2-D Calculations for Oconee Fuels	96
6.2	Discharge Burnups of Trojan Fuels in In-Out Refueling Scheme	103
6.3	Power Peaking Factors of Oconee Fuels in 1-D In-Out and Out-In Refueling Scheme and 2-D In-Out Refueling Scheme	106
6.4	1-D Power Peaking Factors of Trojan Fuels at BOC for Different Refueling Frequencies in Whole Core Controlled Case	107
6.5	1-D Power Peaking Factors of Trojan Fuels at EOC for Different Refueling Frequencies in Central Zone Controlled Case	108
B-1	Block Diagram of 1-D Code	156
C-1	Block Diagram of 2-D Code	182

LIST OF TABLES

Table	Page
3.1 Effect of Burnup Step Size on Discharge Burnup, Burnup Calculations with Burnup Step Size of 1000 MWD/MTU	52
3.2 Effect of Burnup Step Size on Discharge Burnup, Burnup Calculations with Burnup Step Size of 2000 MWD/MTU	53
5.1 Basic Data for Oconee and Trojan Reactors	84
5.2 Design Data of Trojan, Oconee and Standard Westinghouse Fuels	86
5.3 Zone Dimension of Reactor	90
5.4 Summary of Case Studies for Trojan Type Fuel in 1-D Calculations for In-Out Refueling Scheme	91
5.5 Summary of Case Studies for Oconee Type Fuel in Both 1-D and 2-D Calculations for In-Out Refueling Scheme	92
5.6 Summary of Case Studies for Oconee Type Fuel in Both 1-D and 2-D Calculations for Out-In Refueling Scheme	93
6.1 Discharge Burnups of Oconee Fuel in 3, 6, 9 Zone Normal Cycle Whole Core Controlled Case for 1-D Calculations of In-Out Refueling Scheme	112
6.2 Discharge Burnups of Oconee Fuel in 3, 6, 9 Zone Normal Cycle Whole Core Controlled Case for 2-D Calculations of In-Out Refueling Scheme	113
6.3 Discharge Burnups of Oconee Fuel in 3, 6, 9 Zone Normal Cycle Central Zone Controlled Case for 1-D Calculations of In-Out Refueling Scheme	114
6.4 Discharge Burnups of Oconee Fuel in 3, 6 and 9-Zone Normal Cycle Whole Core Controlled Case for 1-D Calculations of Out-In Refueling Scheme	115

Table		Page
6.5.	Discharge Burnups of Oconee Fuel in 3, 6, 9 Zone Normal Cycle Whole Core Controlled Case for 2-D Calculations of Out-In Refueling Scheme	116
6.6	Summary of 1-D and 2-D Calculation Results for Oconee Fuels	117
6.7	Discharge Burnups of Oconee Fuel in 6- and 9-Zone Normal Cycle Whole Core Controlled Case for Enlarged Reactor Size in 1-D Calculation	118
6.8	Discharge Burnups of Oconee Fuel in 6- and 9-Zone Normal Cycle Central Zone Controlled Case for Enlarged Reactor in 1-D Calculation	119
6.9	Discharge Burnup of Oconee Fuel in 6-Zone Coast-down Operation Whole Core Controlled Case for 1-D Calculation	120
6.10	Discharge Burnup of Oconee Fuel in 9-Zone Coast-down Operation Whole Core Controlled Case for 1-D Calculation	121
6.11	Discharge Burnups of All Types of Trojan Fuels in 3-Zone Normal Cycle Whole Core Controlled Case for 1-D Calculation	122
6.12	Discharge Burnups of Trojan 15x15 3 percent Fuel in 6-Zone Normal Cycle Whole Core and Central Zone Controlled Cases	123
6.13	Discharge Burnups of Trojan 15x15 3 percent Fuel in 9-Zone Normal Cycle Whole Core and Central Zone Controlled Cases	124
6.14	Discharge Burnups of Trojan 17x17 2 percent Fuel in 6-Zone Normal Cycle Whole Core and Central Zone Controlled Cases	125
6.15	Discharge Burnups of Trojan 17x17 2 percent Fuel in 9-Zone Normal Cycle Whole Core and Central Zone Controlled Cases	126

Table		Page
6.16	Discharge Burnups of Trojan 17x17 3 percent Fuel in 6-Zone Normal Cycle Whole Core and Central Zone Controlled Cases	127
6.17	Discharge Burnups of Trojan 17x17 3 percent Fuel in 9-Zone Normal Cycle Whole Core and Central Zone Controlled Cases	128
6.18	Discharge Burnups of Trojan 18x18 3 percent Fuel in 6-Zone Normal Cycle Whole Core and Central Zone Controlled Cases	129
6.19	Discharge Burnups of Trojan 18x18 3 percent Fuel in 9-Zone Normal Cycle Whole Core and Central Zone Controlled Cases	130
A-1	Group Constants for Trojan Fuel of 15x15 Lattice Design with 3 percent Enrichment	139
A-2	Group Constants for Trojan Fuel of 17x17 Lattice Design with 2 percent Enrichment	142
A-3	Group Constants for Trojan Fuel of 17x17 Lattice Design with 3 percent Enrichment	145
A-4	Group Constants for Trojan Fuel of 18x18 Lattice Design with 3 percent Enrichment	146
A-5	Group Constants for Oconee Fuel of 15x15 Lattice Design with 3 percent Enrichment	149
B-1	The Format for Group Constants Stored in TAPE1	165
C-1	The Format for the Initial Loadings of the First Core Element (IZ,IR)	188
C-2	The Format for the Trial Functions AT and the Weighting Functions RT Stored in TAPE3	188

Extension of Fuel Burnup in Light Water Reactors by Using a Strict In-Out Refueling Scheme

1. INTRODUCTION

It is always desirable to extract more energy out of nuclear fuel before it is unloaded from the core. This means more efficient use of the natural uranium mined. Today, this desire has become a necessity because of the growing scarcity of uranium and the increasing price of other energy resources, such as oil.

Current reactor fueling schemes do not stress the efficient use of uranium. There are still ways to improve the maneuvering of the reactor so that more energy can be extracted from the fuel.

Fuel performance experience and technological developments made over the past decades have made this improvement possible within a reasonable safety margin. It is the objective of this work to study possible improvements that can be made through modifications in fuel management schemes. The current light water reactors and their fuels have been designed to have a one-year refueling period so that a proper power generation schedule can be set up to meet the seasonal power demand.

In order to maintain a one-year reactivity lifetime, one-third of the core has to be replaced with fresh fuel of around three percent U-235 enrichment each year. Enrichment is kept low so that there will not be too much excess reactivity in the core, and no localized area in the core may have enough reactivity to reach criticality. In addition, the existing fueling schemes tend to load the fuels in such a

fashion as to flatten the flux in the core; this reduces the maximum power density in the fuel for a given total power so that the fuel mechanical integrity is easier to maintain.

One of the fueling schemes is called the out-in loading pattern; in this scheme, when the reactor needs to change its fuel, the fuel bundles around the center are discharged, those in the middle regions are moved toward the center and the fresh fuel bundles are loaded at the periphery of the core.

Another conventional fuel-loading pattern is called the checkerboard pattern. In this pattern, fresh fuel bundles are separated from each other by used fuel bundles. The fresh fuel bundles are never loaded side by side; they are at their closest diagonally, just like squares of the same color on a checkerboard. When newly loaded, the fresh fuels are scattered around the periphery of the core, and moved inward at next refueling. However, fuel is not used most economically in these schemes.

Today, as energy resources are getting scarcer, oil prices drastically increasing, and fuel performance experience piling up, it is becoming more interesting or even necessary to make more efficient use of natural uranium. The current United States nuclear practice of using a once-through fuel cycle, and delaying the reprocessing and recycling of spent fuel, enhances the need to extract as much energy as possible from the fuel before it is unloaded. This is the same as getting as high a burnup in

individual fuel bundles as the reactivity lifetime permits.

To have higher bundle burnup also means that per unit of energy generated less uranium must be mined and there will be less waste to dispose. In a light water reactor, there is a finite reactivity lifetime, and therefore there is a limit to the burnup level the bundle can reach.

Factors (2) affecting the reactivity lifetime of the core are the composition of the core (such as the fuel, the parasitic material and the control rods), leakage, fast fission and non-uniform flux distribution. Once the reactor core and fuels have been designed, the reactivity lifetime of the core becomes a matter of how these factors are maneuvered. Among these factors, the change in the composition of the fuel is the one that affects reactivity lifetime most when power is generated. As energy is extracted from the nuclear fuel, its composition changes. Fission products are created, fissile and fertile materials are produced and destroyed, and other nonfissionable isotopes are formed as a result of neutron capture and fission in fissile, fertile and structural materials of the core. As a result of these changes in the fuel composition, the reactivity of the core can either increase or decrease depending on the balance between fission and nonfission absorption of neutrons by the fuel. The direction of the reactivity change will then determine the reactivity lifetime of the core, either infinite or finite. Control rods are used to compensate for reactivity change during power generation, to maintain

the criticality of the core and to shape neutron flux as desired. The object of this study is to find out how to obtain the highest bundle burnup, i.e., to reach the longest reactivity lifetime through the manipulation of these factors that affect the reactivity lifetime. A strict in-out fueling scheme is hypothetically the one that can yield the highest excess reactivity for a fuel of given enrichment and design. However, in reality, the core management scheme that can lead to the highest burnup of the fuel is not necessarily the most economic way of running a reactor in today's rapidly changing economic environment. This is because the unit cost of power generated by a nuclear reactor consists of plant capital, operation and maintenance, and fuel cycle cost. Good plant economy has to be an optimal combination of all these component costs. An in-out fueling scheme tends to have a high peaking factor. This will force the reactor to be run at a low power level, at the expense of plant economy.

Based on the fact that a finite reactor has a non-uniformly distributed flux, higher at the center of the reactor and lower at the edge, it is believed that in-out refueling will make best use of the high neutron population and neutron importance at the center by loading the fresh fuels into the center and locating the oldest fuels at the edge. This pattern of loading will worsen the power peaking of the core. How much gain the in-out refueling will have on fuel discharge burnup and how serious the peaking will be are explored here. Also considered is the question of how control can be managed to emphasize burnup and decrease peaking.

2. THEORETICAL BASIS

2.1 The Fuel Group Constants and the LEOPARD Code

When a reactor generates power, changes in the composition of the fuels occur. The composition of the fuels can be reasonably translated into neutron cross-sections for nuclear reactor physics purposes. The changes in the composition of the fuel are then expressible by the changes in these cross-sections. They are, in general, neutron energy dependent. However, for simplicity, but with reasonable accuracy, these quantities at many different neutron energies can be combined into parameters in two different neutron energy ranges: fast and slow. The physical quantities thus defined are called group constants. They include diffusion constant D , absorption cross-section Σ_a , fission cross-section Σ_f , neutron generation probability $\nu\Sigma_f$, removal cross-section Σ_r , resonance escape probability P_r and infinite multiplication factor k_∞ .

When the fuel undergoes fission and generates energy, the group constants change. The energy the fuel has generated is measured by a quantity, called burnup, which is defined as the energy generated per unit weight of the fuel and expressed in Megawatt-days per (metric) ton of uranium initially loaded, MWD/MTU.

In order to know how these group constants change as the burnup increases, a computer code named LEOPARD (3,4) is utilized. LEOPARD is a zero-dimension computer code to calculate the group

constants of the fuel at different fuel burnups. It is used to generate homogenized group constants, in either four energy groups or two groups, for a unit cell of the fuel. LEOPARD assumes that the reactor contains a large array of unit fuel cells. Therefore, the unit cell is representative of the reactor. By calculating the fast and thermal neutron spectra of many fine groups within the heterogeneous cell and using these spectra, LEOPARD will collapse the energy dependence of the nuclear constants into two groups (one fast and one thermal) or four groups (three fast and one thermal), while preserving the correct nuclear reaction rate so that neutron behavior in the reactor can be approximated more easily by two-group or four-group diffusion equations without sacrificing too much accuracy. These collapsed constants are called group constants. It is because of these group constants that we become able to model the neutron behavior in a reactor by a set of diffusion equations described later in Section (3.2). Besides the calculations of the group constants at a particular fuel burnup, LEOPARD also traces the changes in the fuel composition due to nuclear reaction under the neutron flux during a certain time period, so that another set of group constants which represent the fuel properties after the change can be generated. Thus, the group constants of the fuel at many different fuel burnup levels are created by LEOPARD.

LEOPARD considers five sets of nuclides, namely (a) uranium-238 chain elements through plutonium 242, (b) uranium-235 chain elements through uranium 236 and fission (c) promethium 149

and samarium 149, (d) iodine 135 and xenon 135, and (e) one pseudo element accounting for all other fission products. These sets of elements are sufficient to represent the fuel. By tracing the change of each nuclide for a certain amount of fluence (flux-time), and solving the nuclear reaction balance equations involving these elements, the composition of the fuel after the amount of fluence (flux-time) can be known. LEOPARD will again calculate another set of fast and thermal fluxes and generate another set of collapsed group constants for the new fuel composition (or fuel burnup). For illustrative purposes, the nuclear reaction balance equations of the first set of elements only are shown in Figure (2.1).

The individual bundle (or zone) fuel burnup calculations are described in Sections (3.5) and (4.4). In those sections we present the accounting of the amount of fluence (flux-time) a fuel bundle (or zone) has received for a given power generation time (or a core average burnup in MWD/MTU). Knowing the fluence (flux-time) of the fuel bundle, the composition of the fuel bundle can be known by referring to the group constants at the fluence (flux-time) generated by LEOPARD. It is LEOPARD that actually does the burnup calculations.

Group constants at different fuel burnups, obtained by LEOPARD calculations for five types of fuel bundle design, are given in Appendix A, Table (A-1) to Table (A-5). Two versions of LEOPARD, the versions of Taiwan Power Company, TPC (10) and of Oregon State University, OSU (11), were used in generating these group constants. Those in Table (A-5) are calculated by the OSU version for fuels which are

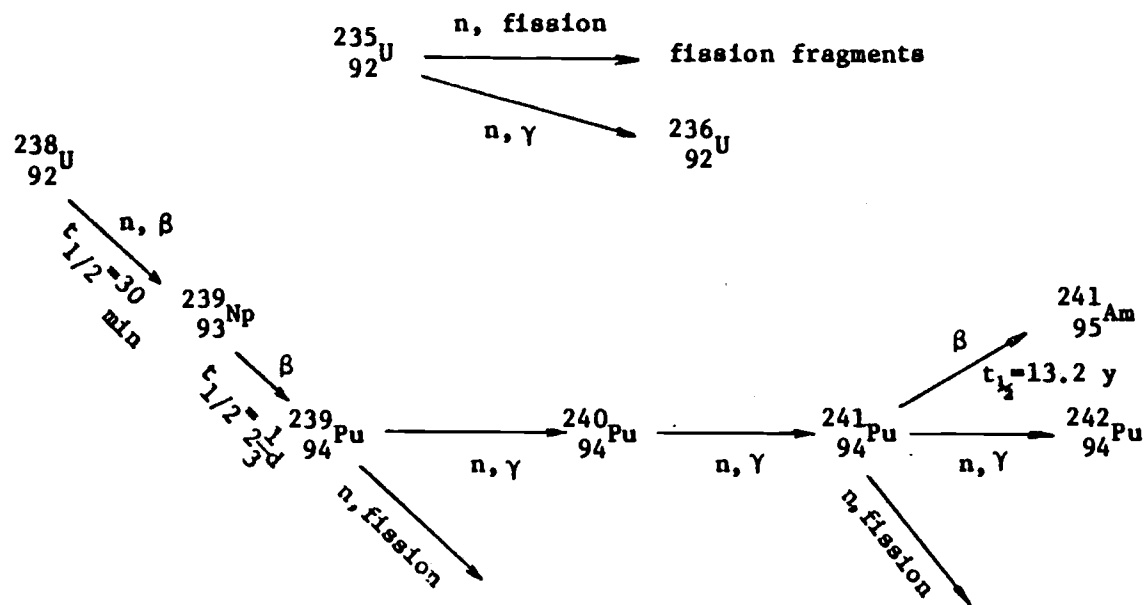


Figure 2.1 Nuclear Reaction Diagrams of U-238 and U-235 Chains.

designated as Oconee fuel because their fuel pins have the same size as those of an actual reactor, "Oconee". Those in Table (A-1) to Table (A-4) are generated by the TPC version for fuels which are called Trojan fuel for the same reason. Group constants for Trojan fuels turned out to be pessimistic when compared with group constants of comparable standard PWR fuels obtained at Battelle Northwest Laboratory (13). The k_{∞} vs. burnup curves for both Taiwan Power Company and Battelle calculations are shown in Figure (2.2). As this figure indicates, the k_{∞} values calculated by TPC and Battelle for identical fuel design have the same zero-burnup value for both calculations, but those from TPC calculations drop at a faster rate as the burnup increases. Effects of these pessimistic group constants will be discussed in Chapter VI. The k_{∞} vs. burnup curves for Trojan and Oconee fuels, as calculated by the two versions of LEOPARD respectively, are shown in Figure (2.3). Design features of these fuels, including standard PWR fuel, are in Table (5.1) and Table (5.2).

The group constants in Appendix A are calculated under the assumption that the reactor is infinitely large. Thus, the multiplication factor is called k-infinity (k_{∞}) because of infinite reactor size. It is defined as the ratio of the number of neutrons in a generation to the number of neutrons in the previous generation, or in mathematical form as,

$$k = \frac{\int v \Sigma_f \phi dV}{\int \Sigma_a dV} \quad (2.1)$$

Because of the infinite size of the reactor in the LEOPARD

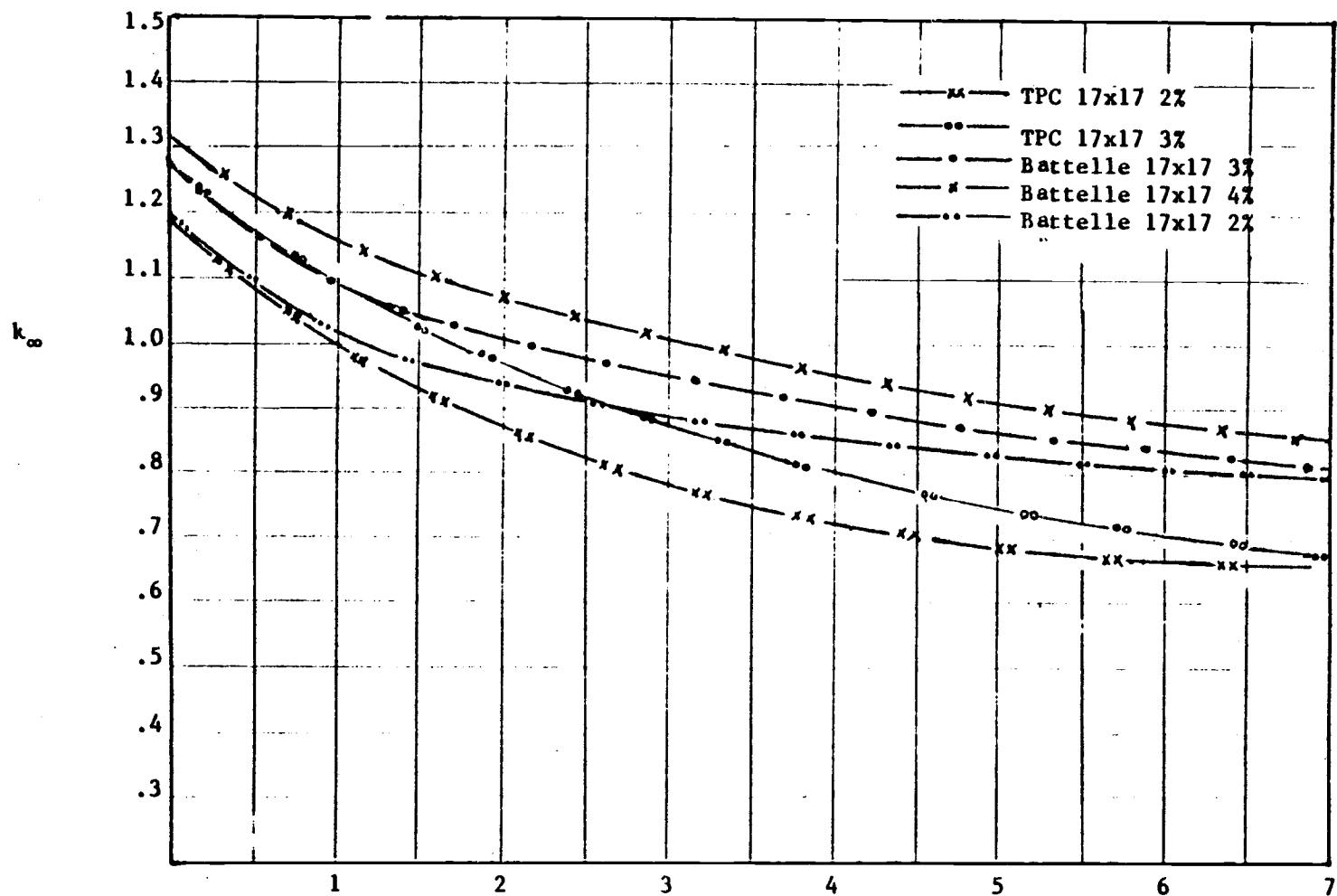


FIGURE 2.2 k_{∞} vs. BURNUP FOR TAIWAN POWER COMPANY $\times 10^4$ MWD/MTU AND BATTELLE CALCULATIONS

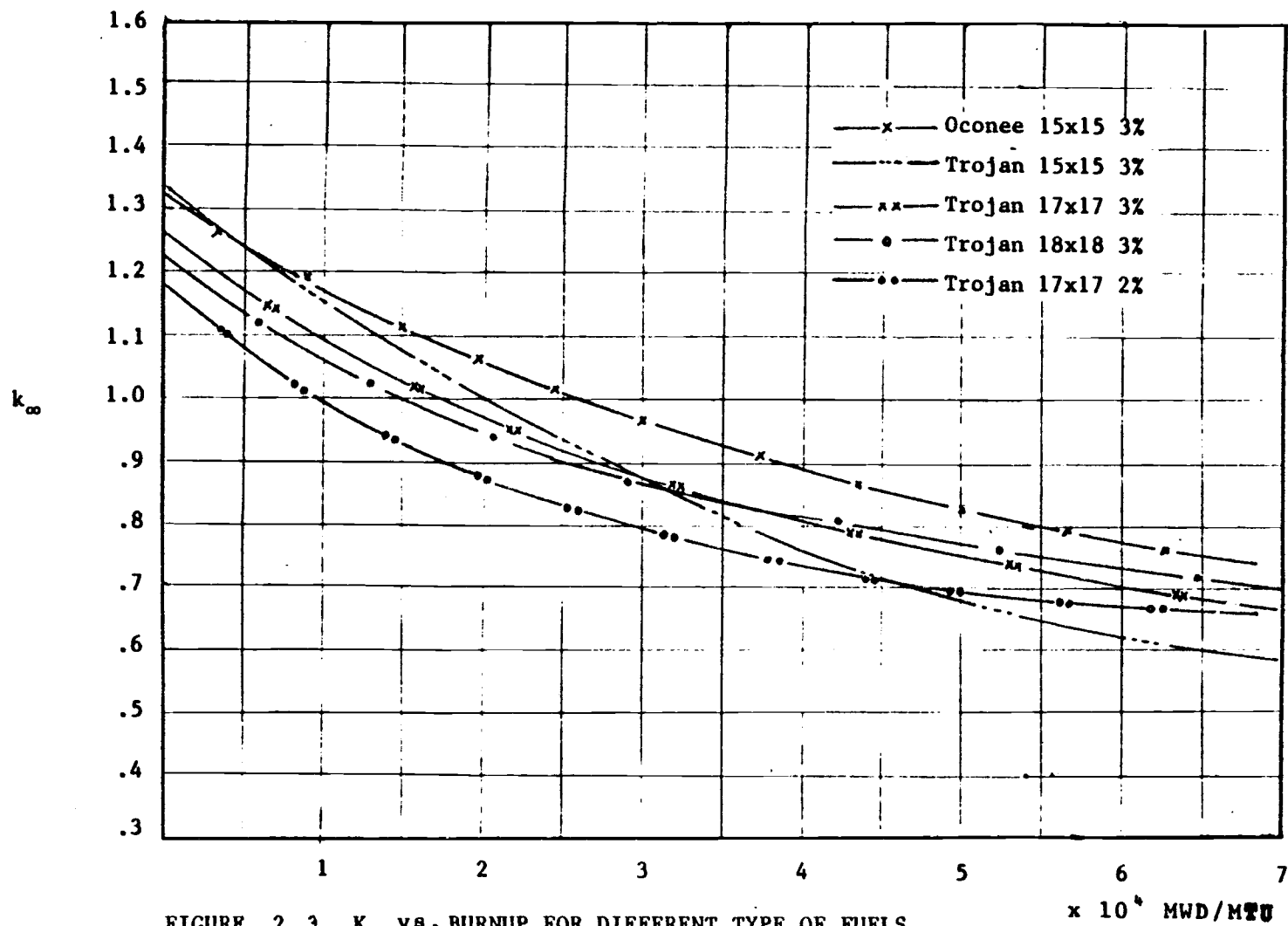


FIGURE 2.3 k_{∞} vs. BURNUP FOR DIFFERENT TYPE OF FUELS

calculation, the flux is flat everywhere in the reactor. Therefore, k_{∞} , $\nu\Sigma_f$, Σ_a , Σ_f and P_r are all local values. When the reactor is of finite size, the multiplication factor of the system, now called effective multiplication factor, k_{eff} or k , can no longer be as large as k_{∞} due to neutron leakage from the core. The relation between k and k_{∞} is, according to the one-group approximations,

$$k = k_{\infty} \frac{1}{1 + M^2 B^2} \quad (2.2)$$

Where M^2 : The migration area of the neutrons in the reactor,
 B^2 : The reactor geometric buckling,

$$\left(\frac{\pi}{H}\right)^2 + \left(\frac{2.405}{R}\right)^2,$$

R : The reactor radius and

H : The reactor height

k is no longer a local value but a global value because it is an integrated value over the whole reactor system. Equation (2.2) is a modified one-group critical equation and is appropriate in a reactor of large size, such as those under study. Both k_{∞} and k are values assuming no reactivity control in the reactor.

2.2 The Theoretical Basis for In-Out Refueling

A strict in-out fueling scheme is defined as the following process. Every time old fuel bundles need to be replaced by fresh

fuel bundles at the end of each power-generation cycle, the fresh fuel bundles are loaded into the central region of the core. The fuel bundles in the ^{old}~~old~~ core are moved toward the edge of the core in sequence without any jumping, and the fuel bundles at the periphery of the core are discharged. In light water reactors, the reason the strict in-out refueling procedure will extract more energy from the fuel bundles than other refueling patterns can be explained qualitatively as follows

A nuclear fuel can be considered as having two properties: freshness and obsolescence. Freshness is equivalent to the $\nu\Sigma_f$ (number of neutrons generated) value of the fuel, and obsolescence is equivalent to the Σ_a (number of neutrons absorbed) value. When the fuel is new, its freshness will be at its maximum value (assuming that the conversion ratio of fissile material is less than one, which is true for a light water thermal reactor) and its obsolescence will be at its minimum value. This fact can be seen by observing the changes in $\nu\Sigma_f$ and Σ_a values with burnup, as in Table (A-1), in the unit cell calculation by the LEOPARD code. When fuel is put into the core to burn, the higher the burnup of the fuel, the lower the freshness and the higher the obsolescence will be. This is illustrated in Figure (2.4).

In order to extract more energy from the fuel, the fuel should stay in the core as long as possible, i.e., as long as the reactivity of the core can be sustained. The reactivity of the core is defined as $\frac{k-1}{k}$, where k is the effective multiplication

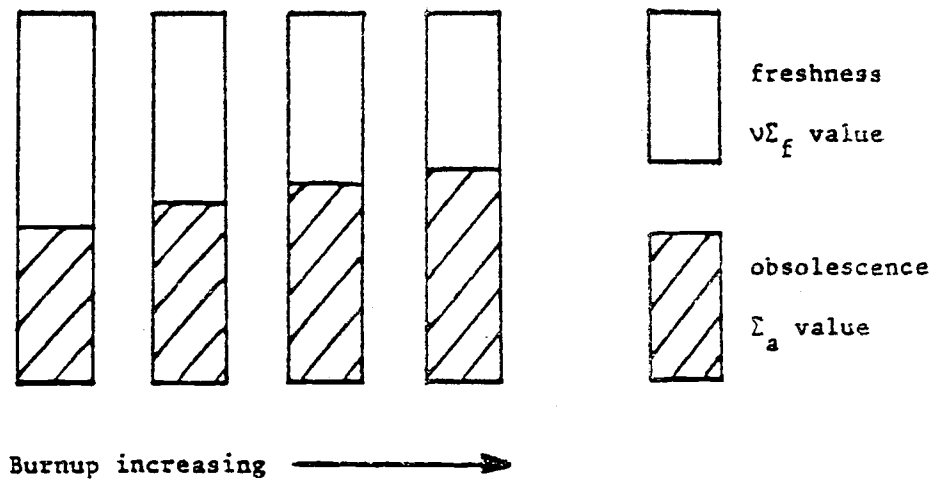


FIGURE 2.4 Fuel freshness and obsolescence vs. burnup

factor of the core, as defined in the previous section. To have a higher reactivity, the core should have a higher k or k_{∞} value. Since k is defined as

$$\frac{\int_c \nu \Sigma_f \phi dV}{\int_c (\Sigma_a \phi + \text{leakage}) dV} \quad (2.3)$$

k will reach its maximum value if $\int_c \nu \Sigma_f \phi dV$ is at its maximum, $\int_c \Sigma_a \phi dV$ and $\int_c (\text{leakage}) dV$ at their minimum.

In light water reactors, a cylindrical core shape is a good approximation. Therefore, the neutron flux in a critical, uniform reactor will have the shape of a zero order Bessel function of the first kind (J_0). It is normally true that the radial neutron flux distribution is a monotonically decreasing function from the

center of the core toward the edge of the core. (Here the axial neutron flux distribution is assumed to be flat.) Then, $\int_c v\Sigma_f \phi dV$ will have a maximum value if we weight the maximum $v\Sigma_f$ value by the maximum flux value, and $\int_c \Sigma_a \phi dV$ will have the minimum value if we weight the maximum value of Σ_a by the minimum flux value. A strict in-out refueling scheme tries to do this by loading the fresh fuels of highest $v\Sigma_f$ value into the center of the core where flux is at its maximum and by keeping the oldest fuels of the lowest Σ_a value at the edge of the core where flux is at its minimum. Moreover, loading the fresh fuels of high neutron productivity at the center and the old fuels of low neutron productivity at the edge will keep the neutron leakage low. Therefore, the in-out refueling scheme should have the highest reactivity, and thus will extract more energy from the fuel than other loading patterns.

The same conclusion can also be derived from perturbation theory in reactor physics (5). In one-group perturbation theory, the reactivity of the perturbed reactor is

$$\rho = \frac{k' - k}{k'} = \frac{\int_{\text{core}} \psi (\delta[v\Sigma_f] - \delta\Sigma_a) \phi dV}{\int_{\text{core}} \psi v\Sigma_f \phi dV} \quad (2.4)$$

where k' = the effective multiplication factor of the perturbed reactor;

k = the effective multiplication factor of the unperturbed reactor;

$\delta\Sigma_f$ = the perturbation in the macroscopic fission cross-section Σ_f due to burnup;

$\delta\Sigma_a$ = the perturbation in the macroscopic absorption cross-section Σ_a due to burnup;

ψ = the adjoint neutron flux;

ϕ = the neutron flux, and

ν = the number of neutrons generated per fission.

Since the neutron flux and the adjoint neutron flux are both monotonically decreasing functions along the radius of the reactor core from the center toward the edge of the core (indeed, in one-group theory, their shapes are identical), and since the denominator is slowly varying, the reactivity will have a maximum value if the fuel bundles with higher fission cross-section relative to an arbitrary reference value (e.g., the value at zero fuel burnup) are put in the center of the core, and the fuel bundles with higher absorption cross-section relative to a reference value (e.g., the value at zero fuel burnup) are put around the edge of the core. This demonstrates qualitatively that a strict in-out refueling scheme will yield the highest reactivity lifetime.

2.3 The Maximum Discharge Burnup and the Self-sustained Lifetime

We know from the previous section that an in-out refueling could yield the highest reactivity lifetime for a given design of fuel. It then becomes interesting to know under what conditions the fuel could reach its maximum discharge burnup and what the maximum discharge burnup should be.

According to our analysis, when the refueling frequency in an in-out refueling scheme is continuous the fuel will reach its maximum discharge burnup. And this maximum discharge burnup will very much depend on the burnup value at which the k_{∞} of the fuel drops below 1. The analysis is as follows.

In the in-out refueling scheme, as refueling becomes more frequent, the cycle length of core will decrease because a smaller amount of fresh fuel is introduced into the core at each reload and the burnup increment for each zone will become smaller and smaller. But the discharge burnup will become larger and larger, with the gain in discharge burnup being roughly proportional to the difference of the reciprocal of the number of refueling batches, $\Delta(\frac{1}{N})$, where N is the number of refueling batches (19). The BOC (Beginning of cycle) and IOC (End of cycle) burnup distributions for different refueling frequencies will then approach each other as Figure (2.5) shows.

In the extreme case of continuous refueling most of the energy output is generated by the fuel in the earliest zones and only a little by the rest of the fuel in other zones. But because of the very limited amount of fuel introduced into the core at each refueling,

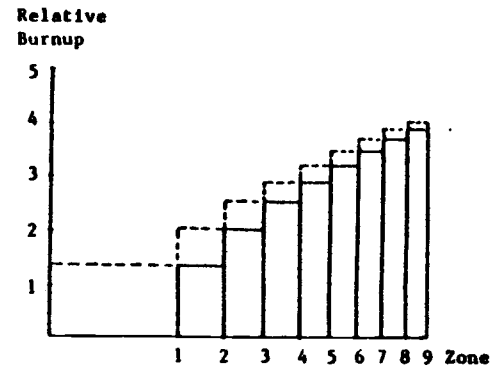
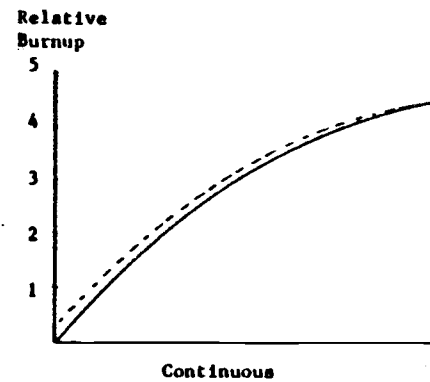
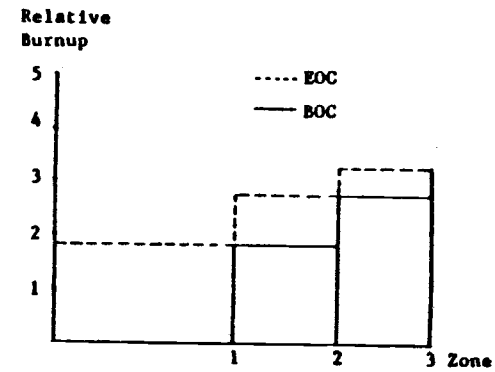
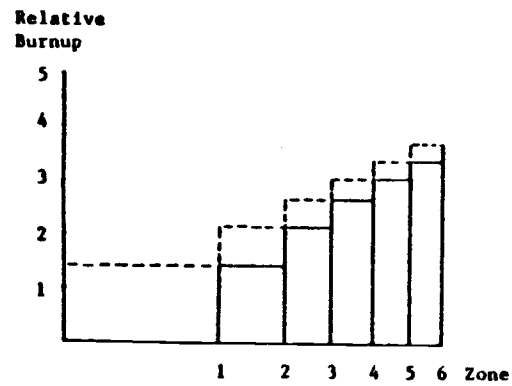


FIGURE 2.5 BOC and EOC burnup distribution for different refueling frequencies (or zones).

the burnup increments in the early (i.e., most recently loaded) zones are small. Consequently, the burnup distributions at BOC and EOC are very much the same and continuous as shown in Figure (2.5). The discharge burnup will reach its limit in the continuous refueling case. Its value can be derived in the following way; it can be different for different types of fuel. At EOC, the k of the reactor should be equal to 1, i.e.,

$$k \equiv \frac{\int v \Sigma f \phi dv}{\int (\Sigma a \phi + \text{leakage}) dv} = 1$$

or

$$\int \left(\frac{v \Sigma f \phi}{\Sigma a} - \phi - \frac{\text{leakage}}{\Sigma a} \right) dv = 0 \quad (2.5)$$

Since $\int \frac{\text{leakage}}{\Sigma a} dv$ is proportional to $(1 + M^2 B^2)$ and $M^2 B^2$ in a reactor is approximately a constant, Equation (2.5), after combined with Equation (2.1), can be written as

$$\int (k_{\infty} - c(1 + M^2 B^2) - 1) \phi dv = \int (k_{\infty} - c_1 - 1) \phi dv = 0, \quad (2.6)$$

where c is the proportional constant, $c_1 = c(1 + M^2 B^2)$. Equation (2.6) is a neutron balance relation in the reactor at its EOC. This balance relation, when shown graphically, is illustrated in Figures (2.6). Figure (2.6-1) is the case when the reactor is large enough so that the outermost fuels in the continuous refueling scheme

have burnups so high that they become a black body to the neutrons, i.e., no neutrons from the interior leak out from the core. In this case the leakage term c_1 in Equation (2.6) is zero. The neutron balance will be that the neutrons generated around the reactor center, represented by the shaded area, in the left, between the ϕ curve and the $k_{\infty}\phi$ curve, are equal to the neutrons needed by the fuels close to the edge of the reactor, represented by the shaded area in the right. The highest burnup at the edge of the core (or the far right) in Figure (2.6-1) is the maximum discharge burnup one can expect to reach in a continuous refueling scheme. This neutron balance is equivalent to having a zero integrated productivity over the time from zero burnup to the maximum discharge burnup, with the productivity defined as the difference in neutron gain and loss per unit of fluxtime.

When the reactor is of finite size, a certain fraction of neutrons leak from the reactor. The c_1 constant in Equation (2.6) can no longer be zero. The neutron balance is then like that in Figure (2.6-2). In this figure, the shaded area is now between $k_{\infty}\phi$ and $(1 + c_1)\phi$ curves rather than $k_{\infty}\phi$ and ϕ curves as in Figure (2.6-1). The area is smaller than that in the non-leakage case and the highest burnup is also lower. Knowing that the leakage is higher for a reactor of higher M^2 and B^2 , it would be beneficial to design a reactor of lower M^2 and B^2 , as far as discharge burnup is concerned. From Figure (2.6-1), it is noted that the higher and longer the k_{∞} of the fuels remains above 1, the larger the shaded area in the left,

Neutron Population

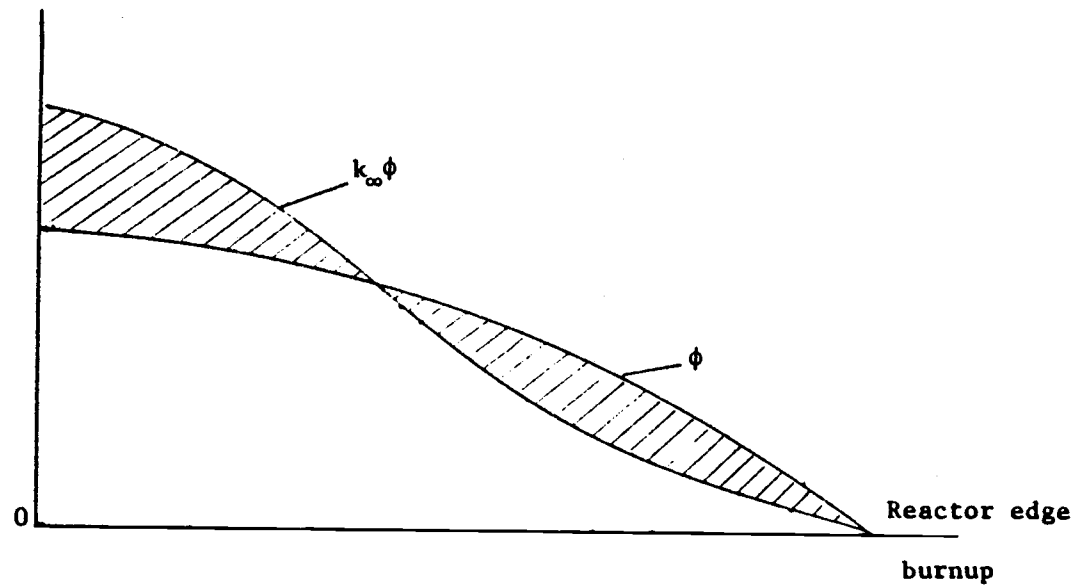


FIGURE 2.6 a Neutron balance relation for reactor of zero leakage in continuous refueling.

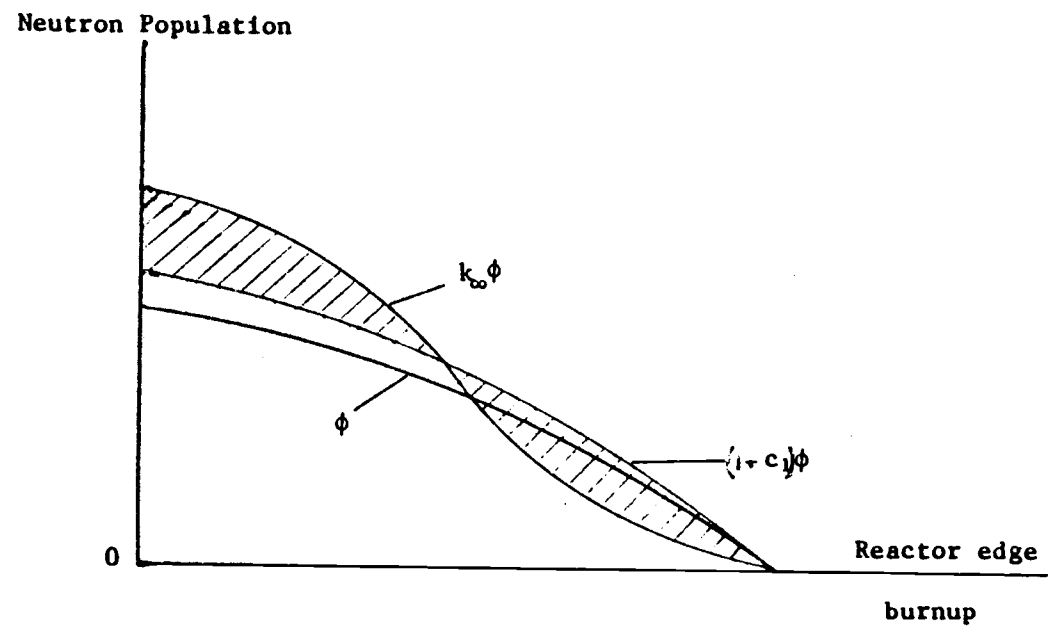


FIGURE 2.6 b Neutron balance relation for finite reactor in continuous refueling.

therefore the higher the maximum discharge burnup. For example, if a fuel has a fertile to fissile conversion ratio greater than 1, the maximum discharge burnup of the fuel theoretically can be infinite.

Since it is hard to know the maximum discharge burnup from Figures (2.6-1) and (2.6-2), an approximation will be made. As a first approximation, if the flux is assumed to be unity everywhere in the reactor, i.e., no leakage, the maximum discharge burnup will be the maximum burnup when the shaded area above the $k_{\infty} = 1$ line in Figure (2.7), is equal to the shaded area below the $k_{\infty} = 1$ line. This approximate maximum discharge burnup is called the self-sustained lifetime of the fuel, because in a time domain, this burnup is the lifetime the fuel can conceptually reach by itself. In other words, the fuel will have its self-sustained lifetime when the extra neutrons the fuel produces before its k_{∞} falls below 1 are preserved and used to sustain its productivity during the period when its k_{∞} is less than 1. Thus, in this case the shaded area in the left in Figure (2.7) is equal to the shaded area in the right. This self-sustained lifetime is equivalent to the maximum burnup the fuel can reach in a uniformly graded fuel management scheme (2). In this scheme, the fuels in any small region are mixed and have a continuous degree of burnup from zero to the maximum; and all these fuels are exposed to the same flux, for the localized flux disturbances due to various burnups are small. These requirements of uniformly graded fuel management are the same as the assumptions made in defining a self-sustained

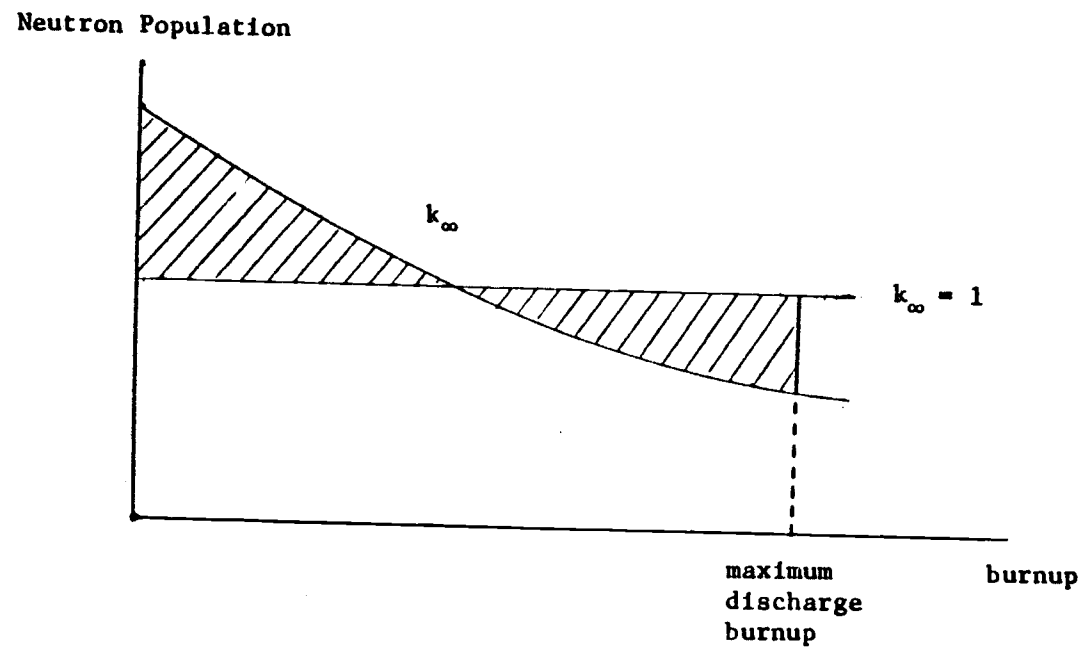


FIGURE 2.7 Neutron balance relation for flat flux.

lifetime of fuel. For the fuels under study, the sustained lifetimes obtained from Figure (2.3) are 61000 MWD/T for Oconee 15x15 three percent enrichment fuel, 45000 MWD/T for Trojan 15x15 three percent enrichment fuel, 41000 MWD/T for Trojan 17x17 three percent enrichment fuel, 36000 MWD/T for Trojan 18x18 three percent enrichment fuel and 22000 MWD/T for Trojan 17x17 two percent enrichment fuel. In the above, all the numbers for Trojan fuels are based on Leopard calculations by TPC's version, but the number for Oconee fuel is from the O.S.U. version.

3. ONE-DIMENSION TWO-GROUP MODEL

3.1 Description of the Algorithm

In order to get a quantitative sense of the advantages and the disadvantages that a strict in-out fueling scheme can have, a one-dimension two-group diffusion code and a two-dimension synthesis (6,7) code have been established to simulate the behaviors of a pressurized light water reactor. A sketch of the reactor and its associated parameters is given in Figure (3.1). In both codes, the group constants, such as Σ_a absorption cross-section, $\nu\Sigma_f$ product of ν and Σ_f macroscopic fission cross-section, D diffusion coefficient, Σ_r removal cross-section, P_r resonance escape probability, and K_∞ the infinite multiplication factor for different bundle burnup used in the diffusion equations, are pre-obtained from the unit cell calculations by the LEOPARD code as described in Section (2.1). In the one-dimension two-group diffusion calculations, the critical neutron flux and a critical boron control absorber concentration are first found through inner and outer iterations of the two-group diffusion equations (see Section (3.2)). An inner iteration is one sweep of the flux iteration through all spatial points. An outer iteration is one loop of inner iterations at the same reactor physical condition. Detailed descriptions are presented in Appendix B and C. Once the critical flux is obtained, a burnup step (power generation) follow using this

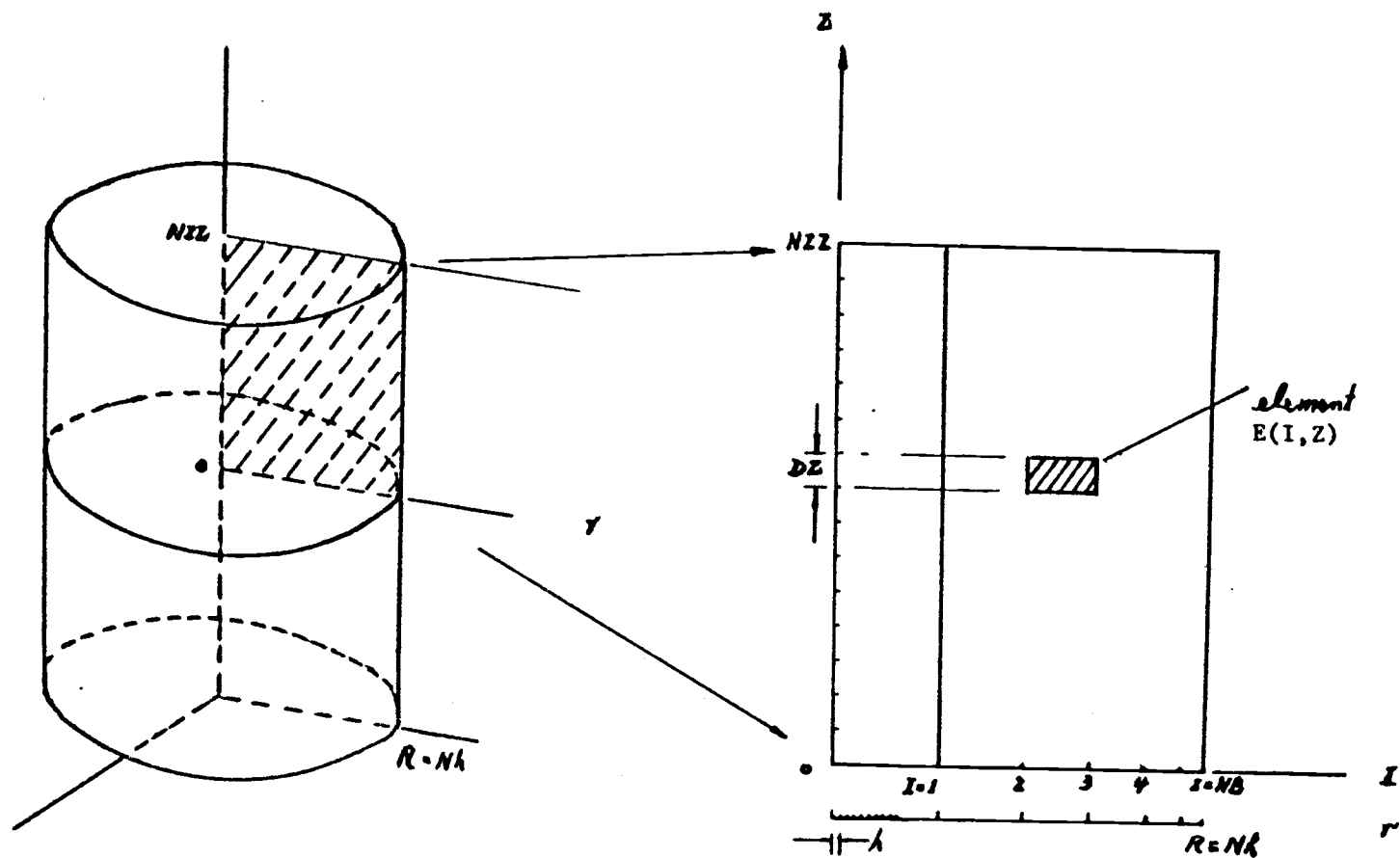


FIGURE 3.1 Sketch of the reactor and its parameters.

critical flux. A burnup step is a power generation process for a given time period in which the energy is created by the fuels due to fissions. The fuels at different locations in the core are exposed to the different levels of the critical neutron flux just computed and undergo different rates of fission. Hence, the amount of energy generated is different for the fuels at different locations, and so each will have its own burnup. Their average over the core is called the core average burnup. It is a measure of the energy the core generated during the burnup step. Both the core average burnup and the individual bundle burnup are in units of Megawatt-days per tonne of uranium fuel, MWD/MTU. Detailed calculation procedures for the individual bundle burnups are presented in Section (3.4). Because of the generation of power, due to nuclear reactions, the fuel composition changes. The group constants of each fuel bundle are then revised according to its corresponding burnup -- which in this work is the zone average burnup--to reflect this change. Another critical flux and burnup calculation is then carried out. Such a process will repeat and repeat until the end of the cycle is reached. Detailed descriptions of the procedure follow.

3.2 The Difference Equations

3.2.1 Neutron fluxes

The set of diffusion equations used to solve for the neutron fluxes is:

$$(1) \quad \nabla^2 \phi^1 - \frac{\Sigma_{a1}}{D_1} \phi^1 + \frac{1}{kD_1} \left(\nu_1 \Sigma_{f1} \phi^1 + \nu_2 \Sigma_{f2} \phi^2 \right) = 0 \quad (3.1)$$

and

$$(2) \quad \nabla^2 \phi^2 - \frac{\Sigma_{a2}}{D_2} \phi^2 + \frac{P \Sigma_{a1}}{D_2} \phi^1 = 0 \quad (3.2)$$

where ϕ^1 = fast group neutron flux;
 ϕ^2 = the thermal group neutron flux;
 Σ_{a1} = the fast group macroscopic removal cross-section
 (the sum of a fast group macroscopic absorption
 and slowing down cross-section);
 Σ_{a2} = the thermal group macroscopic absorption cross-
 section
 ν_1 & ν_2 = the number of neutrons generated per fast and
 thermal fission, respectively;
 Σ_{f1} & Σ_{f2} = macroscopic fission cross-sections of fast and
 thermal groups;
 D_1 & D_2 = the fast and thermal group diffusion coefficients;
 P_r = the resonance escape probability from fast group
 to thermal group, and
 k = the criticality eigenvalue.

This set of diffusion equations when applied in an infinitely
 high cylindrical geometry is:

$$\frac{\partial^2 \phi^1}{\partial r^2} + \frac{1}{r} \frac{\partial \phi^1}{\partial r} - \frac{\Sigma_{a1}}{D_1} \phi^1 + \frac{1}{kD_1} \left(\nu_1 \Sigma_{f1} \phi^1 + \nu_2 \Sigma_{f2} \phi^2 \right) = 0 \quad (3.3)$$

and

$$\frac{\partial^2 \phi^2}{\partial r^2} + \frac{1}{r} \frac{\partial \phi^2}{\partial r} - \frac{\Sigma_{a2}}{D_2} \phi^2 + \frac{P \Sigma_{a1}}{D_2} \phi^1 = 0 \quad (3.4)$$

Here, r is the radial distance in cylindrical geometry and the axial direction length of the reactor is assumed to be infinite.

When the central difference forms (8,9) of $\frac{\partial^2 \phi}{\partial r^2}$ and $\frac{\partial \phi}{\partial r}$ are used, and the successive overrelaxation iterative method (8,9) is employed, the finite difference approximation of Equations (3.3) and (3.4) becomes:

$$\begin{aligned} \phi_{i,n+1}^1 = & - \left(1 + \Delta r^2 \left(\frac{\Sigma_{a1}}{D_1} - \frac{\nu_1 \Sigma_{f1}}{k^n D_1} \right) \right) \phi_{i,n}^1 + \left(1 + \frac{\Delta r}{2r} \right) \\ & \left(\phi_{i+1,n}^1 + Q(\phi_{i+1,n+1}^1 - \phi_{i+1,n}^1) \right) + \left(1 - \frac{\Delta r}{2r} \right) \phi_{i-1,n}^1 \\ & + \frac{\nu_2 \Sigma_{f2}}{k^n D_1} \phi_{i,n}^2 \Delta r^2 \end{aligned} \quad (3.5)$$

and

$$\begin{aligned}
\phi_{i,n+1}^2 = & \left(1 + \frac{\Sigma a_2}{D_2} \Delta r^2\right) \phi_{i,n}^2 + \left(1 + \frac{\Delta r}{2r}\right) \left(\phi_{i+1,n}^2 \right. \\
& \left. + Q(\phi_{i+1,n+1}^2 - \phi_{i+1,n}^2)\right) + \left(1 - \frac{\Delta r}{2r}\right) \phi_{i-1,n}^2 \\
& + \frac{P_r \Sigma a_1 \phi_{i,n}^1}{D_2} \Delta r^2
\end{aligned} \tag{3.6}$$

where i : the radial location
 Δr : distance between mesh points in radial
direction, $\Delta r = hr$
 n : iteration step
 $\phi_{i,n}, \phi_{i,n+1}$: consecutive values of ϕ at i location
 Q : overrelaxation factor.

3.2.2 Adjoint fluxes

The set of equations for adjoint fluxes is:

$$D_1 \nabla^2 \psi^1 - \Sigma_{a_1} \psi^1 + \frac{1}{k} \nu_1 \Sigma_{f_1} \psi^1 + \Sigma_{a_1} P_r \psi^2 = 0 \tag{3.7}$$

$$D_2 \nabla^2 \psi^2 - \Sigma_{a_2} \psi^2 + \frac{1}{k} \nu_2 \Sigma_{f_2} \psi^1 = 0 \tag{3.8}$$

After several steps of derivation, the corresponding difference equations are:

$$\begin{aligned}
\psi_{i,n+1}^1 = & - \left(1 + \Delta r^2 \left(\frac{\Sigma a_1}{D_1} - \frac{v_1 \Sigma f_1}{k^n D_1} \right) \right) \psi_{i,n}^1 \\
& + \left(1 + \frac{\Delta r}{2r} \right) \left(\psi_{i+1,n}^1 + Q(\psi_{i+1,n+1}^1 - \psi_{i+1,n}^1) \right) \\
& + \left(1 - \frac{\Delta r}{2r} \right) \psi_{i-1,n}^1 + \frac{\Sigma a_1 p r}{D_1} \psi_{i,n}^2 \Delta r^2
\end{aligned} \tag{3.9}$$

and

$$\begin{aligned}
\psi_{i,n+1}^2 = & - \left(1 + \Delta r^2 \frac{\Sigma a_2}{D_2} \right) \psi_{i,n}^2 + \left(1 + \frac{\Delta r}{2r} \right) \left(\psi_{i+1,n}^2 \right. \\
& \left. + Q(\psi_{i+1,n+1}^2 - \psi_{i+1,n}^2) \right) + \left(1 - \frac{\Delta r}{2r} \right) \psi_{i-1,n}^2 \\
& + \frac{v_2 \Sigma f_2}{k^n D_2} \psi_{i,n}^1 \Delta r^2
\end{aligned} \tag{3.10}$$

The variables and constants have the same definition as in Section (3.2.1).

3.3 The Boundary Conditions

Equations (3.5) and (3.6) can be solved for critical fluxes ϕ^1 and ϕ^2 by a successive displacement overrelaxation iteration method with the following boundary conditions, and the same boundary conditions were used for the adjoint fluxes.

At the edge of the core, the boundary condition is

$$\frac{\Delta \phi}{\Delta r} = - \frac{\phi}{d} \quad ,$$

where d is the extrapolation distance at the free surface, 2.8 cm for fast flux and 0.666 cm for the thermal flux. (Note: The extrapolation distance in diffusion theory is $2xD$. The diffusion coefficient, D , is 1.4 cm for fast neutron flux and 0.333 cm for thermal flux as obtained from the LEOPARD output; therefore, the extrapolation distance is 2.8 cm for fast neutron flux and 0.666 cm for thermal neutron flux.)

At the center of the core, $\nabla\phi = 0$ at $r = 0$ is used. When this boundary condition is applied to Equations (3.5) and (3.6), the finite difference forms of Equations (3.5) and (3.6) can be written as

$$\begin{aligned} \phi_{0,n+1}^1 = & \phi_{1,n+1}^1 - \frac{\Delta r^2}{2} \left(\Sigma_{a1} - \frac{\nu_1 \Sigma_{f1}}{k^n D_1} \right) \phi_{0,n}^1 \\ & + \frac{\Delta r^2 \nu_2 \Sigma_{f2}}{2k^n D_2} \phi_{0,n}^2 \end{aligned} \quad (3.11)$$

and

$$\phi_{0,n+1}^2 = \phi_{1,n+1}^2 - \frac{\Delta r^2 \Sigma_{f2}}{2D_2} \phi_{0,n}^2 + \frac{\Delta r^2 P_r \Sigma_{f1}}{2D_2} \phi_{0,n+1}^1 \quad (3.12)$$

Equations (3.11) and (3.12) are obtained by multiplying Equations (3.3) and (3.4) by $2\pi r$, integrating from 0 to r (here $r = \Delta r$), rearranging the result into difference form.

Successive overrelaxation is also used for the fluxes at the center. That is,

$\phi'_{0,n+1} = \phi_{0,n} + Q(\phi_{0,n+1} - \phi_{0,n})$ is used as the starting point for the next iteration, where Q is an overrelaxation factor between 1 and 2.

3.4 The Criticality Calculation

3.4.1 The critical fluxes

To start the flux iteration, initial guesses of the fast and thermal neutron fluxes of the shape of the zero order Bessel function of the first kind J_0 are used. They are

$$\phi^1 = 4C \cdot J_0 \left(\frac{2.405r}{R} \right) \quad (3.13)$$

and

$$\phi^2 = C \cdot J_0 \left(\frac{2.405r}{R} \right) \quad (3.14)$$

where 4 = an initial approximation of the ratio of the fast flux to the thermal flux from the LEOPARD run.
 C = a constant chosen so that the fission rate over the whole reactor is approximately correct.

This paper also includes some 1-D calculations for an out-in refueling scheme, a refueling process that is the opposite of the in-out refueling scheme. A detailed description of an out-in refueling scheme is given in Section (5.3). When the out-in refueling scheme is under study, the initial guesses are $\phi^1 = 4C$

and $\phi^2 = C$, rather than those of Equations (3.13) and (3.14), for the actual fluxes in an out-in refueling scheme are not at all well approximated by J_0 Bessel functions. The flat initial guesses $\phi^1 = 4C$ and $\phi^2 = C$ are better, and save computer time in flux iterations.

From equations (3.5) and (3.6), fluxes at neutron generation $n+1$ can be obtained from fluxes at neutron generation n . In this study, the iteration begins at the edge of the core and continues toward the center of the core.

The convergence criterion of the iteration is

$$|CH1| = \left| \frac{\int \phi_{n+1}^1 dV - \int \phi_n^1 dV}{\int \phi_{n+1}^1 dV} \right| < 10^{-5} \quad (3.15)$$

The iteration scheme for the eigenvalue k^n is

$$k^n = k^{n-1} \times \frac{\int v_1 \Sigma_{f1} \phi_n^1 dV + \int v_2 \Sigma_{f2} \phi_n^2 dV}{\int v_1 \Sigma_{f1} \phi_{n-1}^1 dV + \int v_2 \Sigma_{f2} \phi_{n-1}^2 dV} \quad (3.16)$$

3.4.2 The critical boron concentration search

Since this paper includes the study of the effects of reactivity control on discharge burnup and power peaking, the flux calculations described in Section (3.4.1) will search for the critical boron concentration, namely, the boron macroscopic absorption cross section, Σ_a^B (critical), needed to bring the reactor to critical condition, i.e., $k = 1$ and $CH1 < 10^{-5}$. The scheme established

for Σ_a^B (critical) search is followed.

As shown in Section (3.4.1), once the rough k value of the reactor is found after several iterations, the amount of leakage the reactor has can be estimated through the definition of k ,

$$\text{Leakage} = \frac{\int v \Sigma_f \phi dv}{k} - \int \Sigma_a \phi dv \quad (3.17)$$

In order to bring the reactor to a condition $k = 1$ by adding boron, Equation (2.3) can be modified by incorporating Equation (3.17) into it and setting $k = 1$, and be written in the form as,

$$k \text{ (with boron)} = 1 = \frac{\int v \Sigma_f \phi dv}{\frac{\int v \Sigma_f \phi dv}{k \text{ (without boron)}} + \int \Sigma_a^B \phi dv}$$

or

$$\Sigma_a^B = \left(1 - \frac{1}{k \text{ (without boron)}}\right) \frac{\int v \Sigma_f \phi dv}{\int \phi dv} \quad (3.18)$$

Because in our iteration processes, the fluxes and k eigenvalue are both gradually converged quantities, the Σ_a^B value obtained through Equation (3.18) is only an approximate value of Σ_a^B (critical). Repeated adjustments have to be made to reach to Σ_a^B (critical) value. The adjustment process is simply the repeated application of Equation (3.18). In mathematical form, it is

$$\begin{aligned} \Sigma_a^B(\text{critical}) &= Q1 \Sigma_{a,1}^B + Q1 \Sigma_{a,2}^B + Q1 \Sigma_{a,m}^B \\ &= Q1 \sum_{l=1}^m \Sigma_{a,l}^B \end{aligned} \quad (3.19)$$

where m = the number of loops of outer iterations needed to reach critical boron concentration (see Appendix A), four or five loops are usually needed.

$Q1$ = a convergence factor in helping reaching a right boron concentration.

$\Sigma_{a,1}^B$ is the first estimation of boron concentration needed in the first outer iteration when no boron is presented in the core, $\Sigma_{a,2}^B$ is the second estimation of boron needed in the second outer iteration after $\Sigma_{a,1}^B$ is added to the core, $\Sigma_{a,3}^B$ is the estimation after $\Sigma_{a,1}^B + \Sigma_{a,2}^B$ is added, etc. Equation (3.19) is the scheme used in this study.

The effect of the B-10 solution is reflected in the change of the thermal neutron absorption cross-section Σ_{a_2} (Σ_{a_2} with B-10 is equal to Σ_{a_2} without B-10 plus Σ_a^B). Searching for a critical B-10 concentration is called outer iteration. Once a B-10 concentration, not necessarily the critical value at the early iterations, is estimated, the group constant Σ_{a_2} for each fuel bundle, in equations (3.5) and (3.6) is revised according to the amount of B-10 added, and then another inner iteration is initiated. The inner and outer iterations will proceed back and forth until a critical condition (i.e., the B-10 concentration at its critical value, $CH1 < 10^{-5}$, $k = 1$) is reached.

3.4.3 The critical flux verification

The iteration processes just described, used to obtain critical fluxes, are notorious for their slow convergence. Sometimes, even though the convergence criterion Equation (3.15) is met, the flux has really not converged to its critical shape. To be certain that the iterations in our 1-D code will yield flux of right shape, some flux calculation results, from both our 1-D code and an independent 1-D code, called AHRCHB (14), for the same core conditions, are plotted in Figures (3.2) to (3.7) for comparison. AHRCHB is a one-dimension code for reactor criticality calculation. It utilizes the simultaneous solution method (15) rather than the iteration method in solving for the critical fluxes. Curves in Figures (3.2.1) and (3.2.2) are the flux shapes, by our 1-D code and AHRCHB 1-D code respectively, of a 3-zone reactor for an in-out refueling scheme, and those in Figures (3.3.1) and (3.3.2) are the flux shapes also of a 3-zone reactor, but for an out-in refueling scheme. Figures (3.4.1), (3.4.2), (3.5.1) and (3.5.2) are for 6-zone reactor and Figures (3.6.1), (3.6.2), (3.7.1) and (3.7.2) are for 9-zone reactor. As these figures have demonstrated, fluxes by both calculations are in good agreement. However, since AHRCHB 1-D code is superior to our 1-D code, with respect to computation time and stability, AHRCHB is used to calculate the equilibrium discharge burnups for each study case. Our 1-D code is used to generate the trial and weight functions needed for 2-D calculations in Section (4.1).

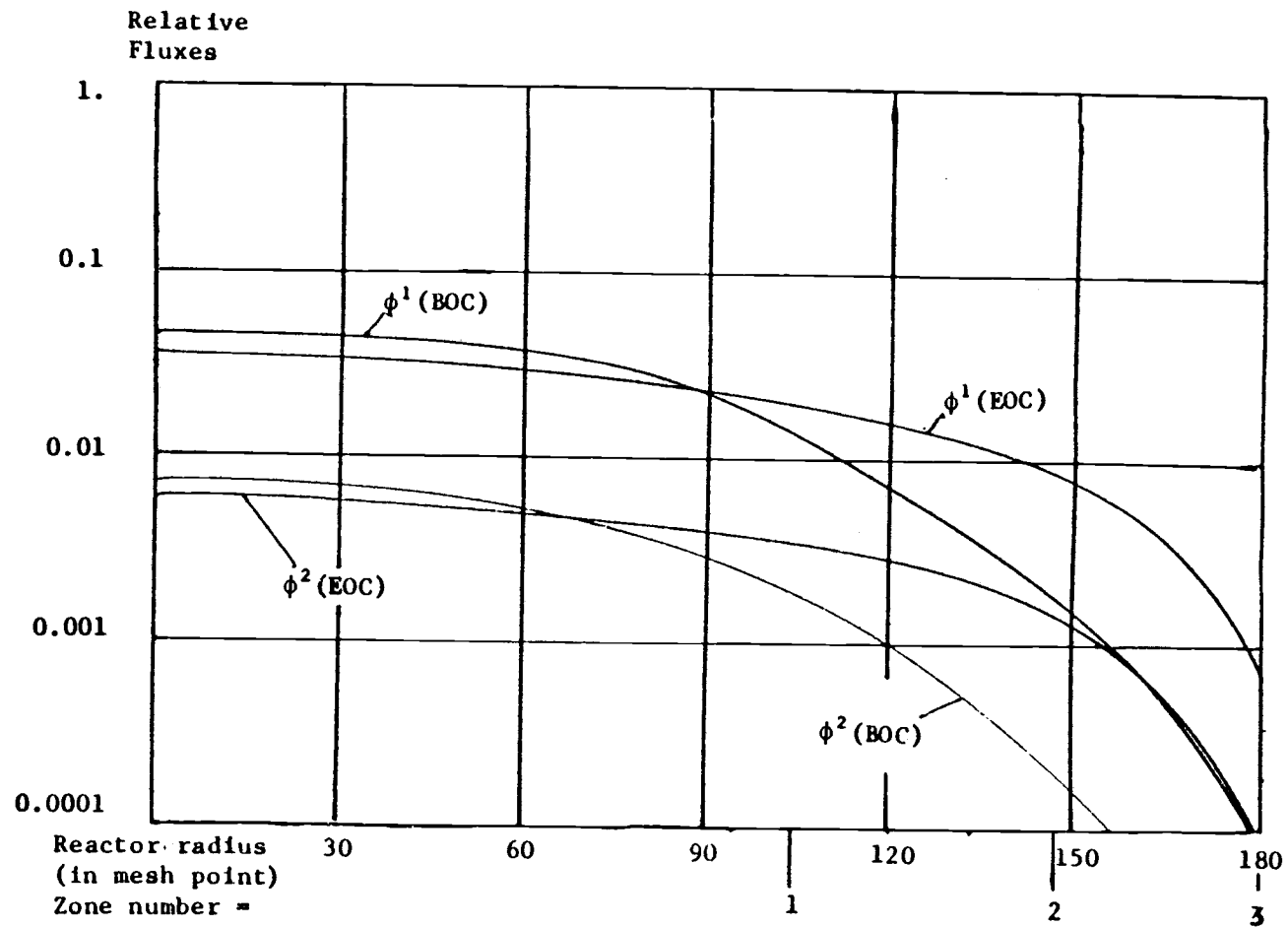


FIGURE 3.2 a BOC and EOC flux distributions of 3-zone cycle for Oconee fuel in in-out refueling scheme by our 1-D code.

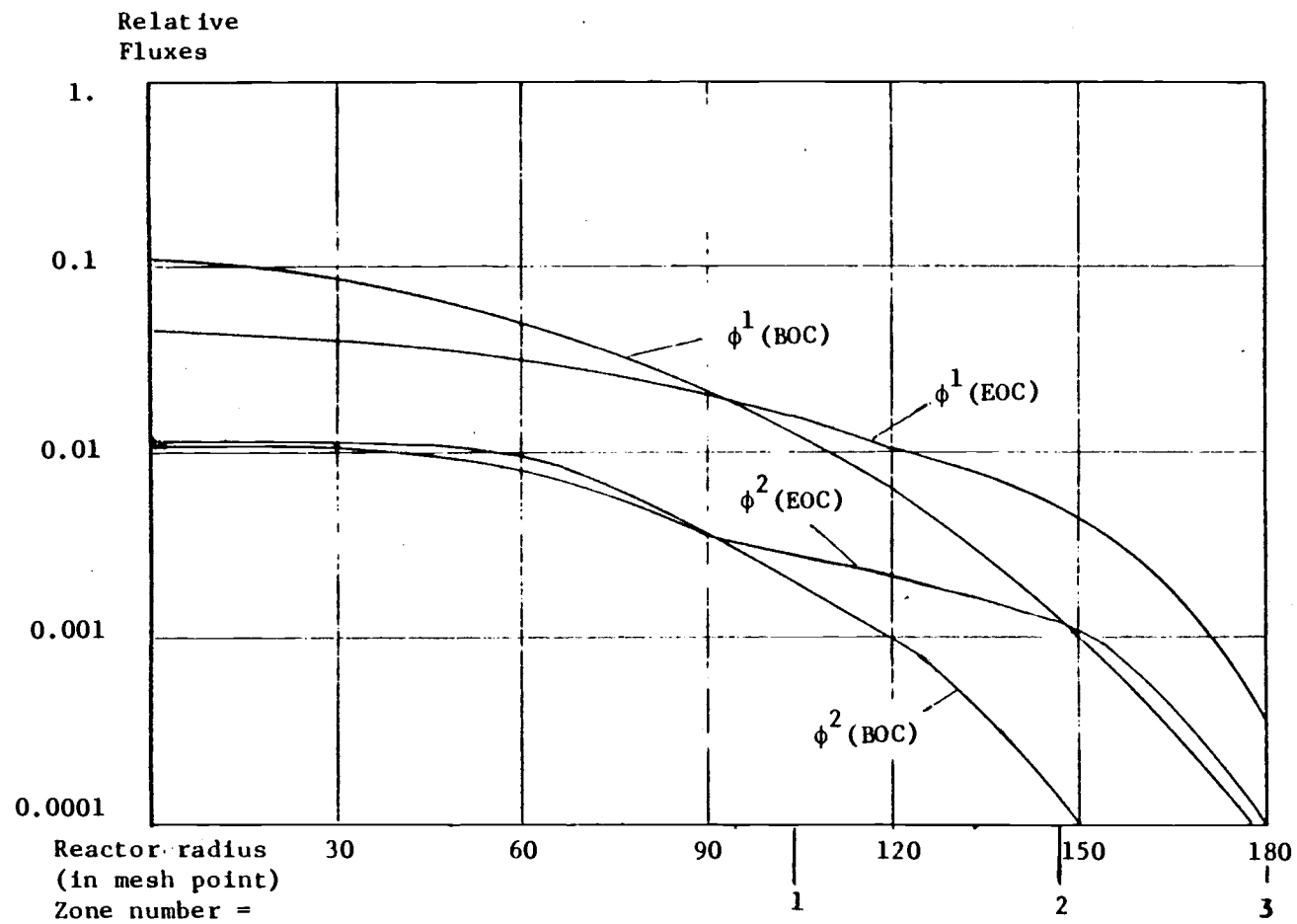


FIGURE 3.2 b BOC and EOC flux distributions of 3-zone cycle for Oconee fuel in in-out refueling scheme by AHRCHB code.

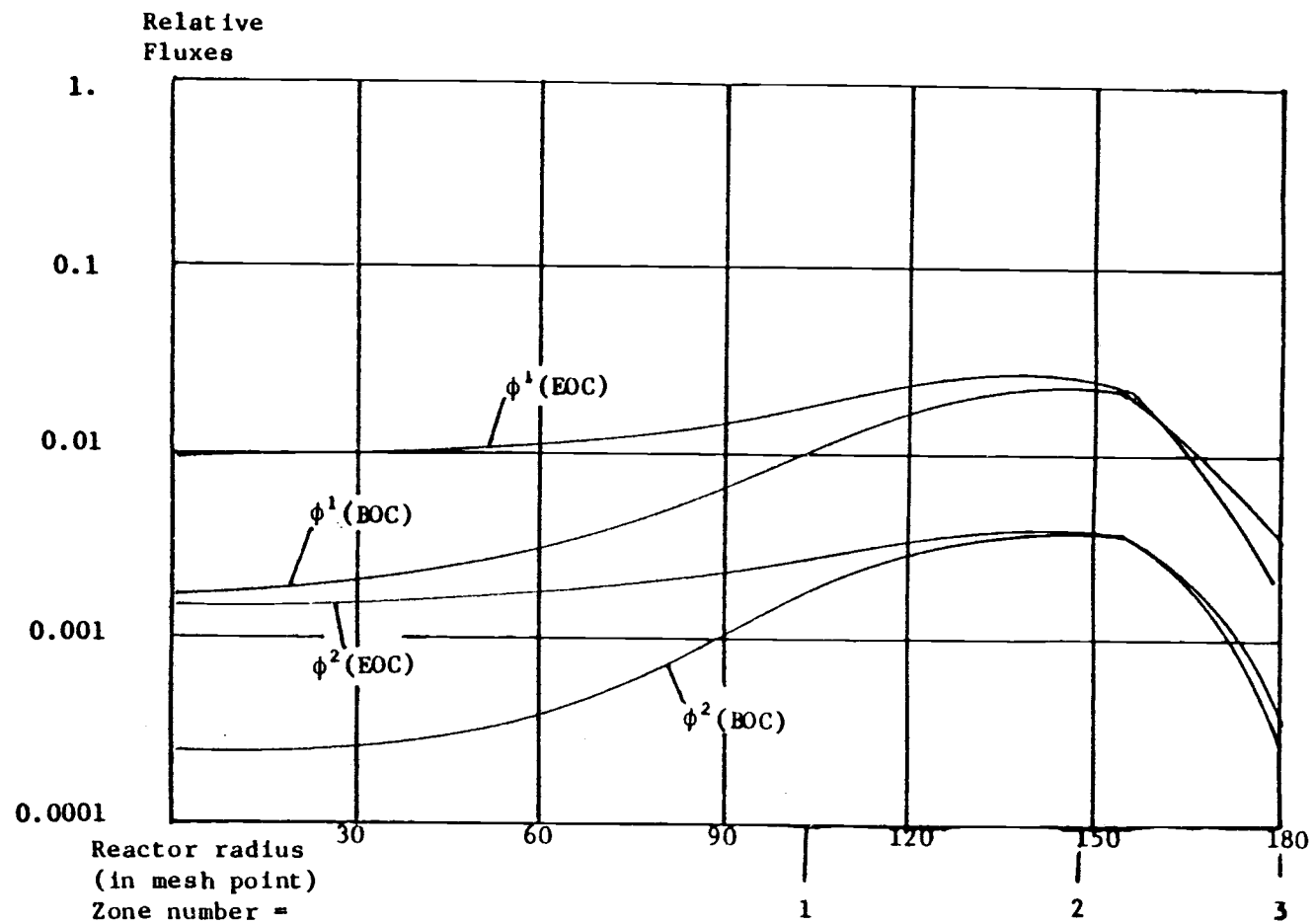


FIGURE 3.3 a BOC and EOC flux distributions of 3-zone cycle for Oconee fuel in out-in refueling scheme by our 1-D code.

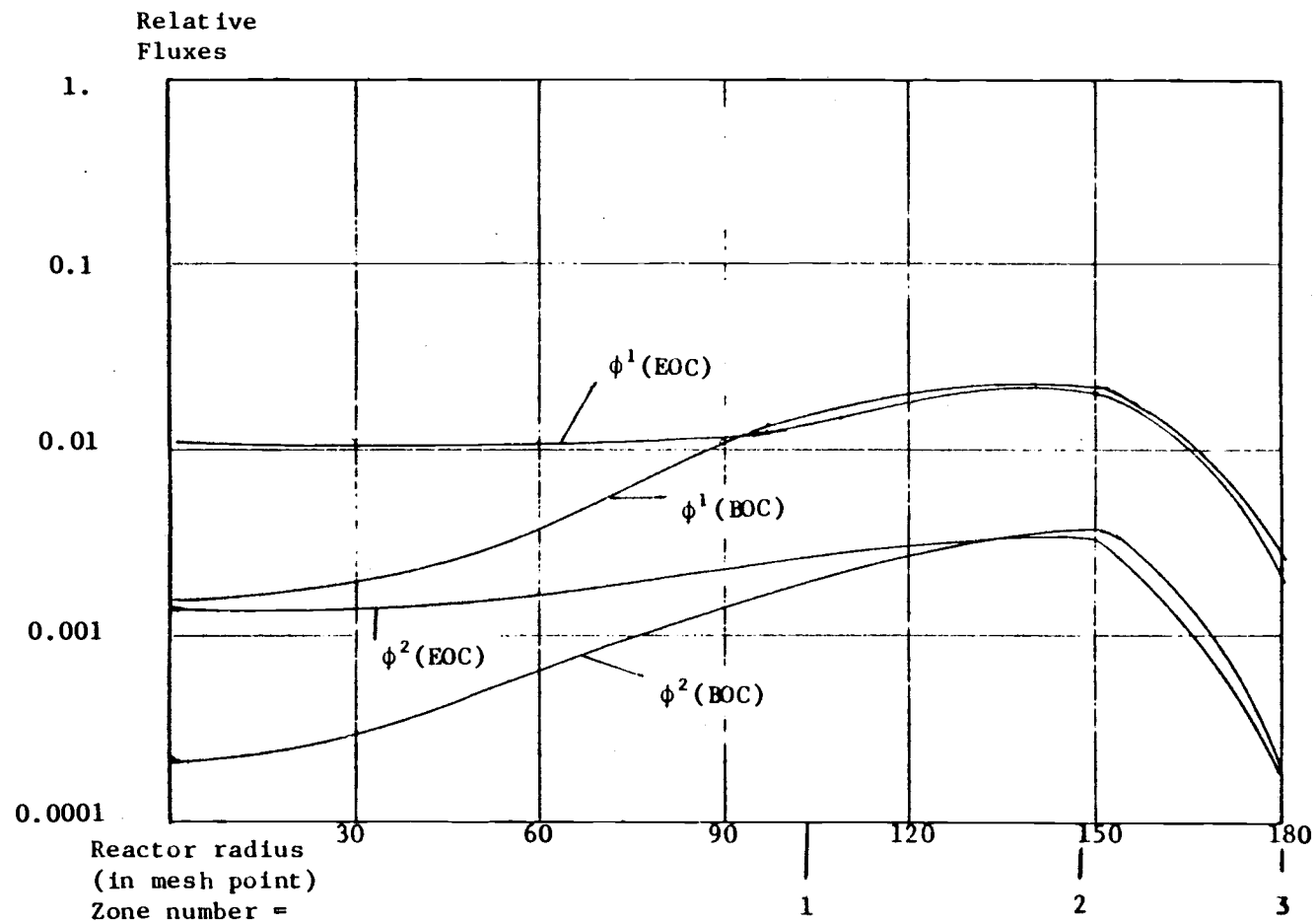


FIGURE 3.3 b BOC and EOC flux distributions of 3-zone cycle for Ocone fuel in out-in refueling scheme by AHRCHB code.

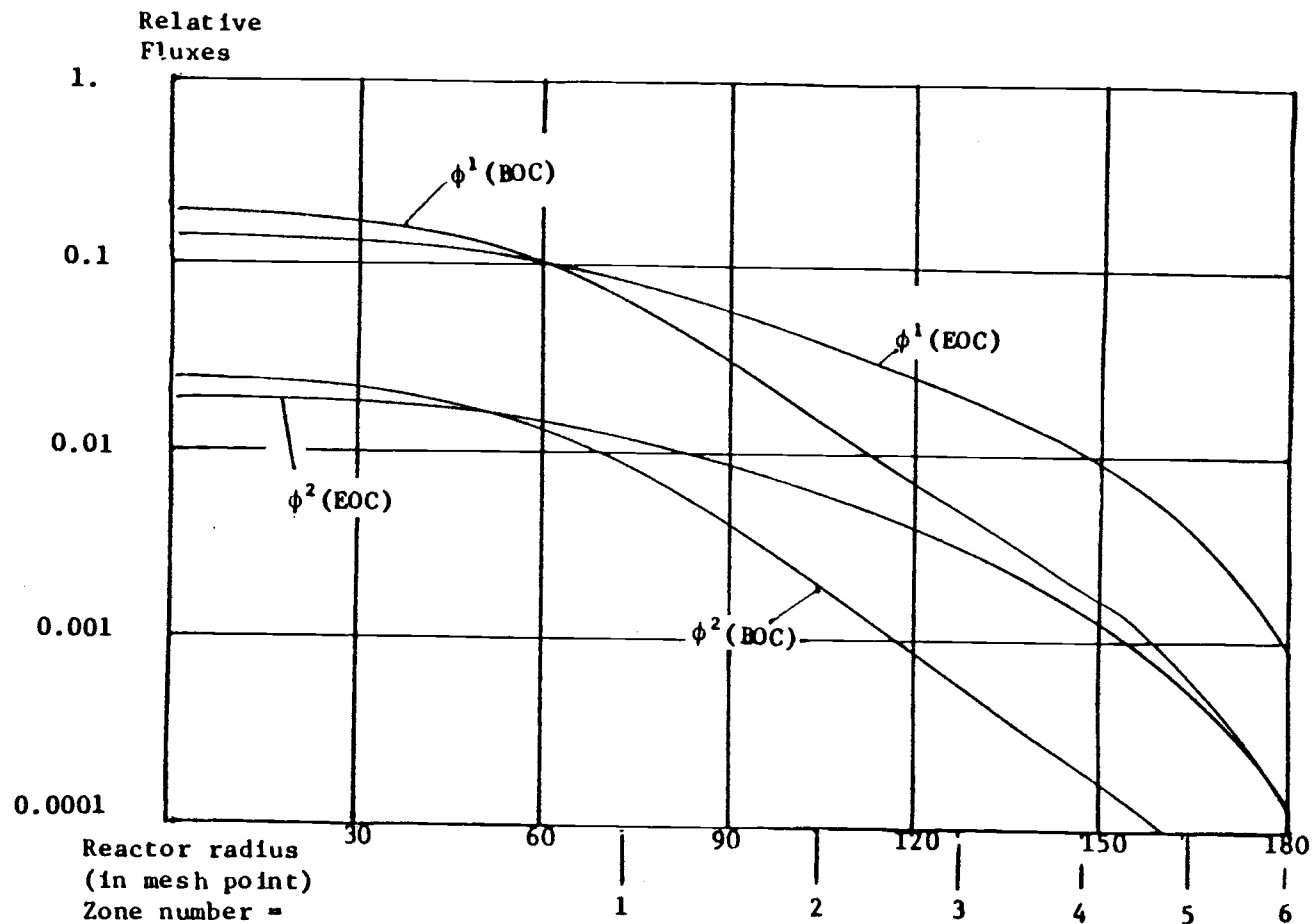
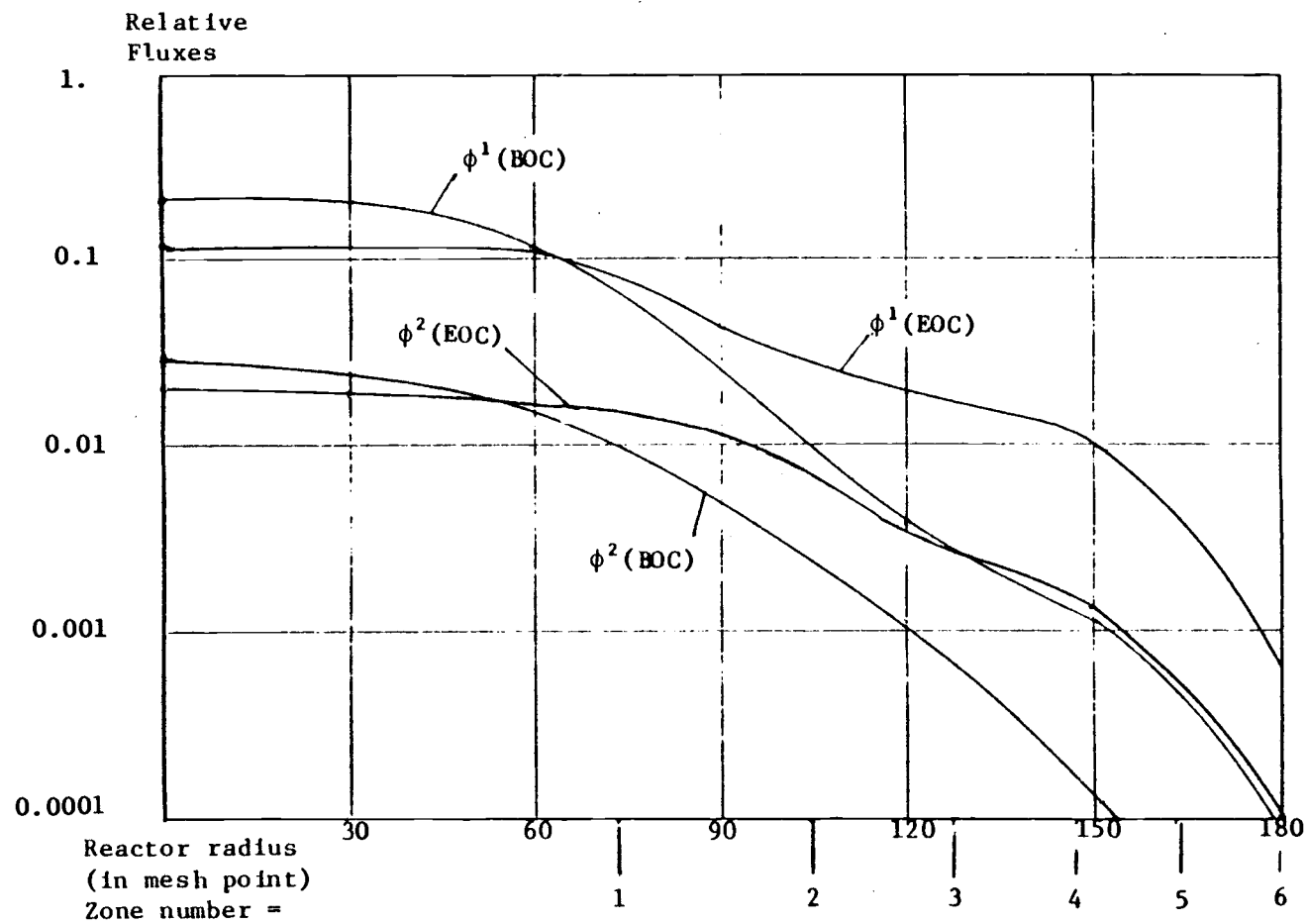


FIGURE 3.4 a BOC and EOC flux distributions of 6-zone cycle for Oconee fuel in in-out refueling scheme by our 1-D code.



41a

FIGURE 3.4b BOC and EOC flux distributions of 6-zone cycle for
Oconee fuel in in-out refueling scheme by AHRCHB code.

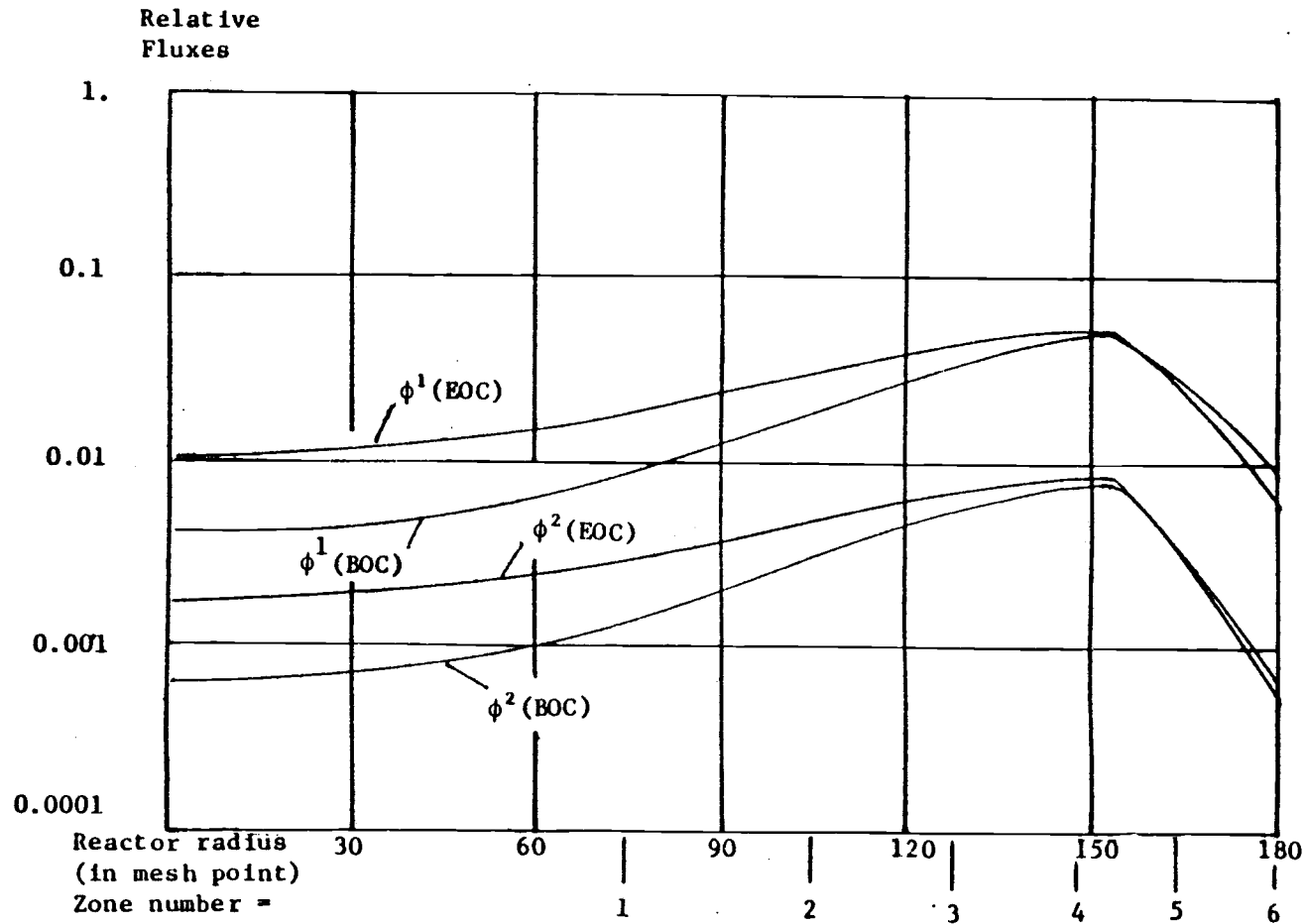


FIGURE 3.5 a BOC and EOC flux distributions of 6-zone cycle for Ocone fuel in out-in refueling scheme by our 1-D code.

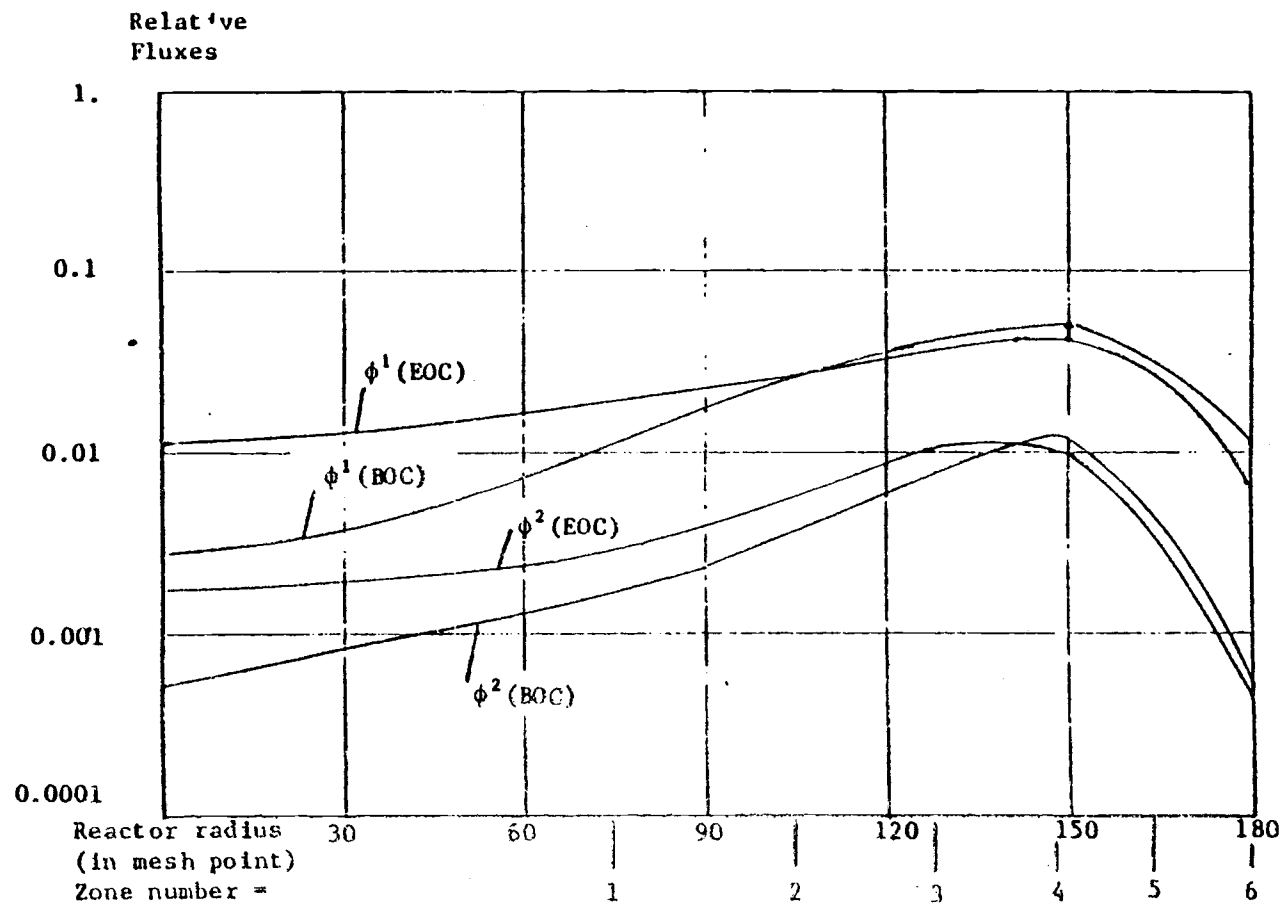


FIGURE 3.5 b BOC and EOC flux distributions of 6-zone cycle for
Oconee fuel in out-in refueling scheme by AHRCHB code.

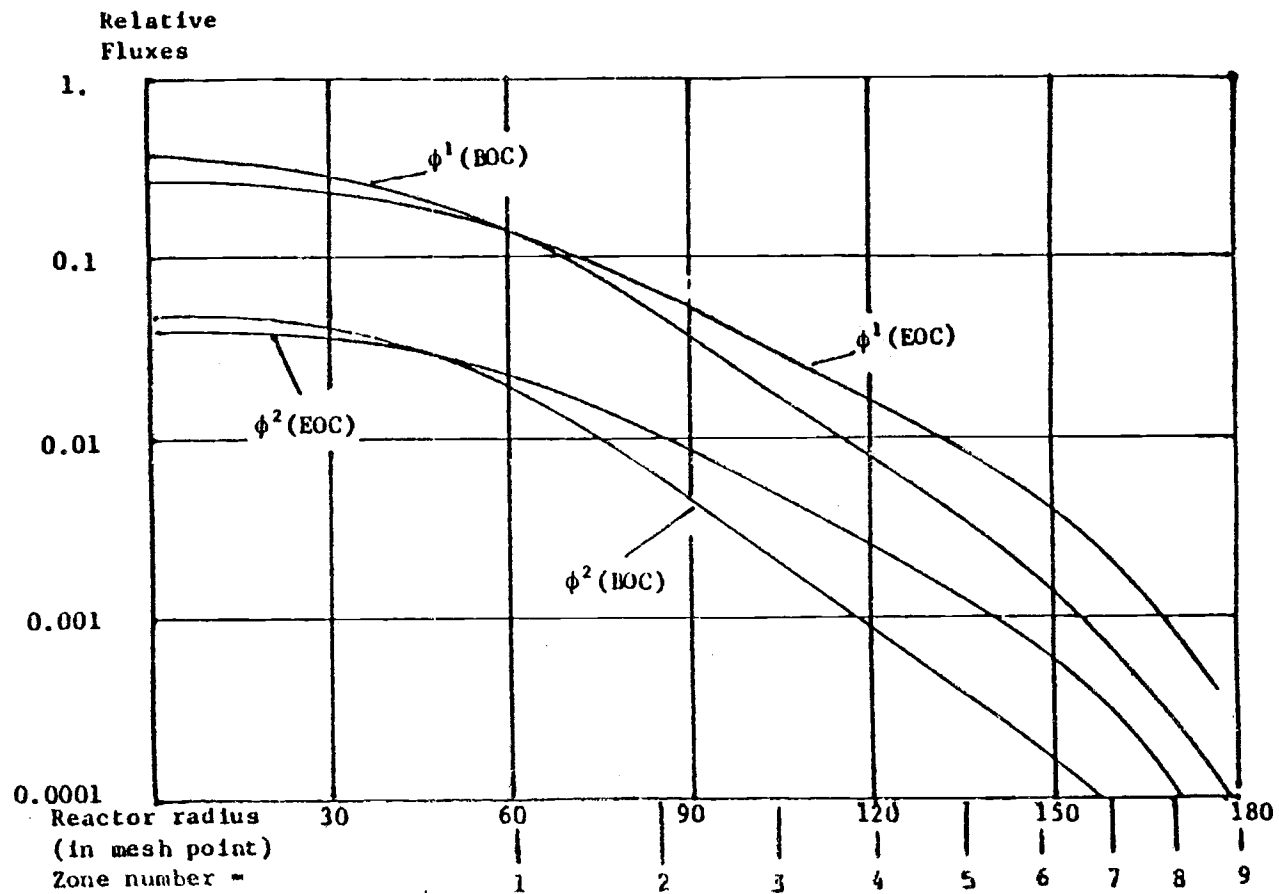


FIGURE 3.6 a BOC and EOC flux distributions of 9-zone cycle for Ocone fuel in in-out refueling scheme by our 1-D code.

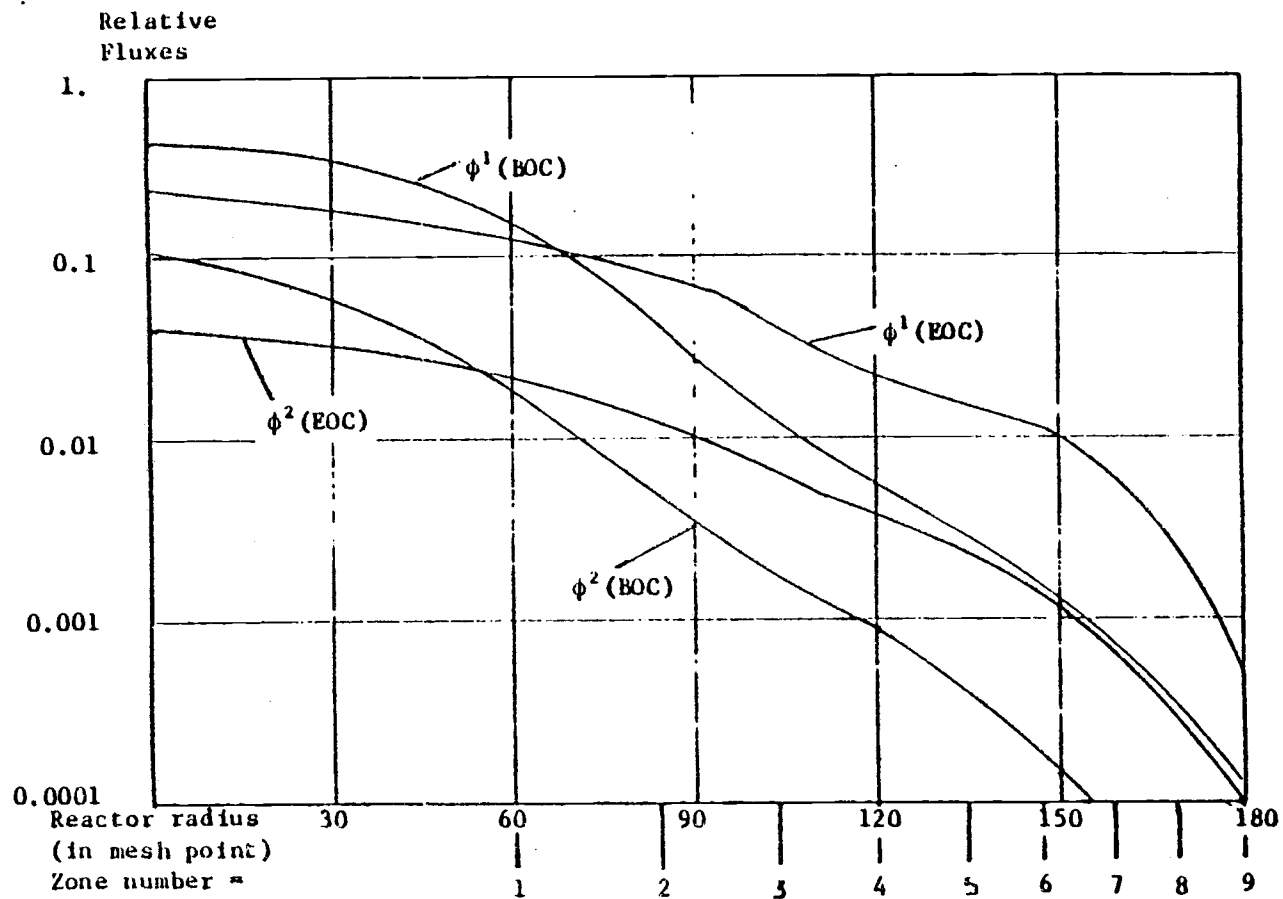


FIGURE 3.6 b BOC and EOC flux distributions of 9-zone cycle for
Oconee fuel in in-out refueling scheme by AIRCHEE code.

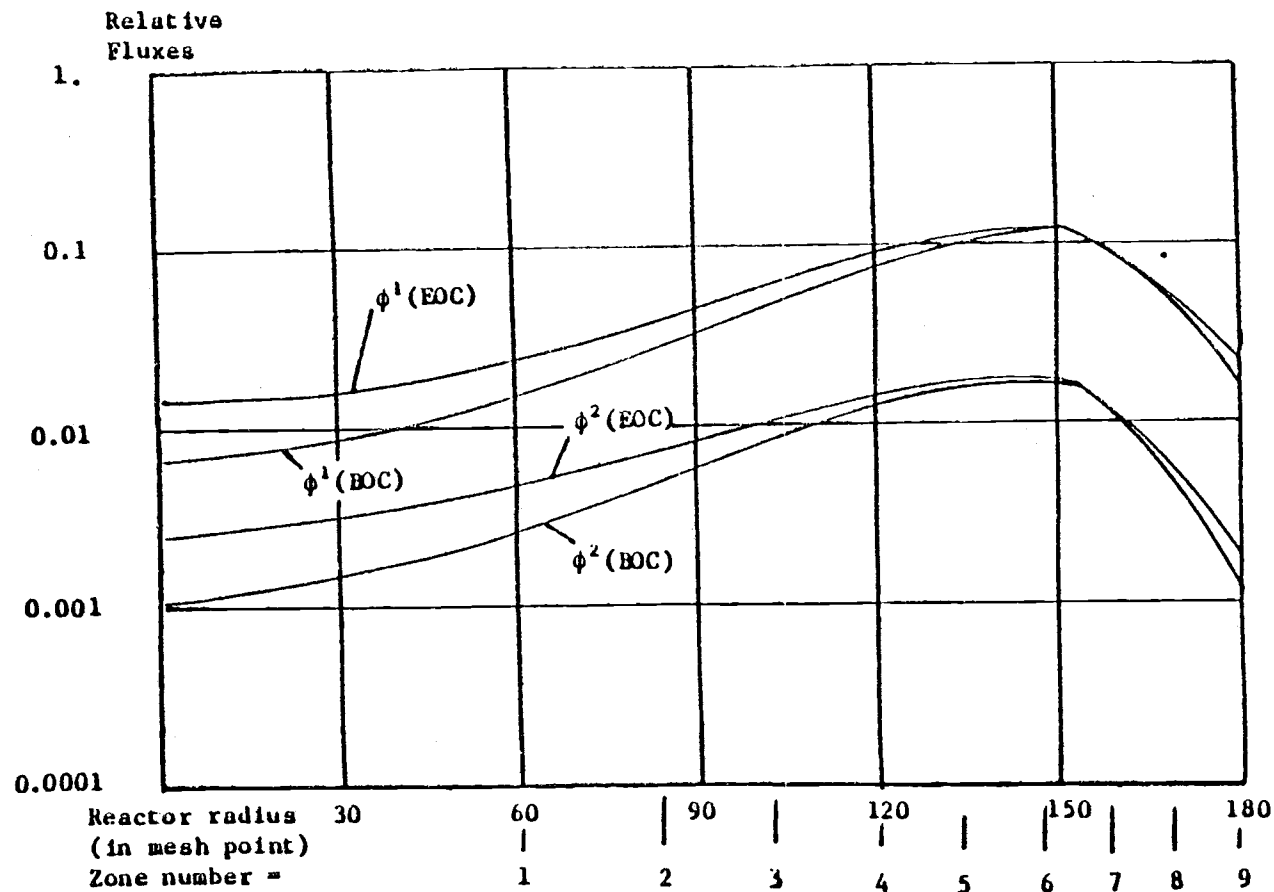


FIGURE 3.7 a BOC and EOC flux distributions of 9-zone cycle for Oconee fuel in out-in refueling scheme by our 1-D code.

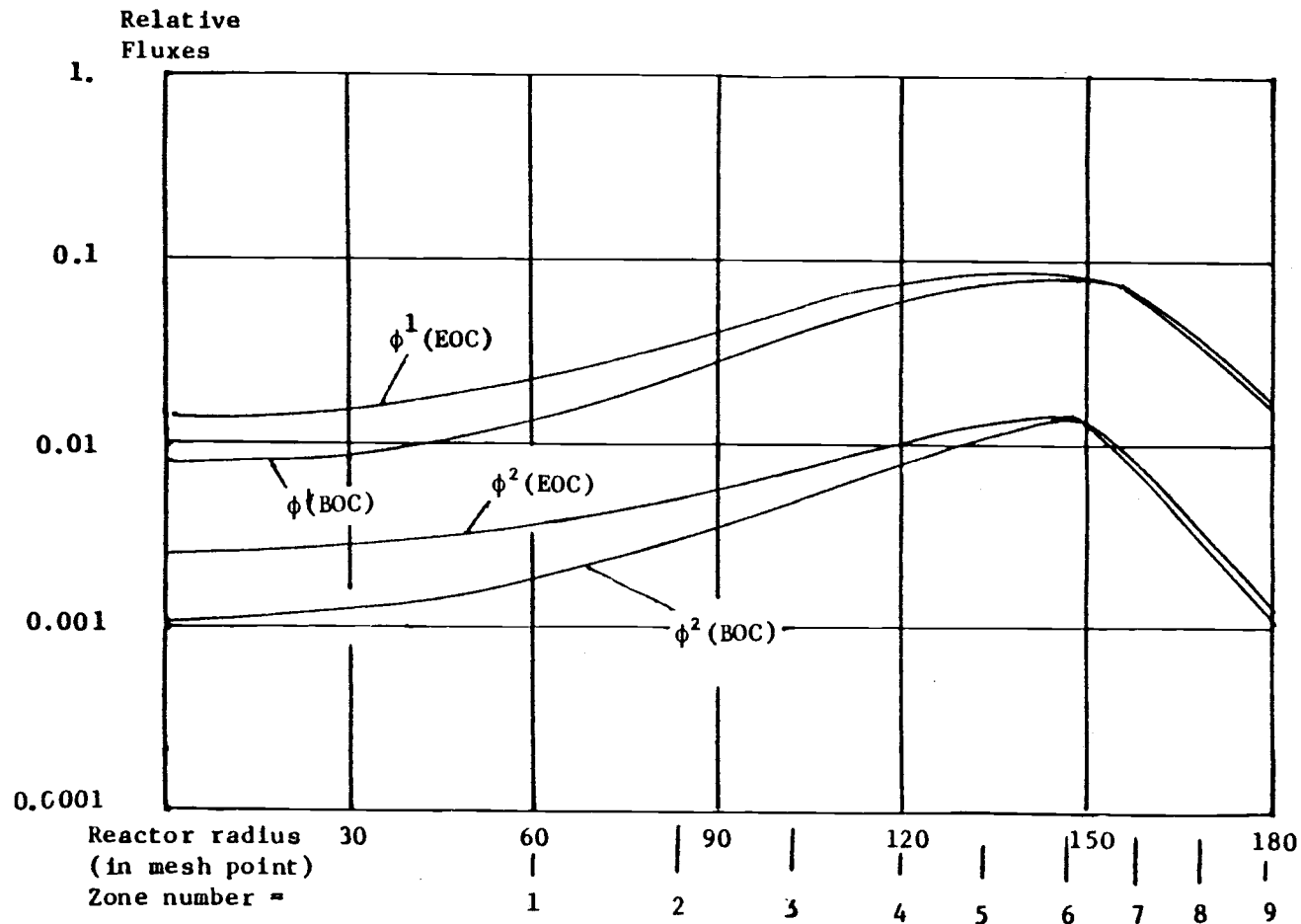


FIGURE 3.7 b BOC and EOC flux distributions of 9-zone cycle for Ocone fuel in out-in refueling scheme by AHRCHB code.

3.5 Individual Bundle Burnup Calculation

3.5.1 Burnup Algorithm

As the reactor reaches its critical condition, the fuels will be burned under the critical fluxes for a pre-selected time step BUC in units of MWD/MTU of core average burnup. That is to say, the fuels in the core will be exposed to the critical fluxes and undergo fissions for a time period so that the integral of fluence (flux-time) times fission cross section over the core volume, after division by the total uranium weight in the core, is equal to the pre-selected core average burnup BUC MWD/MTU. Corresponding to this core average burnup BUC MWD/MTU, the portion of energy contributed by each zone is the integral of fluence times fission cross section over the zone volume. This zone integral, after division by the weight of uranium in the zone, is the zone average burnup.

To find this zone average burnup is actually an allocation process and is done by Equation (3.20), which follows. After the zone average burnups of each zone are found, we then could find new sets of group constants at the new burnup levels, as precalculated by LEOPARD. As described in Section (2.1), it is LEOPARD that actually calculates the fuel composition change due to fissions. The operations described in this section are simply to account for the amount of fluence each zone has been exposed to. Based on these fluences, the group constants which reflect the changes of fuel composition are found from LEOPARD calculation results.

Using the new sets of group constants for each zone in the core, new critical fluxes are found by repeating the processes in Section (3.4) and the core is burned for another burnup time step BUC. In this way, the core is burned in a discrete fashion. The step size (BUC) can be large or small. A step size of approximately 1000 MWD/MTU, a trade-off between computer time consumption and accuracy of the result, is normally used in this calculation. The core cycle lifetime is the period from the beginning of the cycle, BOC, when the fresh fuel bundles are loaded to the end of the cycle, EOC, when the reactor can no longer be critical. EOC here is reached when the B-10 concentration (or equivalent I_a^B value) remaining in the core to keep the core in critical condition is zero and no excess reactivity is left in the core. The core cycle lifetime is approximately proportional to the magnitude of the B-10 concentration needed at BOC for a critical core.

In this study, the core is burned to EOC in four or five time steps. For each time step, the individual zone average burnup can be calculated as

B_I (zone average burnup of I zone, in MWD/MTU)

$$= \frac{P_I \cdot D}{T_I}$$

$$= \frac{P_I \cdot \frac{BUC}{P} \cdot T}{\frac{V_I(\text{zone})}{V_c(\text{core})} \cdot T} = \frac{P_I \cdot \frac{BUC}{P} \cdot V_c(\text{core})}{V_I(\text{zone})}$$

$$\begin{aligned}
&= \frac{P_I \cdot BUC}{\sum_{\text{zone I}} 2\pi \cdot J \cdot h_f^2 \cdot \text{CAL} \cdot P} \cdot \pi (N \cdot \text{hr})^2 \cdot \text{CAL} \\
&= \frac{\gamma \left[\sum_{\text{zone I}} 2\pi \cdot J \cdot h_f^2 (\sum_{f_1} \phi^1(J) + \sum_{f_2} \phi^2(J)) \right] \cdot \pi (N \cdot \text{hr})^2 \cdot BUC}{\gamma \sum_{\text{zone I}} 2\pi \cdot J \cdot h_f^2 \left[\sum_{\text{core}} 2\pi \cdot J \cdot h_f^2 (\sum_{f_1} \phi^1(J) + \sum_{f_2} \phi^2(J)) \right]} \\
&= \frac{N^2 \cdot BUC \cdot \sum_{\text{zone I}} J \cdot (\sum_{f_1} \phi^1(J) + \sum_{f_2} \phi^2(J))}{2 \sum_{\text{zone I}} J \cdot \sum_{\text{core}} J \cdot (\sum_{f_1} \phi^1(J) + \sum_{f_2} \phi^2(J))} \quad (3.20)
\end{aligned}$$

where

- J : the radial coordinate within zone I or core;
- P_I : the power generation rate in zone I, in MWt;
- T_I : the uranium weight in zone I, in tonne;
- T : the total uranium (UO_2) weight in the core, in tonne;
- P : the reactor thermal power, in MWt;
- BUC : the time step, MWD/MTU;
- D : equal to $\frac{BUC}{P} * T$, step size corresponding to BUC, in day;
- N : the total number of mesh points along the core radius;

$\sum_{\text{zone I}}$: the summation over the zone I;

\sum_{core} : the summation over the whole core;

γ : the recoverable energy per fission, $3.2 * 10^{-17}$

MW/sec, and

CAL : the core active length, in cm.

$V_c(\text{core})$: the volume of the whole core, in cm^3 ;

$V_I(\text{zone})$: the volume of zone I, in cm^3 .

Therefore, for every zone, there is a zone average burnup corresponding to each core average burnup step size. Note that this zone average burnup as obtained through Equation (3.20) is the zone volume average of the various burnups within the zone. Instead of summing up these various burnups within the zone separately step after step for finding the cumulative burnup, we apply the zone average burnups for each zone after each step. Justification of this approximation is given in Section (3.5.2). At the end of each burnup time step, the group constants for each zone then have to be revised according to the cumulative burnup for each zone. The group constants for different cumulative burnups are generated by the LEOPARD unit call code. By repeating the burnup steps until EOC, each zone will accumulate an individual burnup value. The fuel bundles in the highest burnup zone will then be discharged from the core, and fresh fuel bundles will be loaded into the core. The highest burnup is called the discharge burnup.

3.5.2 Approximations made in burnup calculation

There are two major approximations that have been made in the burnup calculation, and their possible influences on the accuracy of the burnup must be discussed.

First, the burnup level in a zone is always assumed to be constant. The zone-average fluence is used to calculate a single burnup for the zone, and this burnup is applied throughout the zone to get new group constants (see Equation (3.20)). Second, the critical flux shape is assumed to be constant over the burnup step, being the critical flux shape calculated at beginning of the burnup step. These approximations are made to simplify the calculations and save computation time. They may cause some deviations on the calculation results from their actual values. However, these deviations would not be large enough to destroy the significance of the calculation results for the following reasons. With regard to the first assumption, we realize that in either in-out refueling or out-in refueling the burnups will not be constant in a zone. However, when we move fuels from one zone to another, we will put the least burned assemblies from one zone into the place of another zone where we expect the most burnup will occur in the next cycle, and conversely. Over time, we can expect the burnups within a zone to flatten out. The calculations done by Equation (3.20) are just to simulate such a case. Indeed, flux in a zone varies less the more zones there are, so the approximation should work less well for the three-zone cases. Checking the flux

distributions in Figures (3.2) through (3.7), we could find the worst flux variations occur in the outermost zone in three-zone case, about ± 20 percent about the mean. But there, the burnup is small and therefore the inhomogeneity is not serious in any case. The first approximation is justified.

With regard to the second approximation of assuming constant flux shape over a burnup step, it has been a standard practice long being used to simplify the calculation (18). In general, flux shape is constrained by global considerations, such as total leakage and relative reactivity of regions, and is insensitive to details. Burnup change within a zone during a burnup step would not affect the flux shape much. This can be verified from the fact that the change in flux shape is small even between the BOC and EOC, as shown in Figures (3.2) through (3.7).

Besides, there exists a burnup compensation effect between two consecutive burnup steps that could help reduce the deviation the approximation might cause. The overburn in one area, where flux is relatively high and is assuming to be continually high during a burnup step, will cause the flux in the same area to be relatively low and be compensated by underburn during the next burnup step, and vice versa. Of course, this compensation effect can only reduce the magnitude of deviation. Ideally, the burnup step BUC should be taken as small as possible, and the critical flux used in burnup calculation should be that at the mid-way point of the burnup step rather than that at the beginning of the burnup step. To see how much

effect a large burnup step could be on the equilibrium discharge burnup (see Section(3.6)), two burnup calculations for the same condition are performed, one with fine burnup step size and another large burnup step. Results, as shown in Tables(3.1) and (3.2), convince us that the second approximation would not cause much deviation on discharge burnup.

3.6 Equilibrium Cycle Discharge Burnup

An equilibrium cycle is a reactor operation in which for every consecutive cycle, the amount of energy generated, the level of the discharge burnup, and the cycle length are all constant. When a reactor is new and is just starting up, the fuel bundles of the very first core are all fresh. A transition period, about 3 to 4 cycles, is usually needed before an equilibrium cycle can be reached. This is generally true for different refueling patterns. The one-dimension two-group code which is established in this study to simulate the power generation in a strict in-out refueling scheme also needs 3 or 4, or even more cycle iterations in order to get an equilibrium cycle. To limit the number of simulation cycles of burning before an equilibrium cycle is obtained, two convergence processes are used.

TABLE 3.1 Effect of Burnup Step Size on Discharge Burnup,
Burnup Calculations with Burnup Step Size of
1000 MWD/MTU

Step size	0 MWD/MTU BOC		1000 MWD/MTU		2000 MWD/MTU	
Zone No	Initial Load	Power Peak	Mid-exposure	Power Peak	Mid-exposure	Power Peak
1	0	4.972	5040	4.738	9840	4.502
2	22300	.811	23100	.945	24030	1.061
3	27550	.156	27710	.217	27930	.286
4	29140	.044	29180	.070	29250	.103
5	29780	.013	29790	.023	29820	.037
6	30040	.004	30045	.007	30050	.011

Step size	3000 MWD/MTU		4000 MWD/MTU		5012 MWD/MTU EOC	
Zone No	Mid-exposure	Power Peak	Mid-exposure	Power Peak	Final Burnup	Power Peak
1	14400	4.097	18550	3.682	22210	3.231
2	25070	1.234	26290	1.361	27670	1.465
3	28220	.407	28640	.542	29230	.691
4	29350	.171	29520	.260	29800	.372
5	29860	.069	29930	.116	30060	.178
6	30060	.022	30080	.039	30130	.063

**TABLE 3.2 Effect of Burnup Step Size on Discharge Burnup,
Burnup Calculations with Burnup Step Size of
2000 MWD/MTU**

Step size	0 MWD/MTU BOC		2000 MWD/MTU		4000 MWD/MTU	
Zone No	Initial Load	Power Peak	Mid-exposure	Power Peak	Mid-exposure	Power Peak
1	0	4.972	10080	4.422	19040	3.612
2	22300	.811	23890	1.104	26070	1.385
3	27600	.156	27910	.307	28540	.564
4	29200	.044	29280	.113	29510	.274
5	29800	.013	29830	.042	29910	.123
6	30000	.004	30010	.013	30030	.042

Step size	4970 MWD/MTU EOC					
Zone No	Final Burnup	Power Peak				
1	22490	3.327				
2	27410	1.451				
3	29130	.658				
4	29790	.344				
5	30050	.162				
6	30080	.057				

A. Manually adjust the initial loadings of the cycle

At the end of every power generation simulation cycle, the initial loadings of the next cycle will be determined manually by human judgment, depending on the cycle length, the initial loadings and the final bundle distribution of the current cycle.

B. Automatically adjust the initial loadings of the cycle

It is obvious that when an in-out refueling scheme is followed and the equilibrium stage is reached, the distribution of the bundle (or zone) burnups will monotonically increase from the center toward the edge of the core. Therefore, in the convergence process of equilibrium cycle for an in-out refueling scheme, the core should have an initial loading of fuel such that the bundle burnup distribution along the reactor radius is lowest at the center of the core and increasingly higher toward the edge of the core. A quick convergence toward the equilibrium cycle burnup distribution can be obtained from the individual zone average burnup increments of its preceding cycle. The following relation was used.

$$IL_i^{n+1} = B_i^n \cdot \frac{IL_{NB}^n}{\sum_{j=1}^{NB-1} B_j^n} + IL_{i-1}^{n+1} \frac{COREB^n}{EXCB^n} \quad (3.21)$$

where IL_i^{n+1} = the initial loading in i zone of the $n+1$ th cycle, in MWD/MTU; IL_1^n and IL_1^{n+1} are zero because fresh fuels are loaded into the first zone (the center zone) for each refueling;

B_i^n = the individual zone average burnup increment of the i zone in the n th cycle, in MWD/MTU;

$COREB^n$ = the actual core average burnup of the n th cycle with initial loadings IL_i^n , in MWD/MTU;

$EXCB^n$ = the expected equilibrium cycle core average burnup,

$$\frac{\sum_{j=1}^{NB} (IL_j^n + J \cdot B_j^n)}{(NB)^2},$$

this ratio will be derived later, and

NB = the number of burnup zones.

Equation (3.21) is used to calculate the initial loadings IL_i^{n+1} for the $n+1$ th cycle from the individual zone average burnup increments B_i^n of n th cycle obtained from equation (3.20). Factors used in equation (3.21), such as $\frac{COREB^n}{EXCB^n}$ and $\frac{IL_{NB}^n}{NB-1} \sum_{j=1}^{NB} B_j^n$ help to

accelerate the iteration toward an equilibrium discharge burnup.

These factors are discussed in the following paragraphs.

Assume the zone-average burnups of the initial loadings of the n th cycle are IL_i^n (where i is the zone number and $i=1$ stands

for the innermost zone and NB for the outermost zone; NB is 3, 6, or 9). With this set of initial loadings, the core can obtain a core average burnup COREB^n in this nth cycle, and the individual zone average burnup increments corresponding to this core average burnup COREB^n are B_i^n . If the initial loadings IL_i^n are too low (that is, the individual zone average burnups at the end of the n-1th cycle are too low, or the discharge burnup of the n-1th cycle is lower than the equilibrium discharge burnup DXB^e), the individual zone average burnup increments B_i^n will tend to increase and be larger than the equilibrium individual zone average burnup increments B_i^e . Therefore, the initial loadings IL_i^n have to be adjusted by the multiplication of factors to reduce the initial loadings of the n+1th cycle so that the individual zone average burnups of the n+1th cycle will approach the equilibrium values.

The factor $\frac{\text{IL}_{\text{NB}}^n}{\text{NB}-1 \sum_{j=1}^{\text{NB}} B_j^n}$ in equation (3.21) is actually the ratio of

the initial loading at the outermost zone of the current cycle to the initial loading at the outermost zone for the subsequent cycle if the NB-1 subsequent cycles have the individual zone average burnup increment of B_j^n . This ratio after multiplying by B_j^n will give the next cycle an initial loading of proper shape and magnitudes. Since B_j^n has the same distribution as the flux, it retains the shape information. The factor $\frac{\text{IL}_{\text{NB}}^n}{\text{NB}-1 \sum_{j=1}^{\text{NB}} B_j^n}$ makes an adjustment on the

magnitude of the initial loadings.

The factor $\frac{\text{COREB}^n}{\text{EXCB}^n}$, i.e.,

$$\frac{\text{COREB}^n}{\sum_{j=1}^{NB} (\text{IL}_j^n + j\text{B}_j^n) / (\text{NB})^2}$$

makes a further adjustment on the magnitude of the initial loadings IL_j^{n+1} . When the reactor is close to its equilibrium stage, the sum of the initial loadings IL_j and the individual zone average burnup increment B_j at each zone for cycles approaching the equilibrium cycle is nearly a constant (i.e., the burnup distributions along the core radius at the end of these cycles are approximately the same). Therefore, it is reasonable to assume that the relation

$$\sum_{j=1}^{NB} (\text{IL}_j^{n-1} + \text{B}_j^{n-1}) \approx \sum_{j=1}^{NB} (\text{IL}_j^n + \text{B}_j^n) \approx \sum_{j=1}^{NB} (\text{IL}_j^e + \text{B}_j^e)$$

is true. And so the ratio $\sum_{j=1}^{NB} (\text{IL}_j^n + j\text{B}_j^n) / (\text{NB})^2$ is nearly a constant for cycles approaching the equilibrium cycle.

For cycle n , a ratio designated as EXCB^n is called the expected core average burnup of cycle n because the value of this ratio is close to the equilibrium core average burnup COREB^e , which is the value the actual core average burnup COREB^n is expected to be if the cycle n is an equilibrium cycle. The expected core

average burnup is

$$EXCB^n = \frac{\sum_{j=1}^{NB} (IL_j^n + jB_j^n)}{(NB)^2} \quad (3.22)$$

In equilibrium condition, $EXCB^e = COREB^e$. This relation is derived as follows. For the equilibrium cycle,

$$\begin{aligned} IL_1^e &= 0. \\ IL_2^e &= \sum_{j=1}^1 B_j^e \\ IL_3^e &= \sum_{j=1}^2 B_j^e \\ IL_4^e &= \sum_{j=1}^3 B_j^e \\ IL_5^e &= \sum_{j=1}^4 B_j^e \\ &\vdots \\ &\vdots \\ &\vdots \\ &\vdots \\ IL_{NB}^e &= \sum_{j=1}^{NB-1} B_j^e \end{aligned}$$

The initial loading in zone 2 is the zone average incremental burnup in zone 1. The initial loading in zone 3 is the sum of the individual zone average incremental burnups in zone 1 and zone 2, and so on. Therefore,

$$\sum_{j=1}^{NB} IL_j^e = 0 + \sum_{j=1}^1 B_j^e + \sum_{j=1}^2 B_j^e + \sum_{j=1}^3 B_j^e + \sum_{j=1}^4 B_j^e + \dots + \sum_{j=1}^{NB-1} B_j^e$$

$$\begin{aligned}
&= (NB-1) \cdot B_1^e + (NB-2) \cdot B_2^e + \dots + 2B_{NB-2}^e + B_{NB-1}^e \\
&= NB \cdot B_1^e + NB \cdot B_2^e + \dots + NB \cdot B_{NB-1}^e + NB \cdot B_{NB}^e - \sum_{j=1}^{NB} j \cdot B_j^e \\
&= NB \cdot (B_1^e + B_2^e + \dots + B_{NB-1}^e + B_{NB}^e) - \sum_{j=1}^{NB} j \cdot B_j^e \\
&= NB \cdot NB \cdot COREB^e - \sum_{j=1}^{NB} j \cdot B_j^e
\end{aligned}$$

(Note: for a reactor of NB equi-volumetric zones,

$$COREB = \frac{\sum_{j=1}^{NB} B_j}{NB}.$$

After rearrangement,

$$COREB^e = \frac{\sum_{j=1}^{NB} (IL_j^e + j \cdot B_j^e)}{(NB)^2} \equiv EXCB^e \quad (3.23)$$

For cycles other than an equilibrium cycle, there is a corresponding expected core average burnup $EXCB$ as calculated by Equation (3.22). This $EXCB$ is helpful in accelerating the convergence of cycle toward equilibrium. The expected core average burnup of a cycle other than an equilibrium cycle is always closer to $COREB^e$ (or $EXCB^e$) than the actual core average burnup of the cycle. This statement is proved as follows.

For a reactor divided into NB equi-volumetric zones,

$$\text{COREB}^n = \frac{\sum_{i=1}^{NB} B_i^n}{NB}$$

$$\text{EXCB}^n = \frac{\sum_{i=1}^{NB} iL_i^n + B_i^n}{(NB)^2} \quad ; \quad \text{and}$$

$$\text{COREB}^e = \frac{\sum_{i=1}^{NB} B_i^e}{NB} = \text{EXCB}^e = \frac{\sum_{i=1}^{NB} iL_i^e + iB_i^e}{(NB)^e}$$

It then becomes obvious that

$$\begin{aligned} \text{EXCB}^n - \text{EXCB}^e &= \frac{\sum_{i=1}^{NB} \{iL_i^n - iL_i^e + i(B_i^n - B_i^e)\}}{(NB)^2} \\ &= \frac{\sum_{i=1}^{NB} (iL_i^n + B_i^n) - \sum_{i=1}^{NB} (iL_i^e + B_i^e) + \sum_{i=1}^{NB} (i-1)(B_i^n - B_i^e)}{(NB)^2} \\ &\approx \frac{\sum_{i=1}^{NB} i (B_i^n - B_i^e) - \sum_{i=1}^{NB} (B_i^n - B_i^e)}{(NB)^2} \end{aligned} \quad (3.24)$$

because $\sum_{i=1}^{NB} (iL_i^n + B_i^n) \approx \sum_{i=1}^{NB} (iL_i^e + B_i^e)$ for cycles close to equilibrium cycle, and also

$$\text{COREB}^n - \text{EXCB}^n = \text{COREB}^n - \text{EXCB}^n - \text{COREB}^e + \text{EXCB}^e$$

$$\begin{aligned}
&= \frac{NB \sum_{i=1}^{NB} B_i^n - (\sum_{i=1}^{NB} IL_i^n + iB_i^n) - NB \sum_{i=1}^{NB} B_i^e + (\sum_{i=1}^{NB} IL_i^e + iB_i^e)}{(NB)^2} \\
&= \frac{NB \sum_{i=1}^{NB} (NB-i+1)(B_i^n - B_i^e) + \sum_{i=1}^{NB} (IL_i^e + B_i^e) - \sum_{i=1}^{NB} (IL_i^n + B_i^n)}{(NB)^2} \\
&= \frac{NB \sum_{i=1}^{NB} (NB-i+1)(B_i^n - B_i^e)}{(NB)^2} \tag{3.25}
\end{aligned}$$

For cycles with $\sum_{i=1}^{NB} B_i^n > \sum_{i=1}^{NB} B_i^e$, the right sides of equations (3.24) and (3.25) are all positive, therefore $COREB^n > EXCB^n > EXCB^e$. For cycles with $\sum_{i=1}^{NB} B_i^n < \sum_{i=1}^{NB} B_i^e$, the right sides of equations (3.24) and (3.25) are negative, therefore $COREB^n < EXCB^n < EXCB^e$. As a result, the ratio of the actual core average burnup $COREB^n$ to $EXCB^n$, indicates whether the actual core average burnup $COREB^n$ is higher or lower than the equilibrium core average burnup, depending on whether $COREB^n/EXCB^n$ is larger or smaller than 1. By multiplying this ratio into IL^{n+1} , IL^{n+1} will become much closer to its equilibrium value.

Equation (3.21) was used to accelerate the convergence, and was found effective.

3.7 Extension of the Cycle Length by Coastdown Operation

Once the reactor reaches the end of its cycle at 100 percent

power operation, the reactor can still be kept critical by gradually reducing the power level. This type of operation is called normal coastdown operation. Coastdown operation is possible because light water reactors are designed to have a negative power coefficient for safety reasons. The largest contributor to the negative power coefficient is the negative coolant temperature coefficient. When power decreases, the coolant temperature decreases and so the reactivity of the reactor increases because of the negative coolant temperature coefficient. Further decreasing the coolant temperature by cutting off some of the feedwater heaters can extend the cycle length even further.

The resonance escape probability P_r in the multiplication factor k_∞ ($k_\infty = \eta f P_r \epsilon$) is the factor primarily responsible for being able to extend the cycle length by changing the coolant temperature. P_r in LEOPARD code is defined as:

$$P_r \equiv \frac{\Sigma_{rem}}{\Sigma_{rem} + \Sigma_a} , \quad (3.26)$$

where Σ_{rem} is the macroscopic neutron removal cross-section from fast group to thermal group; Σ_a is the macroscopic neutron absorption cross-section in the fast group.

After differentiating both sides of the equation,

(Note: $d\Sigma_a$ is ignored because Σ_a would not change much due to coolant temperature change.)

$$\begin{aligned}
 dP_r &= \frac{(1-P_r)}{\Sigma_{rem} + \Sigma_a} d\Sigma_{rem} \\
 &= \frac{(1-P_r)\Sigma_{rem}}{\Sigma_{rem} + \Sigma_a} \frac{d\Sigma_{rem}}{\Sigma_{rem}} \\
 &= P_r (1-P_r) \frac{d\rho}{\rho} \quad (3.27)
 \end{aligned}$$

where

$$\frac{d\rho}{\rho} = -\alpha \Delta T$$

α = the volume expansion coefficient of water, and

ρ = water density.

In a typical pressurized light water reactor, when the reactor is coasted down from 100 percent to 90 percent, 80 percent, 70 percent, and 60 percent power, the corresponding core coolant temperature changes from 586°F to 573.5°F, 561°F, 548.5°F, and 536°F, correspondingly (12).

The resonance escape probability P_r for each power level is then

$$P_{r1} = P_{r0} + \Delta P_{r1} = -P_{r0} (1-P_{r0}) \cdot \alpha \cdot (573.5 - 586)$$

$$P_{r2} = P_{r0} + \Delta P_{r2} = -P_{r0} (1-P_{r0}) \cdot \alpha \cdot (561 - 586)$$

$$P_{r_3} = P_{r_0} + \Delta P_{r_3} = -P_{r_0} (1 - P_{r_0}) \cdot \alpha \cdot (548.5 - 586)$$

$$P_{r_4} = P_{r_0} + \Delta P_{r_4} = -P_{r_0} (1 - P_{r_0}) \cdot \alpha \cdot (536 - 586). \quad (3.28)$$

where

$$\alpha = 0.001666/^{\circ}\text{F} ,$$

the volume expansion coefficient of water for temperatures between 586°F and 536°F under the reactor pressure of 2200 psia.

Simulation of the coastdown operation of the reactor can be made by changing the P_r value in the group constants. It has been carried out only in a one-dimension, two-group calculation.

The equilibrium cycle discharge burnup for the coastdown operation can also be obtained in the same way as described in Section (3.6), except that for coastdown operation the end of cycle is extended to 60 percent power level.

4. TWO-DIMENSION TWO-GROUP MODEL

In one-dimension calculations, the axial length of the reactor is assumed infinite; therefore, there is no axial leakage of neutrons. Because of this, one-dimension calculations will overestimate the reactivity life time of the core and the burnup level of the fuel bundles. Therefore, it is necessary to take into account the axial migration of the neutrons in order to obtain an accurate determination of the burnup level of the fuel bundles that a strict in-out refueling scheme can reach. The axial dependence of the neutron flux is evaluated by the "synthesis method" which is described in Sections (4.1), (4.2), and (4.3).

4.1 Description of the algorithm

Because in most cases the flux in a cylindrical reactor is approximately azimuthally symmetrical, the flux can be adequately represented by the r-radial and z-axial components. A three-dimensional problem is therefore simplified to a two-dimensional one. Even in the two-dimensional case, a pure diffusion calculation is rather involved and would consume a great deal of computer time. A method called "spatial synthesis" is used to avoid these difficulties. For illustrative purposes, we may use the sketch of the reactor given in Figure (3.1).

In spatial synthesis, the flux is represented as a linear combination of the products of radial trial functions $T_i(r)$ and axial flux-dependence functions $f_i(z)$, assuming that the r-radial and the z-axial components of the flux are separable. We have used three such products, thus:

$$\phi^1(r,z) = \sum_{i=1}^3 T_{i1}(r) \cdot f_i(z) \quad (4.1)$$

and

$$\phi^2(r,z) = \sum_{i=1}^3 T_{i2}(r) \cdot f_i(z) \quad (4.2)$$

where

$\phi^1(r,z)$ and $\phi^2(r,z)$ = the fast and thermal fluxes
at location (r,z) , respectively;

$T_{i1}(r)$ and $T_{i2}(r)$ = the trial functions for the fast
and thermal fluxes, respectively,
at radial location r ;

i = the index of the trial function
used (3 is chosen for both fast
and thermal fluxes in this paper);

$f_i(z)$ = the i th z -component of the flux at
axial location z , which is the
same for both the fast and thermal fluxes.

The trial functions used in the two-dimension calculations are the fluxes obtained in the one-dimension calculations. They are the fast and thermal fluxes in the one-dimension model (1) at the beginning of cycle with the core slightly supercritical, (2) at the beginning of cycle with the core critical, and (3) at the end of cycle with the core critical.

According to two-group diffusion theory, the governing equation of neutrons is,

$$H\phi = 0, \quad (4.3)$$

where,

$$H = \begin{vmatrix} D_1 \nabla^2 - \Sigma_{a1} + \frac{1}{k} \nu_1 \Sigma_{f1} & \frac{1}{k} \nu_2 \Sigma_{f2} \\ P \Sigma_{ra1} & D_2 \nabla^2 - \Sigma_{a2} \end{vmatrix}$$

$$\phi = \begin{vmatrix} \phi^1 \\ \phi^2 \end{vmatrix}.$$

Since ϕ is synthesized as

$$\phi = \sum_{i=1}^3 \bar{T}_i(r) f_i(z) \quad (4.4)$$

and

$$\bar{T}_i = \begin{vmatrix} T_{i1} \\ T_{i2} \end{vmatrix} ,$$

Equation (4.3) becomes for our case

$$\sum_{i=1}^3 H \bar{T}_i f_i = 0 \quad (4.5)$$

After multiplying the Equation (4.5) by the radially adjoint flux \bar{T}_i^+ of each trial function \bar{T}_i , i.e., \bar{T}_1^+ , \bar{T}_2^+ , and \bar{T}_3^+ , individually, and integrating over the reactor cross-sectional area, the following set of equations can be obtained.

$$\langle \bar{T}_1^+ \sum_{i=1}^3 H \bar{T}_i f_i \rangle_{rdr} = 0 \quad (4.6.1)$$

$$\langle \bar{T}_2^+ \sum_{i=1}^3 H \bar{T}_i f_i \rangle_{rdr} = 0 \quad (4.6.2)$$

$$\langle \bar{T}_3^+ \sum_{i=1}^3 H \bar{T}_i f_i \rangle_{rdr} = 0 \quad (4.6.3)$$

where

$$\bar{T}_j^+ = \begin{vmatrix} T_{j1}^+ & T_{j2}^+ \end{vmatrix} , \text{ and } \langle \rangle_{rdr} \text{ is a symbol meaning}$$

integration over the reactor cross-sectional area.

Thus, for example, take Equation (4.6.1) for derivation.

$$\langle \bar{T}_1^+ \sum_{i=1}^3 H \bar{T}_i f_i \rangle_{rdr} = 0.$$

After expansion,

$$\langle \bar{T}_1^+ H \bar{T}_1 f_1 \rangle_{rdr} + \langle \bar{T}_1^+ H \bar{T}_2 f_2 \rangle_{rdr} + \langle \bar{T}_1^+ H \bar{T}_3 f_3 \rangle_{rdr} = 0 \quad (4.7)$$

Since H in cylindrical coordinates for a right cylindrical reactor is

$$\left[\begin{array}{cc} \frac{D_1}{r} \frac{d}{dr} r \frac{d}{dr} + D_1 \frac{d^2}{dz^2} - \Sigma_{a1} + \frac{1}{k} \nu_1 \Sigma_{f1} & \frac{1}{k} \nu_2 \Sigma_{f2} \\ P_r \Sigma_{a1} & \frac{D_2}{r} \frac{d}{dr} r \frac{d}{dr} + D_2 \frac{d^2}{dz^2} - \Sigma_{a2} \end{array} \right],$$

then further expansion of the first term of Equation (4.7) will lead to the following result:

$$\begin{aligned} \langle \bar{T}_1^+ H \bar{T}_1 f_1 \rangle_{rdr} &= D_1 f_1'' \langle \bar{T}_{11}^+ T_{11} \rangle_{rdr} + D_1 f_1 \langle \bar{T}_{11}^+ \frac{1}{r} \frac{d}{dr} r \frac{d}{dr} T_{11} \rangle_{rdr} \\ &- f_1 \langle \bar{T}_{11}^+ \Sigma_{a1} T_{11} \rangle_{rdr} + f_1 \langle \bar{T}_{11}^+ \frac{\nu_1 \Sigma_{f1}}{k} T_{11} \rangle_{rdr} \\ &+ f_1 \langle \bar{T}_{11}^+ \frac{\nu_2 \Sigma_{f2}}{k} T_{12} \rangle_{rdr} + f_1 \langle \bar{T}_{12}^+ P_r \Sigma_{a1} T_{11} \rangle_{rdr} \\ &+ D_2 f_1'' \langle \bar{T}_{12}^+ T_{12} \rangle_{rdr} + D_2 f_1 \langle \bar{T}_{12}^+ \frac{1}{r} \frac{d}{dr} r \frac{d}{dr} T_{12} \rangle_{rdr} \end{aligned}$$

$$- f_1 \langle T_{12}^+ \sum_{a_2} T_{12} \rangle_{rdr} = 0 . \quad (4.8)$$

By doing the same for the second and the third term of the Equation (4.7), Equation (4.7) becomes

$$\begin{aligned} A_{11} f_1'' + A_{12} f_2'' + A_{13} f_3'' + \frac{\alpha_{11}}{k} f_1 + \frac{\alpha_{12}}{k} f_2 \\ + \frac{\alpha_{13}}{k} f_3 + \beta_{11} f_1 + \beta_{12} f_2 + \beta_{13} f_3 = 0 , \end{aligned} \quad (4.9)$$

where the A's, α 's, and β 's are defined below. A general expression for the Equations (4.6.1), (4.6.2), and (4.6.3) can then be obtained as

$$\begin{aligned} \langle T_j^+ \sum_{i=1}^3 T_{ji} f_i \rangle_{rdr} = \sum_{i=1}^3 (A_{ji} f_i'' + \frac{\alpha_{ji}}{k} f_i + \beta_{ji} f_i) = 0 \\ (j = 1, 2, 3) . \end{aligned} \quad (4.10)$$

where

$$A_{ji} = D_1 \langle T_{j1}^+ T_{i1} \rangle_{rdr} + D_2 \langle T_{j2}^+ T_{i2} \rangle_{rdr} \quad (4.11.1)$$

$$\alpha_{ji} = \langle T_{j1}^+ v_1 \sum_{f_1} T_{i1} \rangle_{rdr} + \langle T_{j2}^+ v_2 \sum_{f_2} T_{i2} \rangle_{rdr} \quad (4.11.2)$$

$$\beta_{ji} = D_1 \langle T_{j1}^+ \frac{1}{r} \frac{d}{dr} r \frac{d}{dr} T_{i1} \rangle_{rdr}$$

$$\begin{aligned}
& + D_2 \langle T_{j_2}^+ \frac{1}{r} \frac{d}{dr} r \frac{d}{dr} T_{i_2} \rangle_{rdr} \\
& + \langle T_{j_1}^+ P_r \Sigma_{a_1} T_{i_1} \rangle_{rdr} \\
& - \langle T_{j_1}^+ \Sigma_{a_1} T_{i_1} \rangle_{rdr} \\
& - \langle T_{j_2}^+ \Sigma_{a_2} T_{i_2} \rangle_{rdr}
\end{aligned} \tag{4.11.3}$$

The finite difference form of Equation (4.10) is

$$\begin{aligned}
& \sum_{i=1}^3 A_{ji} \frac{f_i(z-hz) - 2f_i(z) + f_i(z+hz)}{(\Delta z)^2} + \frac{\alpha_{ji}}{k} f_i(z) \\
& + \beta_{ji} f_i(z) = 0, \quad (j = 1, 2, 3)
\end{aligned} \tag{4.12}$$

with $\Delta z = hz$, the distance between mesh points in the z -direction.

It is an eigenvalue equation, with only one independent variable z .

4.2 Boundary Conditions

Because of the symmetry of the flux about the mid-plane of the core and the vanishing of the flux at the top and the bottom of the core, the following boundary conditions should be met by the solutions to Equation (4.12).

The boundary conditions are, at the midplane,

$$\begin{aligned}
 f_1(+hz) &= f_1(-hz) \\
 f_2(+hz) &= f_2(-hz) \\
 f_3(+hz) &= f_3(-hz)
 \end{aligned}
 \tag{4.13}$$

and, at the end of the core,

$$\begin{aligned}
 f_1\left(\frac{H}{2} + \lambda_{\text{ext}}\right) &= 0 \\
 f_2\left(\frac{H}{2} + \lambda_{\text{ext}}\right) &= 0 \\
 f_3\left(\frac{H}{2} + \lambda_{\text{ext}}\right) &= 0
 \end{aligned}
 \tag{4.14}$$

where λ_{ext} = the extrapolation distance; it is chosen as one uniform distance hz between mesh points for the convenience of calculation, and

H = the height of the reactor.

For a large reactor, small deviations in the extrapolation distance will not affect the reactor behavior. In this paper, the number of mesh points is chosen so that the hz value is 9 cm, approximately the upper and lower reflector savings of LWR's.

4.3 The Criticality Calculation

Because of the symmetry of the flux about the midplane, the

critical fluxes for only half of the core will be solved.

To accelerate the iteration, the successive overrelaxation method is employed in solving $f_1(z)$, $f_2(z)$ and $f_3(z)$. The following steps are used to calculate the critical fluxes.

Step (1)

The governing Equation (4.12), when actually used in iteration, is written in matrix form.

$$\begin{vmatrix} 2A_{11} - (\Delta z)^2 \left(\frac{\alpha_{11}}{k} + \beta_{11} \right) & 2A_{12} - (\Delta z)^2 \left(\frac{\alpha_{12}}{k} + \beta_{12} \right) & 2A_{13} - (\Delta z)^2 \left(\frac{\alpha_{13}}{k} + \beta_{13} \right) \\ 2A_{21} - (\Delta z)^2 \left(\frac{\alpha_{21}}{k} + \beta_{21} \right) & 2A_{22} - (\Delta z)^2 \left(\frac{\alpha_{22}}{k} + \beta_{22} \right) & 2A_{23} - (\Delta z)^2 \left(\frac{\alpha_{23}}{k} + \beta_{23} \right) \\ 2A_{31} - (\Delta z)^2 \left(\frac{\alpha_{31}}{k} + \beta_{31} \right) & 2A_{32} - (\Delta z)^2 \left(\frac{\alpha_{32}}{k} + \beta_{32} \right) & 2A_{33} - (\Delta z)^2 \left(\frac{\alpha_{33}}{k} + \beta_{33} \right) \end{vmatrix} \cdot \begin{vmatrix} f_1(z) \\ f_2(z) \\ f_3(z) \end{vmatrix} =$$

$$\begin{aligned}
 & A_{11} [f_1(z - hz) + f_1(z + hz)] \\
 & + A_{12} [f_2(z - hz) + f_2(z + hz)] \\
 & + A_{13} [f_3(z - hz) + f_3(z + hz)] \\
 \\
 & A_{21} [f_1(z - hz) + f_1(z + hz)] \\
 & + A_{22} [f_2(z - hz) + f_2(z + hz)] \\
 & + A_{23} [f_3(z - hz) + f_3(z + hz)] \\
 \\
 & A_{31} [f_1(z - hz) + f_1(z + hz)] \\
 & + A_{32} [f_2(z - hz) + f_2(z + hz)] \\
 & + A_{33} [f_3(z - hz) + f_3(z + hz)]
 \end{aligned}$$

(4.15)

Equation (4.15), in a successive displacement iterative form, can be simplified and written as

$$\bar{L} f_i^{m+1}(z) = \bar{R} \left[f_i^{m+1}(z - hz) + f_i^m(z + hz) \right] \quad (i = 1, 2, 3) \quad (4.16)$$

where \bar{L} = the left-hand side operator of equation (4.15)

\bar{R} = the right-hand side operator of equation (4.15)

$m, m+1$ = the successive m , and $m+1$ iterations.

Step (2)

To begin the iteration of Equation (4.16), the initial guesses of

$f_1^0(z) = f_2^0(z) = f_3^0(z) = 1$ and the eigenvalue $k = 1$ are used.

The right-hand sides of Equation (4.16) become known values if we utilize the boundary conditions of $f(z)$'s, as described next.

Step (3)

The iteration begins from the midplane of the reactor toward the top of the reactor. Because of the boundary condition Equation (4.13), the right-hand side of Equation (4.16) can be known if we set the first term equal to the second term which is known from previous iterations. Iteration can go on toward the edge of the core and meet the boundary condition (4.14). A standard computer library subroutine LEQTIF (16) is used in solving Equation (4.15).

Step (4)

Once $f_i^{m+1}(z)$ at any z is obtained, $f_i^{m+1}(z)$ is overrelaxed by the relation

$$f_i^{m+1'}(z) = f_i^m(z) + \text{FRX1} \cdot (f_i^{m+1}(z) - f_i^m(z)),$$

where FRX1 is an overrelaxation factor.

At the next spatial point, $f^{m+1'}(z)$ is immediately used for solving $f(z)$. In this work, $\text{FRX1}=1.3$ was employed except for the very first two inner iterations for which $\text{FRX1}=1$ was used.

Step (5)

When one pass of an inner iteration is completed, a new eigenvalue

is calculated

$$k^{m+1} = \frac{\int \nu \Sigma_f \phi_{m+1} dv}{\int \nu \Sigma_f \phi_m dv} k^m ,$$

where ϕ_{m+1} is the flux obtained from $f^{m+1}(z)$ according to Equation (4.4) and ϕ_m from f^m .

Instead of k^{m+1} , a relaxed $k^{m+1'} = \frac{1}{2}(k^{m+1} + k^m)$ is used for the next outer iteration. This relaxed $k^{m+1'}$ helps converge the iteration and avoid instability in $f(z)$ that might happen if k^{m+1} is far from the correct k .

Step (6)

The flux is considered converged if the criteria

$$\frac{\int \phi_{m+1} dv - \int \phi_m dv}{\int \phi_m dv} < 10^{-4} \quad \text{is met.}$$

Step (7)

The core is burned under the converged flux for a burnup step. After this burnup step, another new converged flux under the new core condition is calculated and the core is burned again. This process will go on until the end of the cycle is reached. The burnup algorithm is the same as exhibited in Section 3.4 of the 1-D calculation. Several burnup steps are needed to reach the end of the cycle. The finer the burnup step size, the more accurate the burnup calculation. In our 2-D calculation, the first burnup step is taken as 2000 MWD/MTU,

followed by smaller burnup step sizes. By this means, reasonably accurate results can be obtained at moderate computer cost. The end of cycle occurs when the converged k falls between 1.0002 and .9998.

4.4 Individual Element Burnup and Bundle Average Burnup

As in the one-dimension burnup calculation in Section 3.4, once the critical fluxes are obtained, the element and zone (or bundle) average burnup corresponding to a core average burnup step size of BUC MWD/MTU can be calculated as follows:

1. The element burnup $B(I,Z)$

If we define, $E(I,Z)$ = a fraction of fuel bundle I at axial location Z , as shown in Figure 3.1.
It is called the fuel element $E(I,Z)$;

$T(I,Z)$ = the uranium weight of fuel element $E(I,Z)$, in tonnes;

$P(I,Z)$ = the power generation rate in fuel element $E(I,Z)$;
in MWt;

$V(I,Z)$ = the volume occupied by fuel element $E(I,Z)$, in cm^3 ;

V = the total reactor volume, in cm^3 ;

P = the total reactor power generation rate, in MWt;

- T = the total uranium weight in core, in tonnes;
- h_z = the distance between mesh points in Z direction, in cm and
- NZZ = the number of divisions in Z direction for half the core height.

Then, the element burnup $B(I,Z)$ of the element $E(I,Z)$ corresponding to a power generation period D (or the equivalent core average burnup step BUC) is

$$B(I,Z) = \frac{P(I,Z) \cdot D}{T(I,Z)} \quad (4.17)$$

Since $D = \frac{BUC}{P} \cdot T$ and $T(I,Z) = \frac{V(I,Z)}{V} \cdot T$, equation (4.16) becomes

$$B(I,Z) = \frac{P(I,Z) \cdot BUC \cdot V}{P \cdot V(I,Z)} \quad (4.18)$$

Equation (4.18) is the one used to calculate the element burnup $B(I,Z)$.

2. The zone (or bundle) average burnup ZBU(I)

The zone average burnup $ZBU(I)$ is simply the average of the element burnup $B(I,Z)$ in Zone I.

$$ZBU(I) = \frac{\sum_{Z=1}^{NZZ} B(I,Z)}{NZZ} \quad \text{MWD/MTU} \quad (4.19)$$

By repeating the burnup calculations several times the reactor will reach to its end of cycle. If the cycle just run is not an equilibrium one, another cycle with new initial loadings of the core will follow. The processes in reaching an equilibrium cycle are next.

4.5 Equilibrium Cycle Discharge Burnup

In reality, an equilibrium cycle in which the core average burnup and the discharge element burnups remain constant for each cycle is very difficult to reach, because power generation manipulations, required to meet the power demand, are hardly the same from cycle to cycle. The outcome of the manipulations in the previous cycle affects the behavior of the reactor in the following cycle, thus making the cycles different from each other. Therefore, an equilibrium cycle is only a theoretical state of reactor operations. To simplify the problem, no core manipulation is employed, and all cycles are to have identical energy demands. Even after ignoring all the power generation manipulations, searching for an equilibrium cycle has different methods from the ones used in the one-dimension case. Basically, they are averaging operations which make use of relationships inherent in the equilibrium cycle between the initial loadings and individual bundle incremental burnups. These procedures are divided into four steps.

Step (1)

First, we define $IL^n(I,Z)$ = the burnup of the fuel element $E(I,Z)$

at the beginning of cycle n , it is called the initial loading of the core of cycle n , in MWD/MTU;

$B^n(I,Z)$ = the total burnup increment of element $E(I,Z)$ during cycle n , in MWD/MTU;

$IL^e(I,Z)$ = the initial loading of core for an equilibrium cycle, in MWD/MTU, and

$B^e(I,Z)$ = the total burnup increment of element $E(I,Z)$ for an equilibrium cycle, in MWD/MTU.

In searching for an equilibrium cycle, we begin from the first cycle with an initial loading of $IL^1(I,Z)$ for each fuel element $E(I,Z)$.

Burn the core until the end of the cycle. As a result of the power generation in the cycle, each element $E(I,Z)$ gains an incremental burnup of $B^1(I,Z)$ corresponding to the power generated in the cycle. The superscript 1 denotes the first cycle.

Step (2)

An initial loading $IL^1(I,Z)$ higher or lower than the equilibrium cycle value $IL^e(I,Z)$ will lead to an incremental element burnup $B^1(I,Z)$ lower or higher than the incremental element burnup $B^e(I,Z)$ of the equilibrium cycle. Because the values of $B^1(I,Z)$ for the first zone of the first cycle are the initial loadings for the second zone of the second cycle in the in-out refueling scheme (and

$B^1(2,Z) + IL^1(2,Z)$ are the initial loadings for the third zone of the second cycle, and so on), a poor guess of the initial loadings $IL(I,Z)$ will make the reactor cycle lengths for the following cycles swing above and below the equilibrium cycle length. Thus, it will be difficult to converge to the equilibrium cycle. In order to avoid the swing and speed up the convergence, some deliberate modifications on the initial loadings of the next cycle must be made based on information from the previous cycle. Taking the second cycle as an example, the average of $IL^1(2,Z)$ and $B^1(1,Z)$ of the first cycle instead of only $B^1(1,Z)$ is adopted as the initial loading for the second zone of the second cycle.

Step (3)

The initial loading of the third zone is taken as the sum of $IL^1(2,Z)$ and $\frac{1}{2}(IL^1(2,Z) + B^1(1,Z)) \times B^1(2,Z)$. The same averaging operations are applied to all other zones for initial loadings. That is

$$IL^2(2,Z) = IL^1(1,Z) + \frac{1}{2}(IL^1(2,Z) + B^1(1,Z)) \times B^1(2,Z)$$

$$IL^2(3,Z) = IL^2(2,Z) + \frac{1}{2}(IL^1(2,Z) + B^1(1,Z)) \times B^1(3,Z)$$

$$IL^2(4,Z) = IL^2(3,Z) + \frac{1}{2}(IL^1(2,Z) + B^1(1,Z)) \times B^1(4,Z)$$

$$IL^2(NB,Z) = IL^2(NB-1,Z) + \frac{1}{2}(IL^1(2,Z) + B^1(1,Z)) \times B^1(NB,Z)$$

where NB = the number of zones; and

$IL^n(1,Z) = 0$ for every cycle $n = 1, 2, 3, \dots$ because fresh fuels are loaded into the first zone for every cycle.

Step (4)

With the new initial loadings obtained from Step (2) and Step (3), another power generation cycle is run.

Step (5)

Continue repeating steps (2), (3) and (4) until the conditions of the equilibrium cycle are reached, i.e., until

$$IL^{n+1}(I,Z) = IL^n(I,Z) \text{ and}$$

$$B^{n+1}(I,Z) = B^n(I,Z).$$

In this study, a less restricted condition,

$$\sum_{I=1}^{NB} \sum_{Z=1}^{NZZ} (IL^{n+1}(I,Z) + B^{n+1}(I,Z) - IL^n(I,Z) - B^n(I,Z)) < 5000$$

MWD/MTU is used.

The burnups of the outermost elements ($B(NB,Z), Z=1, NZZ$) are the equilibrium cycle discharge burnups.

5. CASE STUDIES AND DISCUSSION

Cases concerning the effects on the equilibrium discharge burnup, of the way of flux peaking control, the lattice design, enrichment, coastdown operation, and the batch size of replacement fuel are under study in this paper.

Reactors employed for these studies are reactors of Oconee and Trojan size. By this, we mean that we did not really study the Oconee and Trojan reactors, rather we used some of the characteristics of these reactors to define parameters of very idealized reactors for study. For this reason, "Oconee" and "Trojan" as used to describe calculations done here are just shorthand for referring to these idealized reactors. Likewise, the fuels designated here as "Oconee fuel" or "Trojan fuel" are also idealized fuels with fuel pins of the same size either as actual Oconee fuel pins or as Trojan fuel pins, rather than actual Oconee fuel or Trojan fuel. As a matter of fact, the Trojan fuels under study here have a more pessimistic set of group constants than what we expected the actual Trojan fuel should have, even though both have the same fuel pin size. (See Section (2.1) Confusions with the real reactor cases should be avoided. The basic parameters of these idealized reactors are summarized in Table (5.1).

5.1 Effect of Flux Peaking Control

As discussed before, the in-out refueling scheme has a higher

Table 5.1. Basic data for Oconee and Trojan reactors.

	Oconee	Enlarged Oconee	Trojan
Reactor Radius, cm	163.5	200	170
Reactor Height, cm	366	366	365
Power, MWT	2568	3842	3411

Note: In this work, when a reactor is loaded with fuels of different lattice design, the core does not necessarily contain an integral number of fuel assemblies. Actually, the core, within its radius is fully occupied by fuel rods with rod dimensions and pitch as specified for a particular lattice. Therefore, the amount of uranium loaded into the core depends on the number of fuel rods in the reactor volume. The reactor is then divided into zones of equi-volume for study. Zone dimensions are in Table 5.3.

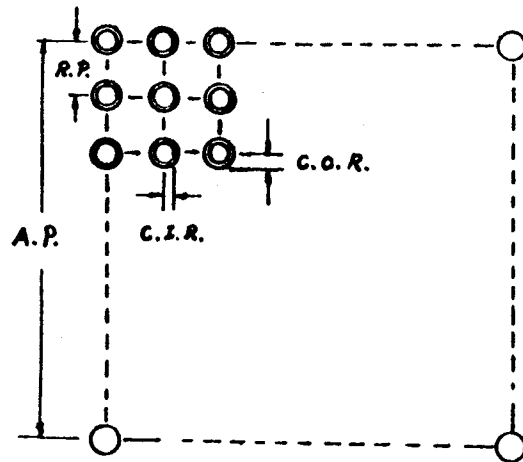
peaking factor than conventional refueling schemes because fresh fuels are intentionally loaded into regions of higher flux in the in-out refueling scheme, and so flux peaking is exacerbated. Nevertheless, it is always desirable to avoid a flux with too high a peaking factor. One way to avoid peaking is to derate the reactor system, but it is a costly way, for it will reduce the capacity of the system and damage the system economics. An alternate way to reduce the peaking problem without derating the system is to confine the control poison, boron, only to the central zone, where the peaking usually occurs. Therefore, the reactor is studied under two different kinds of control, i.e., whole core control and central zone control.

5.2 Effect of Bundle Lattice Design and Enrichment

In addition to the type of control used, fuel bundle lattice design and enrichment have long been known to be very important factors in safety and fuel economics. In order to see how fuels with different lattice design and different enrichment will function in the in-out refueling scheme, Trojan fuels of three lattice designs and two enrichments, i.e., 15x15 with 3% enrichment, 17x17 with 2% enrichment, 17x17 with 3% enrichment and 18x18 with 3% enrichment, and Oconee fuels of 15x15 with 3% enrichment are studied in this paper. Bundle design data and the sketches of these fuels are shown in Table (5.2) and Figure (5.1), respectively.

Table 5.2. Design data of Trojan, Oconee and standard Westinghouse fuels.

	Standard PWR 17x17	Trojan 15x15	Trojan 17x17	Trojan 17x17	Trojan 18x18	Oconee 15x15
Cold Pallet O.R. cm	.4095	.4095	.4095	.4095	.4095	.47
Clad I.R cm	.4178	.4100	.4100	.4100	.4100	.4788
Clad O.R cm	.4749	.4749	.4749	.4749	.4749	.5461
Cold Pitch cm	1.26	1.43	1.26	1.26	1.19	1.45
Power Density W/cm ³	105.7	102	102	102	102	83,382
Resonance temp °F.	1550	1500	1500	1500	1500	1540
Pellet temp °F.	1350	1500	1500	1500	1500	1500
Clad temp °F.	640	650	650	650	650	630
Moderator temp °F.	590	580	580	580	580	579.3
Moderator Pressure Psia	2250	2220	2220	2220	2220	2200
Assembly Pitch cm	21.5	21.5	21.5	21.5	21.5	21.8
Enrichment %	3%	3%	2%	3%	3%	3%



Abbr.	Full Name
C. I. R	Cladding Inside Radius
C. O. R	Cladding Outside Radius
R. P.	Rod Pitch
A. P.	Assembly Pitch

NOTE: In this study, the 15x15 fuel bundle has 225 fuel rods, the 17x17 fuel has 289 rods and the 18x18 fuel has 324 fuel rods. In actual fuel design, because some control rod thimbles are included, less fuel rods are in the fuel bundle. The actual 15x15 fuel bundle has 208 rods, the 17x17 fuel has 264 rods. No actual 18x18 fuel has ever been designed.

FIGURE 5.1 Sketch of the fuel bundle and its parameters.

5.3 Effect of Batch Size

Most current light water reactors have a one-year refueling period, based on the same period of seasonal power demand. For reasons of system maintenance and fuel economics, refueling schemes of different periods, such as 18 months or six months (17) have been investigated by the nuclear industry. It is the number of fuel batches (or zones) employed for refueling that has the major bearing on the length of the cycle period. In view of this, cases of 3, 6 and 9 zone cycles are analyzed for both Trojan and Oconee fuel. However, in order to see how much gain in discharge burnup the in-out refueling can have for different batch size when compared to an out-in refueling scheme, cases of 3, 6 and 9 zone cycles in out-in refueling scheme are also studied, but only for Oconee fuel. An out-in refueling scheme under this study is defined to be one such that, when refueling is required, the fuel bundles in the innermost zone are discharged, the fuels in the outer zones are moved inward in a sequential fashion and the fresh fuels are loaded into the outermost zone. It is a process just opposite to the in-out refueling scheme. Although the out-in refueling scheme just defined is not exactly the same as the standard out-in refueling scheme (in which new fuel is added to the outside but all other fuels are in general shuffled and scattered so that no distinctive zones can be identified,) these two out-in refueling schemes will not be very much different as far as discharge burnup is concerned.

This is particularly the case for our burnup calculations, in which the burnup of fuels in each zone are homogenized over the zone; the homogenization of zone burnup has somewhat the same effect as scattering the fuels throughout the inner zones.

Zone dimensions of reactors are shown in Table (5.3).

5.4 Effect of Coastdown Operation

Coastdown is a strategy very commonly used to meet seasonal power demands when unexpected shutdowns of the reactor force the end of normal cycle to coincide with a period of higher power demand and when, therefore, a reactor shut-down for refueling is inappropriate to maintaining the reliability of the power supply. Here, because only a general understanding of the effect of the coastdown operation is needed, the coastdown operation is surveyed only in one-dimension 9-zone and 6-zone in-out cases for Oconee fuel.

5.5 Effect of Reactor Size on Fuel Discharge Burnup

Reactors of two different sizes, Oconee size and enlarged Oconee size, loaded with same type of Oconee fuel were also studied to see the effect of reactor size on fuel discharge burnup in in-out refueling scheme. Basic data of these reactors are shown in Table (5.1). Tables (5.4), (5.5) and (5.6) are the summary of the cases under study.

Table 5.3. Zone dimension of reactor.

Zone number		1	2	3	4	5	6	7	8	9
OCONEE REACTOR	3 zone cycle	94.4	133.5	163.5						
	6 zone cycle	66.7	94.4	115.6	133.5	149.3	163.5			
	9 zone cycle	54.5	77.1	94.4	109.0	121.8	133.5	144.2	154.1	163.5
ENLARGED OCONEE REACTOR	3 zone cycle	115.5	163.3	200.0						
	6 zone cycle	81.6	115.5	141.4	163.3	182.6	200.0			
	9 zone cycle	66.7	94.3	115.5	133.3	149.1	163.3	176.4	188.5	200.0
TROJAN REACTOR	3 zone cycle	98.1	138.8	170.0						
	6 zone cycle	73.5	98.1	120.2	138.8	155.2	170.0			
	9 zone cycle	56.6	80.1	98.1	113.3	126.7	138.8	149.9	160.3	170.0

Note: The value is the outside radius of each zone in cm.

Table 5.4 Summary of case studies for Trojan type fuel in 1-D calculations for in-out refueling scheme.

	9 Zone	6 Zone	3 Zone
	Normal	Normal	Normal
15x15 3%	Whole Core	Whole Core	Whole Core
	Central Zone	Central Zone	
17x17 2%	Whole Core	Whole Core	Whole Core
	Central Zone	Central Zone	
17x17 3%	Whole Core	Whole Core	Whole Core
	Central Zone	Central Zone	
18x18 3%	Whole Core	Whole Core	Whole Core
	Central Zone	Central Zone	

Table 5.5 Summary of case studies for Oconee type fuel in both 1-D and 2-D calculations for in-out refueling scheme.

	9 Zone	6 Zone	3 Zone
OCONEE REACTOR SIZE	<ul style="list-style-type: none"> a. Whole core controlled in both 1-D and 2-D b. Central zone controlled in 1-D only c. Coastdown operation 	<ul style="list-style-type: none"> a. Whole core controlled in both 1-D and 2-D b. Central zone controlled in 1-D only c. Coastdown operation 	<ul style="list-style-type: none"> a. Whole core controlled in both 1-D and 2-D b. Central zone controlled in 1-D only
ENLARGED OCONEE REACTOR SIZE	<ul style="list-style-type: none"> a. Whole core controlled in 1-D b. Central zone controlled in 1-D 	<ul style="list-style-type: none"> a. Whole core controlled in 1-D b. Central zone controlled in 1-D 	

Table 5.6 Summary of case studies for Oconee type fuel in 1-D and 2-D calculations for out-in refueling scheme.

	9 Zone	6 Zone	3 Zone
OCONEE REACTOR SIZE	Whole core controlled 1-D & 2-D	Whole core controlled 1-D & 2-D	Whole core controlled 1-D & 2-D

6. RESULTS AND DISCUSSIONS

All the calculation results are summarized in Tables (6.1) to (6.19). Each table contains the same information for different study cases. They are the zone average burnup levels and the power peaking factors at BOC and EOC, and the cycle length. Tables (6.1) to (6.2) are the results of 1-D and 2-D calculations for Oconee fuels in whole core controlled cases, at 3, 6 and 9 zone refueling frequencies, in the in-out refueling scheme. Table (6.3) is the result of 1-D in-out refueling calculations for Oconee fuels in central zone controlled cases. Tables (6.4) and (6.5) are the results of 1-D and 2-D out-in refueling calculations for Oconee fuels. Table (6.6) is a summary of Tables (6.1) to (6.5). Table (6.7) to (6.8) are results of the enlarged Oconee reactor in 1-D calculation for 6-zone and 9-zone normal cycle in both whole core controlled cases and central zone controlled cases. Table (6.9) and (6.10) are results of the coastdown cycle for 6-zone and 9-zone whole core controlled cases respectively for Oconee reactor. Tables (6.11) to (6.19) are results for Trojan fuels. The discharge burnups and the highest power peaking factors from these tables are further categorized and plotted into Figures (6.1) to (6.5) for illustration and comparison purposes. Figure (6.1) is the discharge burnup for Oconee fuels and Figure (6.2) for Trojan fuels. Figure (6.3) is the highest power peaking factors for Oconee fuels and Figures (6.4) and (6.5) are both for Trojan fuels, one for the whole core controlled case, the other for the central zone controlled case.

As described in Sections (2.2) and (2.3) and verified by the results summarized in Table (6.1) to (6.19), the in-out refueling scheme can best simulate a reactor of zero leakage and thus utilize the fuels best in the sense of neutron economics. This conclusion, among others, is explained in the following:

6.1 The Discharge Burnup Advantage

6.1.1 1-D Calculation Results

Figure (6.1) shows that both in-out and out-in refueling schemes will extract more energy out of fuels, in other words, higher discharge burnup, as refueling frequency increases. It reaffirmed the relation that the slope of discharge burnup with refueling frequency, other things being equal, is approximately proportional to $-1/N$ (19), where N is the number of cycles that the fuel remains in the core before discharge; this is the same as the number of batches. This is because the amount of control poison that must be present on the average is roughly proportional to the k change from BOC to EOC, and the k change decreases as refueling frequency increases. This figure also indicates that at any given refueling frequency, the central zone controlled cases yield higher discharge burnups than the whole core controlled ones, in both an in-out or out-in refueling scheme. This tendency is already established when only three batches are used. The discharge burnups of the in-out refueling scheme in the whole core controlled cases for the same

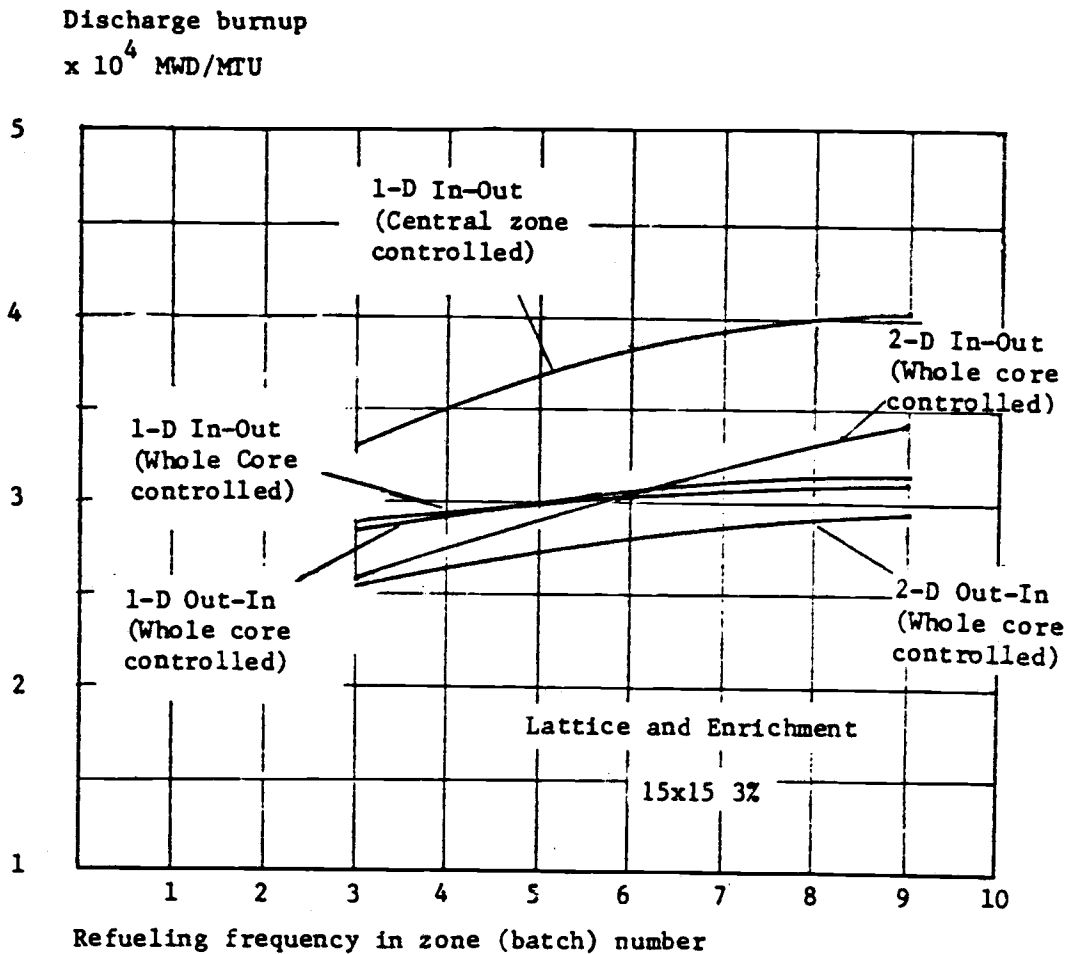


FIGURE 6.1 Comparison of discharge burnups of in-out and out-in refueling schemes in 1-D and 2-D calculations for Ocone fuel.

refueling frequency are very comparable. Take the 3 zone cases in Table (6.1) and (6.4) for example. The in-out refueling has a cycle length of 9600 MWD/MT and a discharge burnup of 28700 MWD/MT, while the out-in refueling has a cycle length of 9400 MWD/MT and a discharge burnup of 28400 MWD/MT.

This is mainly because both the in-out and out-in refuelings have the same batch size of fresh fuels loaded each cycle, and the cycle length depends very much on the batch size. However, the out-in refueling scheme needs a relative fresher core than the in-out refueling scheme, both at EOC and BOC. This occurs because the out-in refueling scheme has a larger neutron leakage and less utilization of neutron importance than the in-out refueling scheme. Therefore when an equilibrium status is reached, the out-in refueling scheme must have a relative fresh core in order to maintain critical. This by itself shows that before reaching an equilibrium status the in-out refueling scheme must already have extracted more energy from fuel than the out-in refueling scheme. This is due to its inherent characteristics of low neutron leakage and high neutron importance at the core center. However, its full potential for increasing burnup can not be realized if we allow the fuel at the core center to burn or to use up its excess reactivity in the very early stage of the cycle (a very high power peaking at the core center) as we did in the whole core controlled case. The

in-out refueling scheme, nevertheless, is capable of sustaining a longer cycle length and a higher discharge burnup for the same refueling batch size than the out-in refueling scheme if we control the burnup rate of the fuels at the core center at a lower rate (a low power peaking at the core center than in the whole core controlled case) as in the central zone controlled case.

This has demonstrated the importance of the proper maneuvering of the reactivity of the fresh fuels at the core center in an in-out refueling scheme if a higher discharge burnup is desired. The calculation results of the enlarged Oconee reactor in Table(6.7) and(6.8) further illustrate the predominance of the reactivity effect of the fresh fuels at the core center on discharge burnup. According to the inference in Section (2.3), a reactor of lower B^2 (or larger radius) should yield a higher discharge burnup than a reactor of higher B^2 (or smaller radius) if other things are the same. The results in Table(6.7) and(6.8), when compared with those in Table(6.1) and(6.3) show just the opposite. This seems to be contrary to our inference. However, if we look at the higher power peaking of the enlarged Oconee reactor, we then realize that the faster consumption of the reactivity of the fresh fuels at the core center of the enlarged reactor due to the higher power peaking is responsible for having lower discharge burnup. In other words, the power peaking has much more influence than the B^2 value on discharge burnup.

It is clear from the results as shown in Figure (6.1) or

in Table(6.1)to(6.5)that the actual discharge burnups we have calculated have uncertainties of a few percent. Correspondingly, we can not draw any conclusions beyond the observation that the in-out refueling scheme (central zone controlled) for Oconee reactor leads to about 15% discharge burnup improvement over the out-in case.

Of course, for getting a real sense of the discharge burnup gain one has to compare the 2-D results which take into consideration the axial leakage and the axial-radial flux interaction. This will be discussed in the next subsection.

As explained in Section (2.1), the group constants of Trojan fuels are somewhat pessimistic when compared with those of compatible Standard PWR fuels. These pessimistic group constants of the Trojan fuels are considered responsible for the low discharge burnups for all 1-D calculations for Trojan fuels. Nevertheless, the 1-D calculation results for the Trojan fuels are still illustrative in many aspects of the in-out refueling scheme except for the absolute discharge values.

6.1.2 2-D calculation adjustment

Some 2-D calculations for Oconee fuels are made to see how the axial leakage and the axial-radial flux interaction which are taken into account in 2-D calculation but not in 1-D calculation will affect the equilibrium discharge burnup. Results of these calculations are shown in Tables (6.2) and (6.5) and also in Figure (6.1) and (6.3). By comparing the 1-D and the 2-D results, several observations could be made. First, unlike the 1-D calculation, the 2-D calculation results

indicate a clear benefit in discharge burnup for in-out refueling scheme over out-in refueling scheme, especially when refueling frequency is high. Second, the effects of axial leakage and axial-radial flux interaction are obvious and predominant when refueling frequency is low. This can be seen from the fact that for both in-out and out-in refueling schemes, the discharge burnups of 2-D calculations are at their lowest values below the corresponding 1-D results for 3-zone refueling cases and are getting close to the 1-D results as refueling frequency increases. Another fact that the core average exposures of the fuels at BOC and EOC of 2-D calculations are lower than those of 1-D calculations for both in-out and out-in refueling schemes reveals also the effects of axial leakage and axial-radial flux interaction. Third, the importance of power peaking at the core center to discharge burnup is reemphasized by the following phenomena. That is, the in-out refueling scheme in 2-D calculations tend to have lower power peaking than in 1-D calculations. As a result, the discharge burnup of the 2-D calculation becomes higher than the 1-D calculation for the 9-zone refueling case while the core average exposures of fuels at BOC and EOC respectively remain about the same for both 2-D and 1-D calculations.

6.2 Batch Size and Maximum Cycle Length

The cycle length of a one-batch refueling scheme is greater than for a multi-batch refueling scheme, and is given by the burnup at which the original reactor is just critical. The highest cycle length will reach its maximum if the reactor is of infinite size (no leakage) with one-batch refueling. All fuels in a reactor of infinite size start

fresh and burn at the same rate because of flat flux. The cycle will end when all the fuels reach a burnup level such that k_{∞} has dropped to 1. In this case, the behavior of one individual fuel sample can be representative of the whole core. The maximum cycle length can then be known from the k_{∞} vs. burnup curve of the unit cell calculation as shown in Figure (2.2). For the fuels under study, their corresponding maximum cycle lengths, that is, the burnup level of the fuel when its $k_{\infty} = 1$ in Figure (2.2), are 25000 MWD/MTU for Oconee fuel, 20000 MWD/MTU for 17x17 three percent Trojan fuel, 15000 MWD/MTU for 18x18 three percent Trojan fuel and 9000 MWD/MTU for 17x17 two percent Trojan fuel.

In reality, the cycle length of the reactor is far less than the maximum cycle length, partly because of the reactor is not run with a one-batch refueling scheme and partly because of the neutron leakage of a reactor of finite size.

A proper choice of cycle length should depend on a variety of factors, such as seasonal power demand, facility inspection and maintenance scheduling and the fuel cycle cost. Our studies show that the cycle lengths of three, six, nine-batch, in-out refueling cycles in whole core controlled case are 352, 185, and 129 EFPD (Equivalent Full Power Days) correspondingly. These are calculated from cycle length in MWD/MTU, reactor power level in MW, and fuel loaded in MTU. For example, 352 days = $\left[9600 \text{ MWD/MTU (cycle length in Table 6.1)} \times 94.1 \text{ MTU (fuel loaded)} \right] \div 2568 \text{ MW (Reactor Power level)}$. The six-batch cycle has a cycle length of about half a year which could be of interest to the industry

considering that it is typical for seasonal demand for electricity to show minima twice a year (spring and fall).

6.3 Enrichment Effects on the Discharge Burnup

As was discussed in Sections (2.1) and (6.1), the group constants of the Trojan fuels used in this study are somewhat pessimistic, therefore the magnitude of the discharge burnups obtained by 1-D calculations are lower than they should be. But because these group constants are generated by the same version of LEOPARD (10) and show the same degree of pessimism, the 1-D calculation results obtained from these group constants will still be illustrative in a relative sense. These results were summarized in Tables (6.11) to (6.18) or in Figure (6.2).

It is clear from this figure that enrichment increase could improve the discharge burnup. However, the gain in discharge burnup per unit enrichment increment decreases as the enrichment level increases. Although there is no calculation result to prove this statement, it can be inferred from the discussion in Section (2.3), which states that the maximum discharge burnup an in-out refueling scheme can reach is dependent on the area under the k_{∞} curve but above the $k_{\infty} = 1$ line in Figure (2.7). As enrichment increases the effect of enrichment on k_{∞} decreases as shown by the k_{∞} curves of the standard PWR fuels for three different enrichments in Figure (2.1); when this happens, the effect on the area mentioned above likewise decreases, justifying our original statement. This fact is also pointed out in reference (2) from a different point of view.

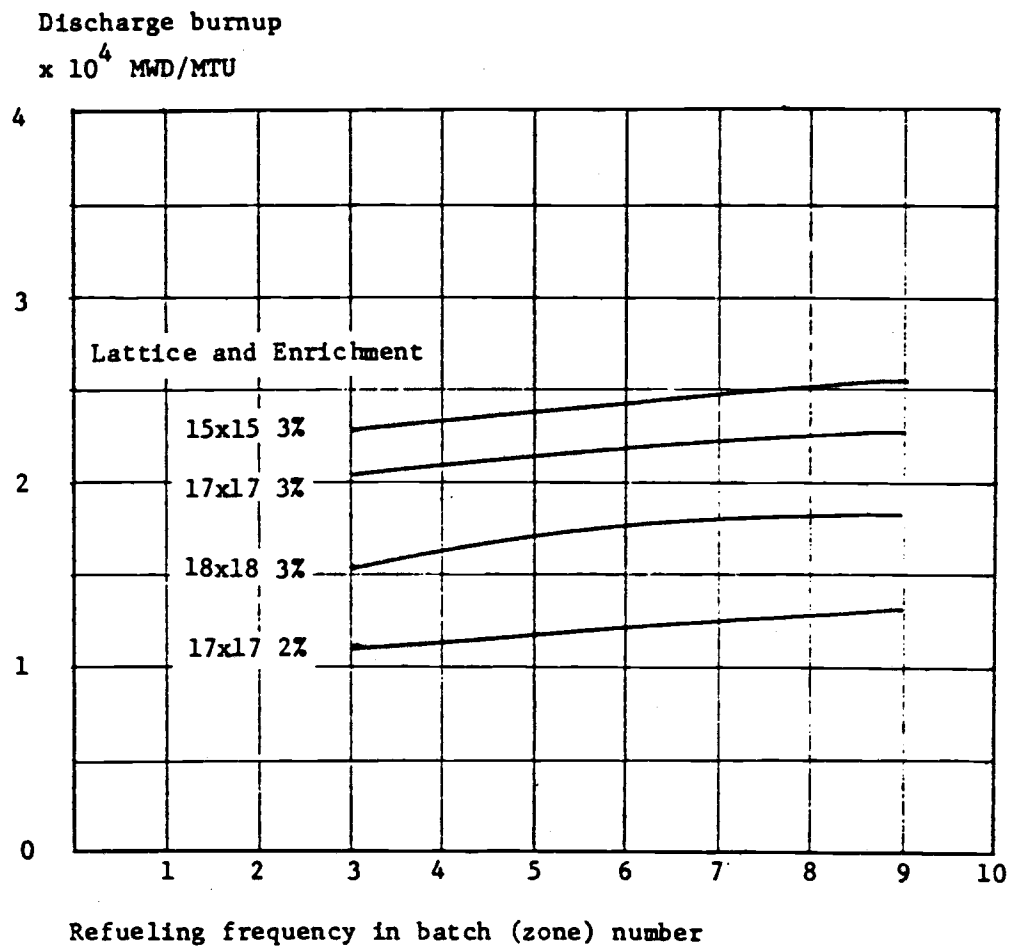


FIGURE 6.2 Discharge burnups of all types of Trojan fuel in in-out refueling scheme.

6.4 Effect of Bundle Lattice Design on Discharge Burnup

Figure (6.2) also shows that for fuels with the same enrichment, the fuels of loose lattice design can yield higher discharge burnups. This is because in a light water reactor, it is the thermal neutrons that are primarily responsible for causing fission reactions and among the three lattice designs, the 15x15 fuels have the best neutron thermalization, the 17x17 fuels the next, and the 18x18 fuels the worst. As a result of this, among the three percent enrichment cases, the 15x15 fuels exhibit the highest zero-burnup k_{∞} value, and the 18x18 fuels the lowest. However, we also note from Figure (2.2) that the k_{∞} value drops faster as the fuel burnup increases for the fuels of looser lattice design, because of the smaller amount of fissile material converted during power generation. According to the discussions in Section (2.3), this faster decrease of the k_{∞} value of the looser lattice fuels is harmful to discharge burnup gain. Between the two conflicting effects on discharge burnup of the higher zero burnup k_{∞} value and the faster decrease of the k_{∞} value of the looser lattice fuels, our results indicate that it is the former that has a stronger influence on the discharge burnup in the in-out refueling scheme--at least within the range of lattice design changes we considered.

6.5 The Peaking Factor

The crux of the in-out refueling scheme is to load the fresh

fuel into the region of high flux to fully exploit the high reactivity of the fresh fuel and the high neutron importance of the flux at the reactor center. Having a high peaking factor becomes natural to the in-out refueling scheme. This fact can be seen from Figures (6.3), (6.4) and (6.5), a summary of the calculation results in Tables (6.1) to (6.19), from which we see that all power peaking factors in the central zone in whole core controlled cases are higher than 1.6, a standard value for the conventional refueling scheme. It can also be seen from Figure (6.4) that fuels with higher zero burnup k_{∞} value will yield higher discharge burnup, but also higher power peaking, noting that the magnitude of the zero burnup k_{∞} values of all the fuels under study, from high to low, are in the sequence of Oconee 15x15 three percent fuel, Trojan 15x15 three percent fuel, Trojan 17x17 three percent fuel, Trojan 18x18 three percent fuel and Trojan 17x17 two percent fuel as shown in Table (A-1) to Table (A-5) or in Figure (2.2). Another fact is that the larger the number of zones, the more serious the peaking problem. For instance, both the Oconee and the Trojan 15x15 three percent fuels, having the highest zero burnup k_{∞} values among the fuels, exhibit radial power peaking factors as high as 6.882 and 7.123 respectively in the 9 zone, normal cycle, whole core controlled case, as shown in Table (6.1) and (6.13), while the peaking factors for 6 zone cases are 4.972 and 5.094 as shown in Table (6.1) and (6.12). The 2-D calculation results in Figure (6.3) or Table (6.2) and (6.5),

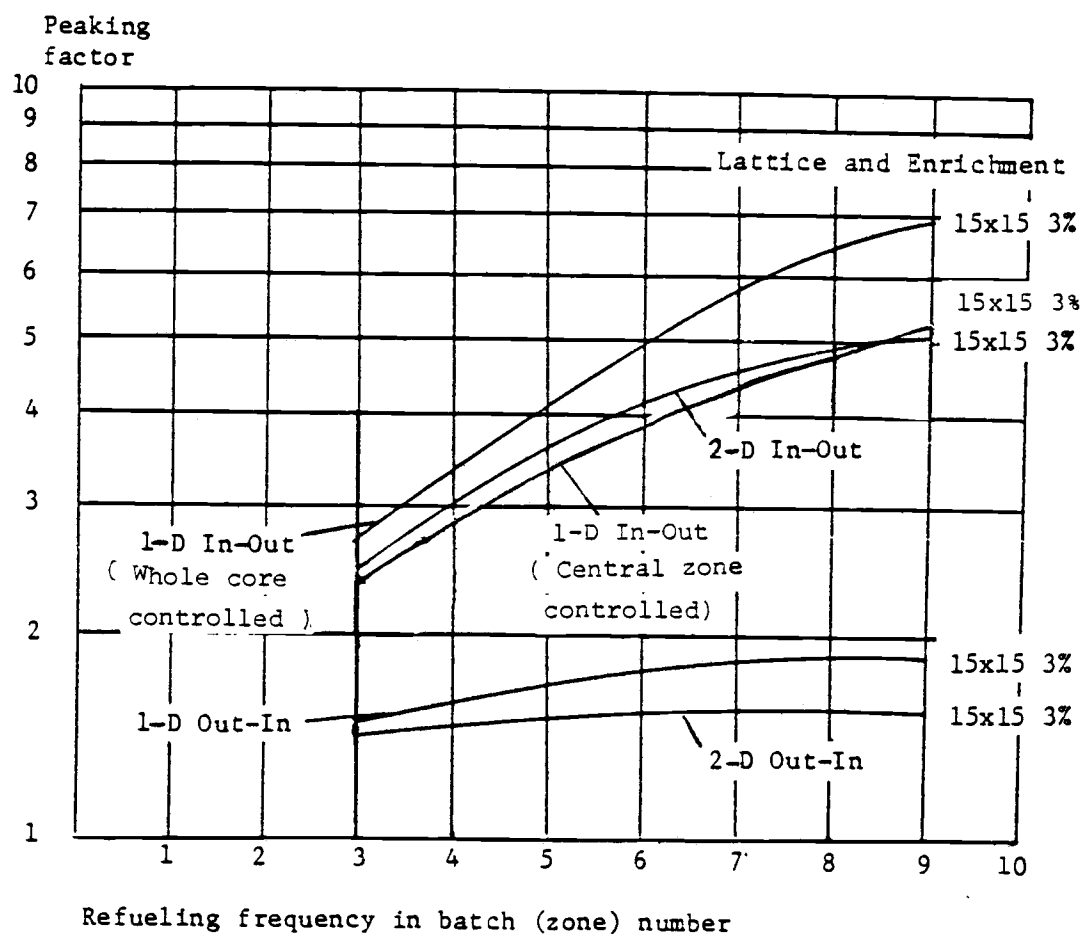


FIGURE 6.3 Power peaking factors of Oconee fuel in 1-D in-out and out-in refueling schemes and 2-D in-out and out-in refueling schemes.

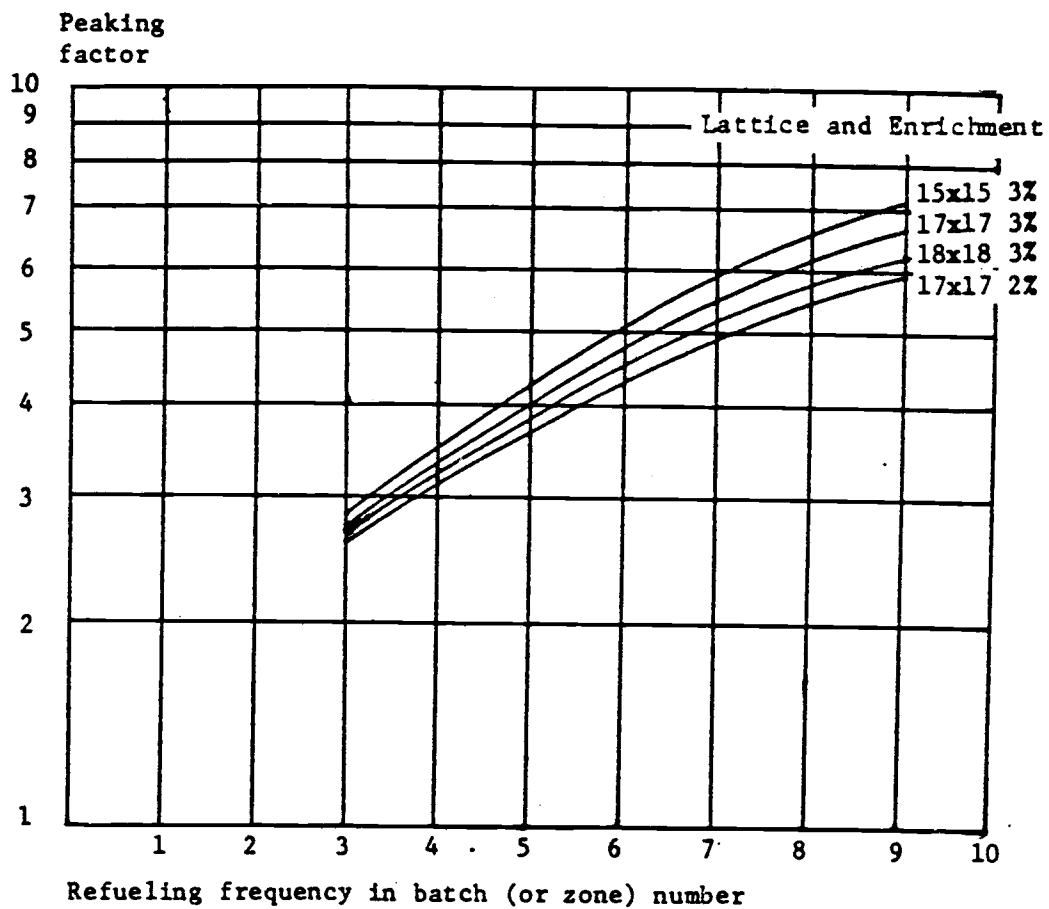


FIGURE 6.4 1-D calculated peaking factors of Trojan fuels at BOC for different refueling frequency in whole core controlled case.

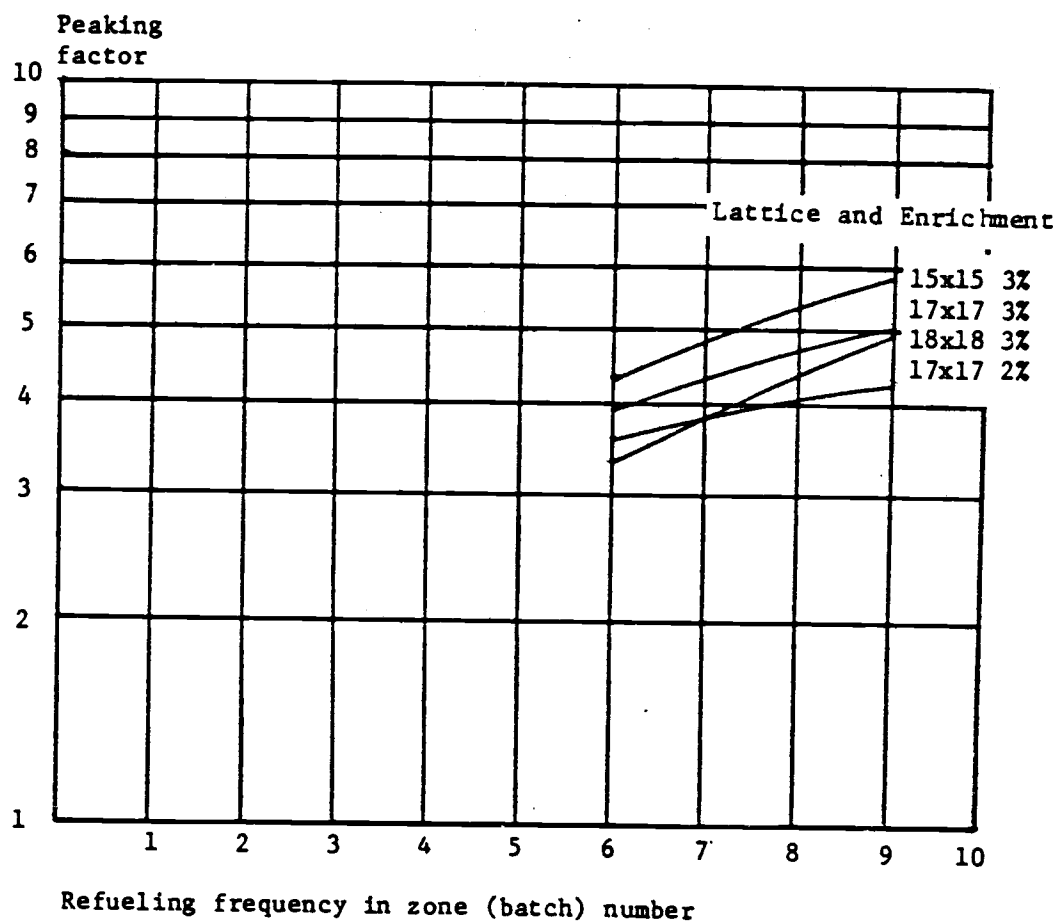


FIGURE 6.5 1-D calculated peaking factors of Trojan fuels at EOC for different refueling frequency in central zone controlled case.

however, show that when the axial leakage is taken into account, the peaking problem in the in-out refueling scheme is not as serious as in 1-D cases. A survey of the peaking factors in Table (6.1) to Table (6.19) reveals that in an in-out refueling scheme, the most serious peaking during a cycle occurs at the reactor center at BOC when fresh fuels are loaded. This is the reason that only the peaking factors at BOC were shown in Figure (6.4). The high power peaking at the reactor center indicates that during a reactor cycle life, the energy contribution from the fuels occupying the inner half of the core volume amounts to more than 80 percent of the total power output of the core.

In the out-in refueling scheme, the 1-D calculation results for Oconee fuel, as shown in Figure (6.3) indicate that just as in the in-out refueling scheme, the power peaking increases with the refueling frequency, but power peaking magnitudes are much less than their counterparts in the in-out refueling scheme.

6.6 Central Zone Reactivity Control

In order to reduce the high power peaking, the reactivity control material is confined to the central zone only.

Contrary to the whole core controlled case, the worst peaking occurs at EOC rather than at BOC as in the whole core controlled case. Its magnitude is comparable to that of the whole core controlled case at EOC and is significantly lower than that

of the whole core controlled case at BOC. Figure (6.5) shows that the power peaking factors at EOC in the central zone controlled case are lower than 6.0 for all Trojan fuels although still higher than the 1.6 value of the conventional refueling scheme. In addition to this benefit of depressing the power peaking, the central zone reactivity control can also extend the cycle lengths and therefore the discharge burnups, compared to those of the whole core controlled case. This extension capability can be explained in two ways. First, in the central zone controlled case, the neutron absorber is added to the central zone only, where the neutron importance is the highest in the core. The number of neutrons absorbed by the absorber in order to keep the reactor at a critical condition need not be as many as in the whole core controlled case. Therefore, the central zone controlled case has better neutron economics and so can have a longer cycle length. Secondly, because of the lower peak flux distribution in the central zone controlled case, the fuels in the central zone have a lesser share of power generation than they have in the whole core controlled case. This leads to a result that at EOC the bundle burnup distribution has a shape lower at the center and higher at the edge when compared with that of the whole core controlled case. Due to the higher reactivity of the lower burnup fuels in the center, the reactor can maintain an end of cycle condition with higher discharge burnup at the edge than the reactor in the whole core controlled case can. This ad-

vantage of the cycle length extension of the central zone controlled scheme diminishes as the refueling period approaches zero (continuous refueling), because the amount of reactivity control that is needed decreases.

6.7 Effects of Coastdown Operation on the Discharge Burnup

Only two cases of coastdown operation were studied. They are 9 zone and 6 zone whole core controlled cases for Oconee fuels. The results are summarized in Tables (6.9) and (6.10). They reveal that coastdown operation could elongate the total cycle length when compared with the normal cycle length, but will sacrifice the length of full power operation. As a result, the plant capacity factor is drastically reduced. Therefore, it would be unprofitable to adopt coastdown operation, except when continual power demand happens to coincide with the end of normal cycle and coastdown operation becomes necessary in order to meet this demand. Another adverse effect of coastdown operation is the worsening of power peaking at the central zone at the BOC. This can be seen when compared to the result in Table (6.1) with that in Table (6.9) and Table (6.1) with Table (6.10). This is because the coastdown operation tends to steepen the burnup distribution at EOC, i.e., the fuels near the reactor center having a higher burnup level but the fuels close to the periphery of the reactor having an even higher burnup level for the coastdown case than for the normal cycle case. Therefore, at BOC the fresh fuels will share even more power generation than in normal cycle case.

Table 6.1 Discharge burnup of Oconee fuel in 3,6,9 zone normal cycle whole core controlled case for 1-D calculations of in-out refueling scheme.

15x15 3% 3 zone. Normal cycle, Whole core controlled 1-D				
Zone No.	Initial Load	Power Peak	Final Burnup	Power Peak
1	0	2.730	24000	2.120
2	24000	.248	28100	.705
3	28100	.021	28700	.174
Cycle length 9600 MWD/MTU				

15x15 3% 6 zone. Normal cycle, Whole core controlled 1-D				
Zone No.	Initial Load	Power Peak	Final Burnup	Power Peak
1	0	4.972	22300	3.231
2	22300	.811	27600	1.465
3	27600	.156	29200	.691
4	29200	.044	29800	.372
5	29800	.013	30000	.178
6	30000	.004	30200	.063
Cycle length 5040 MWD/MTU				

15x15 3% 9 zone. Normal cycle, Whole core controlled 1-D				
Zone No.	Initial Load	Power Peak	Final Burnup	Power Peak
1	0	6.882	20900	4.426
2	20900	1.490	27200	2.092
3	27200	.396	29500	1.070
4	29500	.136	30600	.603
5	30600	.054	31100	.357
6	31100	.024	31400	.223
7	31400	.011	31500	.134
8	31500	.005	31600	.071
9	31600	.002	31650	.025
Cycle length 3520 MWD/MTU				

Table 6.2 Discharge burnup of Oconee fuel in 3,6,9 zone normal cycle whole core controlled case for 2-D calculations of in-out refueling scheme.

15x15 3% 3 zone. Normal cycle, Whole core controlled 2-D				
Zone No.	Initial Load	Power Peak	Final Burnup	Power Peak
1	0	2.564	21000	2.039
2	21000	.353	24300	.744
3	24300	.079	26000	.215
Cycle length 8670 MWD/MTU				

15x15 3% 6 zone. Normal cycle, Whole core controlled 2-D				
Zone No.	Initial Load	Power Peak	Final Burnup	Power Peak
1	0	4.225	20000	3.084
2	20000	.781	25000	1.406
3	25000	.453	27700	.764
4	27700	.324	29400	.444
5	29400	.195	30400	.241
6	30400	.071	30700	.087
Cycle length 5120 MWD/MTU				

15x15 3% 9 zone. Normal cycle, Whole core controlled 2-D				
Zone No.	Initial Load	Power Peak	Final Burnup	Power Peak
1	0	5.222	18800	3.894
2	18800	1.155	24300	1.938
3	24300	.670	27500	1.138
4	27500	.574	29900	.743
5	29900	.485	31800	.509
6	31800	.384	33100	.350
7	33100	.274	34100	.231
8	34100	.165	34680	.136
9	34680	.064	34900	.052
Cycle length 3880 MWD/MTU				

Table 6.3 Discharge burnup of Oconee fuel in 3, 6, 9 zone normal cycle central zone controlled case for 1-D calculations of in-out refueling scheme.

15x15 3% 3 zone. Normal cycle, Central zone controlled 1-D				
Zone No.	Initial Load	Power Peak	Final Burnup	Power Peak
1	0	1.787	23300	2.307
2	23300	.971	31400	.577
3	31400	.242	33300	.117
Cycle length 11100 MWD/MTU				

15x15 3% 6 zone. Normal cycle, Central zone controlled 1-D				
Zone No.	Initial Load	Power Peak	Final Burnup	Power Peak
1	0	2.726	21300	3.916
2	21300	1.907	31100	1.324
3	31100	.817	35400	.461
4	35400	.358	37500	.193
5	37500	.146	38500	.078
6	39500	.047	38700	.025
Cycle length 6400 MWD/MTU				

15x15 3% 9 zone. Normal cycle, Central zone controlled 1-D				
Zone No.	Initial Load	Power Peak	Final Burnup	Power Peak
1	0	3.642	19800	5.286
2	19800	2.709	30600	2.054
3	30600	1.320	35700	.849
4	35700	.644	38000	.396
5	38000	.333	39300	.202
6	39300	.185	40000	.111
7	40000	.100	40360	.060
8	40360	.050	40550	.030
9	40550	.017	40600	.010
Cycle length 4510 MWD/MTU				

Table 6.4 Discharge burnup of Oconee fuel in 3,6,9 zone normal cycle whole core controlled case for 1-D calculations of out-in refueling scheme.

15x15 3% 3 zone. Normal cycle, Whole core controlled 1-D				
Zone No.	Initial Load	Power Peak	Final Burnup	Power Peak
1	24000	.385	28400	.715
2	11000	1.408	24000	1.275
3	0	1.211	11000	1.011
Cycle length 9400 MWD/MTU				

15x15 3% 6 zone. Normal cycle, Whole core controlled 1-D				
Zone No.	Initial Load	Power Peak	Final Burnup	Power Peak
1	29500	.189	31000	.459
2	26500	.536	29500	.782
3	22000	1.023	26500	1.103
4	13500	1.613	22000	1.447
5	4700	1.725	13500	1.423
6	0	.914	4700	.787
Cycle length 5160 MWD/MTU				

15x15 3% 9 zone. Normal cycle, Whole core controlled 1-D				
Zone No.	Initial Load	Power Peak	Final Burnup	Power Peak
1	31200	.145	32000	.264
2	29900	.327	31200	.465
3	27700	.594	29900	.720
4	24200	.952	27700	1.025
5	19500	1.347	24200	1.328
6	13800	1.732	19500	1.608
7	7680	1.824	13800	1.664
8	2400	1.446	7680	1.337
9	0	.633	2400	.591
Cycle length 3560 MWD/MTU				

Table 6.5 Discharge burnup of Oconee fuel in 3,6,9 zone normal cycle whole core controlled case for 2-D calculations of out-in refueling scheme.

15x15 3% 3 zone. Normal cycle, Whole core controlled 2-D				
Zone No.	Initial Load	Power Peak	Final Burnup	Power Peak
1	19000	.716	25800	.913
2	8030	1.328	19000	1.215
3	0	.956	8030	.873
Cycle length 8600 MWD/MTU				

15x15 3% 6 zone. Normal cycle, Whole core controlled 2-D				
Zone No.	Initial Load	Power Peak	Final Burnup	Power Peak
1	25100	.620	28000	.776
2	21000	.825	25100	.899
3	15400	1.138	21000	1.115
4	9000	1.393	15400	1.309
5	3100	1.322	9000	1.243
6	0	.709	3100	.666
Cycle length 4600 MWD/MTU				

15x15 3% 9 zone. Normal cycle, Whole core controlled 2-D				
Zone No.	Initial Load	Power Peak	Final Burnup	Power Peak
1	25890	.748	28800	.905
2	24130	.769	25890	.889
3	21880	.872	24130	.942
4	18890	1.032	21880	1.047
5	15050	1.221	18890	1.177
6	10460	1.374	15050	1.285
7	5710	1.364	10460	1.258
8	1800	1.089	5710	1.009
9	0	.509	1800	.467
Cycle length 3200 MWD/MTU				

**Table 6.6 Summary of 1-D and 2-D Calculation Results
for Oconee Fuels**

in MWD/MTU

3-Zone Refueling	Cycle Length	Discharge Burnup	Core Average Exposure BOC	Core Average Exposure EOC
1-D In-Out Whole Core Controlled	9600	28700	17360	26930
2-D In-Out Whole Core Controlled	8670	26000	15100	23766
1-D Out-In Whole Core Controlled	9400	28400	11666	21133
2-D Out-In Whole Core Controlled	8600	25800	9010	17610
1-D In-Out Central Zone Controlled	11100	33300	18230	29300

6-Zone Refueling	Cycle Length	Discharge Burnup	Core Average Exposure BOC	Core Average Exposure EOC
1-D In-Out Whole Core Controlled	5040	30200	23150	28180
2-D In-Out Whole Core Controlled	5120	30700	22080	27200
1-D Out-In Whole Core Controlled	5160	31000	16033	21200
2-D Out-In Whole Core Controlled	4600	28000	12266	16933
1-D In-Out Central Zone Controlled	6400	38700	27400	33916

9-Zone Refueling	Cycle Length	Discharge Burnup	Core Average Exposure BOC	Core Average Exposure EOC
1-D In-Out Whole Core Controlled	3520	31650	25970	29497
2-D In-Out Whole Core Controlled	3880	34900	26020	29897
1-D Out-In Whole Core Controlled	3560	32000	17375	20931
2-D Out-In Whole Core Controlled	3200	28800	13756	16956
1-D In-Out Central Zone Controlled	4510	40600	31600	36100

TABLE 6.7 Discharge burnups of Oconee fuel in 6 and 9 zone
normal cycle whole core controlled case for enlarged
reactor size in 1-D calculation

15x15 3Z, 6 Zone, Normal Cycle, Whole Core Controlled				
Zone No.	Initial Load	Power Peak	Final Burnup	Power Peak
1	0	5.255	22800	3.491
2	22800	.637	27200	1.418
3	27200	.085	28300	.603
4	28300	.018	28700	.303
5	28700	.004	28800	.139
6	28800	.001	28920	.047
cycle length 4820 MWD/MTU				

15x15 3Z, 9 Zone, Normal Cycle, Whole Core Controlled				
Zone No.	Initial Load	Power Peak	Final Burnup	Power Peak
1	0	7.481	22500	4.827
2	22500	1.189	27800	2.050
3	27800	.233	29500	.953
4	29500	.063	30100	.513
5	30100	.021	30400	.292
6	30400	.008	30600	.178
7	30600	.003	30670	.104
8	30670	.001	30700	.055
9	30700	.000	30780	.019
cycle length 3420 MWD/MTU				

Table 6.8 Discharge burnups of Oconee fuel in 6 and 9 zone normal cycle central zone controlled case for enlarged reactor in 1-D calculation.

15x15 3%, 6 Zone, Normal Cycle, Central zone controlled				
Zone No	Initial Load	Power Peak	Final Burnup	Power Peak
1	0	2.746	22300	4.198
2	22300	1.992	31700	1.227
3	31700	.793	35200	.369
4	35200	.315	36500	.139
5	36500	.118	37100	.052
6	37100	.036	37200	.016
cycle length 6200 MWD/MTU				

15x15 3%, 6 Zone, Normal Cycle, Central Zone Controlled				
Zone No	Initial Load	Power Peak	Final Burnup	Power Peak
1	0	4.082	21500	5.806
2	21500	2.722	31400	1.940
3	31400	1.198	35500	.700
4	35500	.525	37400	.294
5	37400	.246	38200	.135
6	38200	.125	38700	.069
	38700	.063	38900	.035
	38900	.030	39020	.016
	39020	.010	39080	.005
cycle length 4340 MWD/MTU				

TABLE 6.9 Discharge burnups of Oconee fuel in 6 zone, coastdown operation,
whole core controlled case for 1-D calculation

Oconee 15x15 3%, 6 Zone, Coastdown Operation, Whole Core Controlled						
Zone No.	Initial Load ⁺	Power Peak	Mid-Load [*]	Power Peak	Final Burnup ^Δ	Power Peak
1	0	5.050	21500	3.907	24600	3.319
2	24600	.765	28900	1.307	30500	1.468
3	30500	.135	31700	.468	32400	.659
4	32400	.035	32900	.205	33100	.340
5	33100	.010	33300	.085	33500	.159
6	33500	.003	33540	.028	33580	.055
Full power cycle length= 4630 MWD/MTU Total cycle length= 5590 MWD/MTU						

+ Zone average burnup at the beginning of cycle

* Zone average burnup at the end of full power operation

Δ Zone average burnup at the end of total cycle

TABLE 6.10 Discharge burnups of Oconee fuel in 9 zone,
coastdown operation, whole core controlled
case for 1-D calculation

Oconee 15x15 3%, 9 Zone, Coastdown Operation, Whole Core Controlled						
Zone No.	Initial Load ⁺	Power Peak	Mid-Load [*]	Power Peak	Final Burnup Δ	Power Peak
1	0	7.029	20500	5.004	23400	4.390
2	23400	1.427	28000	2.070	30500	2.120
3	30500	.354	32000	.922	33200	1.075
4	33200	.115	34000	.463	34400	.600
5	34400	.044	34600	.252	34900	.357
6	34900	.019	35100	.147	35300	.224
7	35300	.008	35400	.084	35500	.135
8	35500	.004	35540	.043	35560	.072
9	35560	.001	35580	.015	35600	.026
Full power cycle length= 3253 MWD/MTU Total cycle length= 3960 MWD/MTU						

+ Zone average burnup at the beginning of cycle

* Zone average burnup at the end of full power operation

Δ Zone average burnup at the end of total cycle

TABLE 6.11 Discharge burnups of Trojan fuels in 3 zone,
normal cycle whole core controlled case for
1-D calculation

122

15x15 3Z, 3 Zone, Normal Cycle, Whole Core Controlled				
Zone No.	Initial Load	Power Peak	Final Burnup	Power Peak
1	0	2.762	20000	2.236
2	20000	.223	22800	.629
3	22800	.015	23100	.135
cycle length 7700 MWD/MTU				

17x17 2Z, 3 Zone, Normal Cycle, Whole Core Controlled				
Zone No.	Initial Load	Power Peak	Final Burnup	Power Peak
1	0	2.570	9300	2.189
2	9300	.380	11200	.658
3	11200	.048	11400	.153
cycle length 3800 MWD/MTU				

17x17 3Z, 3 Zone, Normal Cycle, Whole Core Controlled				
Zone No.	Initial Load	Power Peak	Final Burnup	Power Peak
1	0	2.689	17100	2.149
2	17100	.286	20000	.686
3	28000	.026	20400	.164
cycle length 6800 MWD/MTU				

18x18 3Z, 3 Zone, Normal Cycle, Whole Core Controlled				
Zone No.	Initial Load	Power Peak	Final Burnup	Power Peak
1	0	2.618	13700	2.014
2	13700	.343	16100	.776
3	16100	.039	16500	.210
cycle length 5500 MWD/MTU				

TABLE 6.12 Discharge burnups of Trojan 15x15 3% fuel
in 6 zone, normal cycle, whole core and
central zone controlled cases

123

15x15 3%, 6 Zone, Normal Cycle, Whole Core Controlled				
Zone No	Initial Load	Power Peak	Final Burnup	Power Peak
1	0	5.094	19200	4.522
2	19200	.755	23000	1.080
3	23000	.116	23900	.269
4	23900	.027	24100	.090
5	24100	.007	24300	.031
6	24300	.002	24360	.009
cycle length 4060 MWD/MTU				

15x15 3%, 6 Zone, Normal Cycle, Central Zone Controlled				
Zone No	Initial Load	Power Peak	Final Burnup	Power Peak
1	0	2.649	18000	4.344
2	18000	2.193	28000	1.203
3	28000	.781	31500	.312
4	31500	.265	32600	.099
5	32600	.087	33000	.032
6	33000	.025	33100	.009
cycle length 5520 MWD/MTU				

TABLE 6.13 Discharge burnups of Trojan 15x15 3% fuels
in 9 zone normal cycle, whole core and
central zone controlled cases

124

15x15 3%, 9 Zone, Normal Cycle, Whole Core Controlled				
Zone No	Initial Load	Power Peak	Final Burnup	Power Peak
1	0	7.123	17900	5.064
2	17900	1.420	22900	2.093
3	22900	.314	24500	.910
4	24500	.091	25200	.444
5	25200	.031	25500	.233
6	25500	.012	25600	.132
7	25600	.005	25700	.073
8	25700	.002	25750	.037
9	25750	.001	25770	.012
cycle length 2870 MWD/MTU				

15x15 3%, 9 Zone, Normal Cycle, Central Zone Controlled				
Zone No	Initial Load	Power Peak	Final Burnup	Power Peak
1	0	3.741	17100	5.846
2	17100	3.086	27000	2.031
3	27000	1.291	31000	.682
4	31000	.505	32700	.254
5	32700	.210	33400	.104
6	33400	.096	33700	.047
7	33700	.044	33880	.027
8	33880	.020	33950	.010
9	33950	.006	33970	.003
cycle length 3770 MWD/MTU				

TABLE 6.14 Discharge burnups of Trojan 17x17 2% fuels
in 6 zone normal cycle whole core and central
zone controlled cases

125

17x17 2%, 6 Zone, Normal Cycle, Whole Core Controlled				
Zone No	Initial Load	Power Peak	Final Burnup	Power Peak
1	0	4.358	8300	3.871
2	8300	1.157	10800	1.328
3	10800	.318	11700	.474
4	11700	.114	12000	.209
5	12000	.041	12150	.088
6	12150	.012	12200	.029
cycle length 2030 MWD/MTU				

17x17 2%, 6 Zone, Normal Cycle, Central Zone Controlled				
Zone No	Initial Load	Power Peak	Final Burnup	Power Peak
1	0	2.594	8170	3.554
2	8170	1.896	12700	1.471
3	12700	.878	14700	.571
4	14700	.404	15600	.257
5	15600	.172	15900	.108
6	15900	.056	16000	.036
cycle length 2660 MWD/MTU				

TABLE 6.15 Discharge burnups of Trojan 17x17 2% fuels in
9 zone, normal cycle, whole core and central
zone controlled cases

17x17 2%, 9 Zone, Normal Cycle, Whole Core Controlled				
Zone No	Initial Load	Power Peak	Final Burnup	Power Peak
1	0	5.914	8250	4.534
2	8250	1.907	11300	2.127
3	11300	.659	12600	1.049
4	12600	.276	13200	.566
5	13200	.127	13500	.325
6	13500	.064	13700	.199
7	13700	.033	13800	.117
8	13800	.016	13840	.062
9	13840	.005	13880	.021
cycle length 1540 MWD/MTU				

17x17 2%, 9 Zone, Normal Cycle, Central Zone Controlled				
Zone No	Initial Load	Power Peak	Final Burnup	Power Peak
1	0	3.144	7150	4.338
2	7150	2.728	12100	2.344
3	12100	1.481	14800	1.122
4	14800	.775	16200	.565
5	16200	.416	16900	.301
6	16900	.236	17400	.171
7	17400	.131	17600	.095
8	17600	.067	17700	.048
9	17700	.023	17750	.016
cycle length 1970 MWD/MTU				

TABLE 6.16 Discharge burnups of Trojan 17x17 3%
fuels in 6 zone normal cycle whole core
and central zone controlled cases

17x17 3%, 6 Zone, Normal Cycle, Whole Core Controlled				
Zone No	Initial Load	Power Peak	Final Burnup	Power Peak
1	0	4.836	16000	3.455
2	16000	.916	20000	1.444
3	20000	.180	21300	.613
4	21300	.051	21800	.303
5	21800	.015	21980	.137
6	21980	.004	22100	.047
cycle length 3680 MWD/MTU				

17x17 3%, 6 Zone, Normal Cycle, Central Zone Controlled				
Zone No	Initial Load	Power Peak	Final Burnup	Power Peak
1	0	2.546	14800	3.952
2	14800	2.070	23500	1.355
3	23500	.858	27000	.439
4	27000	.350	28500	.170
5	28500	.134	29000	.065
6	29000	.042	29200	.020
cycle length 4860 MWD/MTU				

TABLE 6.17 Discharge burnups of Trojan 17x17 3% fuels
in 9 zone normal cycle whole core and
central zone controlled cases

17x17 3%, 9 Zone, Normal Cycle, Whole Core Controlled				
Zone No	Initial Load	Power Peak	Final Burnup	Power Peak
1	0	6.612	14700	4.495
2	14700	1.657	19500	2.141
3	19500	.458	21200	1.056
4	21200	.160	22000	.576
5	22000	.063	22400	.330
6	22400	.028	22600	.201
7	22600	.013	22700	.118
8	22700	.006	22800	.062
9	22800	.002	22820	.022
cycle length 2540 MWD/MTU				

17x17 3%, 9 Zone, Normal Cycle, Central Zones Controlled				
Zone No	Initial Load	Power Peak	Final Burnup	Power Peak
1	0	3.330	13600	5.151
2	13600	2.904	22200	2.169
3	22200	1.434	26300	.891
4	26300	.673	28300	.403
5	28300	.331	29300	.195
6	29300	.176	29800	.103
7	29800	.092	30000	.054
8	30000	.045	30200	.026
9	30200	.015	30250	.009
cycle length 3360 MWD/MTU				

TABLE 5.18 Discharge burnups of Trojan 18x18 3% fuels
in 6 zone normal cycle whole core and central
zone controlled cases

18x18 3%, 6 Zone, Normal Cycle, Whole Core Controlled				
Zone No	Initial Load	Power Peak	Final Burnup	Power Peak
1	0	4.585	12700	3.757
2	12700	1.048	16400	1.372
3	16400	.250	17600	.509
4	17600	.081	18000	.230
5	18000	.027	18200	.099
6	18200	.008	18270	.033
cycle length 3050 MWD/MTU				

18x18 3%, 6 Zone, Normal Cycle, Central Zone Controlled				
Zone No	Initial Load	Power Peak	Final Burnup	Power Peak
1	0	2.509	11600	3.356
2	11600	1.969	18800	1.592
3	18800	.897	22000	.631
4	22000	.404	23400	.274
5	23400	.167	24000	.112
6	24000	.054	24200	.036
cycle length 4030 MWD/MTU				

TABLE 6.19 Discharge burnups of Trojan 18x18 3% fuels
in 9 zone normal cycle whole core and central
zone controlled cases

18x18 3%, 9 Zone, Normal Cycle, Whole Core Controlled				
Zone No	Initial Load	Power Peak	Final Burnup	Power Peak
1	0	6.187	11500	5.249
2	11500	1.797	15400	2.011
3	15400	.584	17000	.856
4	17000	.233	17700	.417
5	17700	.105	18000	.222
6	18000	.052	18200	.127
7	18200	.026	18300	.070
8	18300	.012	18400	.036
9	18400	.004	18420	.012
cycle length 2050 MWD/MTU				

18x18 3%, 9 Zone, Normal Cycle, Central Zone Controlled				
Zone No	Initial Load	Power Peak	Final Burnup	Power Peak
1	0	3.226	10500	4.936
2	10500	2.715	17200	2.098
3	17200	1.454	21000	.956
4	21000	.756	23500	.480
5	23500	.405	25000	.254
6	25000	.230	25500	.143
7	25500	.128	26100	.079
8	26100	.065	26200	.040
9	26200	.022	26280	.014
cycle length 2920 MWD/MTU				

7. CONCLUSION

We learn from this study that an in-out refueling scheme is a natural process that a refueling pattern should follow if the fuel is going to deliver the most energy it can during its residence time in the reactor. Therefore, from the fuel maneuvering point of view, we should adopt an in-out refueling pattern in order to make best use of the fuel of a fixed design. From the fuel design point of view, we know from the discussion in Section (2.3), although no particular attempt of proof was made here, that if a fuel is to remain longer in the core so that higher burnup level can be obtained, the fuel should have a high initial k_{∞} value and a slowly decreasing k_{∞} against burnup, because both characteristics will result in a larger shaded area above $k_{\infty} = 1$ line in Figure (2.7) and thus a reactor of longer cycle length can be maintained by the fuel. To have a higher k_{∞} , one could increase the enrichment of the fuel. But to have a slowly decreasing k_{∞} against burnup, the fuel has to have high high fertile to fissile conversion ratio. This may require a reactor to be designed so that it could be operated under a higher energy spectrum, such as the case of breeder reactor, which makes a higher conversion ratio possible. This is out of our scope, but is mentioned here for reference purposes. A fuel of tighter lattice could also have a higher fertile to fissile conversion ratio and thus reduces the k decrease rate against burnup, but it reduces the

magnitude of k_{∞} too. These conflicting effects of lattice design on discharge burnup turn out in our case to lead to the preference of looser lattice fuel.

As far as the existing light water reactor is concerned, to increase the enrichment is the option available. However, in today's energy-scarce economy, the gain in discharge burnup by increasing enrichment may not be able to offset the energy cost increase needed for increasing the enrichment. To increase fuel utilization without incurring energy cost increases as the enrichment is increased, one resort would be to manufacture the fuel with a looser lattice design. A fuel with looser lattice, as our study has demonstrated, could have a net positive effect on discharge burnup. This is due to the stronger positive influence of a higher zero-burnup k_{∞} over the weaker negative effect of a lower fertile to fissile conversion ratio of the looser lattice. This suggestion of using a looser lattice fuel is contrary to the fuel design trend in the past. For years, fuel designers for the light-water reactors have been prone to a tighten lattice fuel design, based on the consideration that a tighter lattice design, such as 18x18 fuel would allow the reactor to maintain a higher licensed maximum power density with the fuels at a lower specific power level, thus reserving more Departure from Nucleate Boiling, DNB, margin (21) for heat transfer but bearing a higher carrying charge of fuel. When whole plant economy is concerned, a higher power density reactor would be more economical, if the uranium price is low. But as uranium price increases,

a looser lattice fuel could become more attractive, as far as fuel saving is concerned, even though it may reduce the reactor power density if a DNB margin must be preserved. It would be therefore worthwhile for the light-water reactor owners to consider using the fuels of looser lattice design. One more concern could help justify this suggestion. That is, in a once-through fuel cycle management scenario and a high uranium price market, the loss in plutonium due to lower fertile to fissile conversion ratio of a looser lattice fuel could be easily offset by the gain in discharge burnup of the same fuel due to better neutron thermalization.

From the viewpoint of refueling pattern maneuvering, the in-out refueling scheme is the best scheme one ought to follow if a maximum fuel discharge burnup is desired. Knowing this and also knowing that very large gains in discharge burnup are available from frequent refueling, an in-out refueling scheme with short cycle length deserves more study. A short cycle length undoubtedly will reduce plant availability since more reactor shutdowns are required for refuelings. This drawback in plant availability, of course, can be minimized and would not become a big obstacle to the adoption of an in-out refueling scheme with short cycle length if the refueling time can be reduced. In addition to the fuel cost saving, a short cycle length, such as a six-month cycle, has also some other potential benefits resulting from considerations of system load requirement, facilities inspection and maintenance planning that are interesting the nuclear industry.

The conventional out-in refueling scheme has a flatter power distribution than the in-out refueling scheme; the reactor can be run at a higher power density without risking exceeding the thermohydraulic safety margin when a power excursion happens.

The in-out refueling scheme has a very undesirable characteristic, namely, a high power peaking. In order to keep a required safety margin at the hot spot, the high peaking power distribution in an in-out refueling scheme will force such a reactor to run at a low power density or derated power level. This, consequently, will damage the plant economy unless the fuel in the core can tolerate a very high power peaking without losing its physical integrity. To minimize the disadvantage of the high power peaking, one can suppress the power peaking at the core center either by clustering the control rods at the central zone or by mixing the fresh fuels, which supposedly should be loaded into the reactor central zone in the in-out refueling scheme, with the fuels of higher burnup, or by the combination of both. How high a power peak the fuel can be subject to will determine the strategy of power control. It is also possible that a new reactor can be built economically to tolerate higher peaks; for example, by using large vessels for lower power reactors. Further study is needed in these respects.

As a summary of the above discussions, in view of the definite gain on discharge burnup by in-out refueling, the lesser severity of power peaking in a 6-zone scheme, the advantage of central zone reactivity control on both cycle length and power peaking and the matching of the cycle length of the 6-zone scheme with the 6-month

cycle operation schedule that is compatible with seasonal electrical demand loads, it is recommended that further efforts could be concentrated on the economic and technical studies of a 6-zone in-out refueling scheme with the first and second central batches scattered, and control concentrated in the more reactive zones.

From the results of this study, although the in-out refueling scheme is very promising in easing the cost of fuel in today's light-water reactor, other engineering compromises, such as designing reactors of lower power density and arranging for new control schemes that suppress power peaking, are needed. A combination of burnable poison and careful control rod placement might be useful for control.

Some anticipated future problems may be alleviated by the adoption of in-out refueling. For example, the life span of the reactor vessel might be improved because there would be decreased neutron flux and fluence there. Also, improvements in fuel design and manufacture are in the direction of requiring less DNB margin so that higher power peaking would be tolerable.

BIBLIOGRAPHY

1. B. I. Spinrad., "A Limiting Problem for High-Peaking, Low Leakage Fuel Management," unpublished.
2. B. I. Spinrad, J. C. Carter, and C. Eggler., "Reactivity Changes and Reactivity Lifetimes of Fixed-Fuel Elements in Thermal Reactors," Proc. Second U. N. Conf. on Peaceful Uses of At. Energy., V5, P/835, 1958.
3. R. F. Barry., "LEOPARD-A Spectrum Dependent Non-Spatial Depletion Code for the IBM-7094," WCAP-3269-26 (Sept. 1963).
4. L. E. Strawbridge., "Calculation of Lattice Parameters and Criticality for Uniform Water Moderated Lattices," WCAP-3269-26 (Sept. 1963).
5. J. R. Lamarsh., "Introduction to Nuclear Reactor Theory," Addison-Wesley Publishing Co., Inc., 1966.
6. Kaplan, S. "Synthesis Methods in Reactor Analysis". In: "Advances in Nuclear Science and Technology," ed. by P. Greebler and E. J. Hensly. Vol. 3. New York, Academic, 1966. P. 233-266.
7. Nenhold, R. J. "Multiple Weighting Functions in Fast Reactor Space-Energy Synthesis," Nuclear Science and Engineering 44:204-220, 1971.
8. K. E. Atkinson., "An Introduction to Numerical Analysis," John Wiley and Sons, New York, 1966.
9. B. Carnahan, H. A. Luther, J. O. Wilkes., "Applied Numerical Method," John Wiley and Sons, Inc.

10. Taiwan Power Company's Version of LEOPARD Code, a Version for Boiling Light-Water Reactor, Personal Communication.
11. Oregon State University's Version of LEOPARD Code.
12. R. A. Matzie, D. C. Leung, Y. Liu, R. W. Beekmann., "The Benefits of Cycle Stretchout In PWR Extended Burnup Fuel Cycles," TIS-6469.
13. Group Constants Provided by A. W. Prichard, Battelle, Pacific Northwest Laboratory, Personal Communication.
14. A. H. Robinson., "AHRCHB-A One-Dimension Two or Four Diffusion Criticality Code using Chebyshev Extrapolation to Converge the Fission Source," Personal Communication.
15. An IMSL Library Routine, LEQTLF "A solution to system of linear equations", IMSL Inc., Houston, Texas.
16. F. Scheid., "Theory and problems of numerical analysis."
17. E. D. Fuller, A. L. Phillips, F. E. Wicks, H. N. Andrews, C. A. Olmstead, H. G. Houser., "Optimizing the refuel cycle: two views-18 months and 6 months," Nuclear News, Sept, 1973., P.71.
18. J. Pop-Jordanov., "Lattice Cell Burnup Calculation," Unpublished
19. Station Nuclear Engineering Manual, General Electric Co., P. 22-1.
20. "Power Reactor 1978," Nuclear Engineering International, July 1978, Supplement.
21. "PWR Reference Core Report" WCAP 8185, Sept, 1973.

APPENDIX A

GROUP CONSTANTS OF TROJAN AND OCONEE FUELS

TABLE A-1 Group Constants for Trojan fuel of 15x15 lattice design with 3% enrichment

BURNUP	INDEX	1	2	3	4	5	6
BURNUP	RANGE						
FROM	MWD/T	0.00	20.00	60.00	100.00	500.00	1000.00
TO	MWD/T	20.00	60.00	100.00	500.00	1000.00	2000.00
D_1		1.458169	1.460925	1.463142	1.463543	1.465201	1.466400
D_1		.365567	.365596	.365596	.365566	.365229	.364831
Σ_{a1}		.568117E-02	.568922E-02	.569375E-02	.569203E-02	.566641E-02	.563073E-02
Σ_{a2}		.120065	.119469	.119011	.118954	.118865	.118840
$\nu_1 \Sigma f_1$.265760E-01	.266953E-01	.267886E-01	.268048E-01	.268674E-01	.269090E-01
$\nu_2 \Sigma f_2$.723682E-01	.738184E-01	.749769E-01	.751825E-01	.759693E-01	.764049E-01
k_{∞}		1.351505	1.323745	1.302397	1.298761	1.285036	1.276286
P_r		.68581	.68639	.68682	.68686	.68675	.68629
Σf_1		.220464E-02	.220792E-02	.220964E-02	.220875E-02	.219642E-02	.217960E-02
Σf_2		.778921E-01	.781995E-01	.784443E-01	.784864E-01	.786185E-01	.786163E-01
MATERIAL	BUCKLING	.579900E-02	.537870E-02	.505090E-02	.499460E-02	.478110E-02	.464340E-02

BURNUP	INDEX	7	8	9	10	11	12
BURNUP	RANGE						
FROM	MWD/T	2000.00	3000.00	5000.00	7000.00	9000.00	11000.00
TO	MWD/T	3000.00	5000.00	7000.00	9000.00	11000.00	13000.00
D_1		1.468646	1.471137	1.476158	1.481397	1.486762	1.492334
D_1		.364122	.363514	.362538	.361790	.361211	.360761
Σ_{a1}		.555671E-02	.548157E-02	.532952E-02	.517799E-02	.502854E-02	.488216E-02
Σ_{a2}		.118586	.118047	.116320	.113996	.111254	.108209
$\nu_1 \Sigma f_1$.269832E-01	.270657E-01	.272263E-01	.273875E-01	.275457E-01	.277029E-01
$\nu_2 \Sigma f_2$.769364E-01	.772842E-01	.775615E-01	.774215E-01	.769740E-01	.762921E-01
k_{∞}		1.261093	1.245350	1.213180	1.181408	1.150554	1.120725
P_r		.68487	.68306	.67878	.67434	.67011	.66626
Σf_1		.214520E-02	.211068E-02	.204174E-02	.197373E-02	.190711E-02	.184219E-02
Σf_2		.784258E-01	.780789E-01	.770353E-01	.756605E-01	.740536E-01	.722792E-01
MATERIAL	BUCKLING	.440160E-02	.413350E-02	.361430E-02	.309240E-02	.257800E-02	.206230E-02

TABLE A-1 CONTINUED

BURNUP	INDEX	13	14	15	16	17	18
BURNUP	RANGE						
FROM	MWD/T	13000.00	15000.00	17000.00	19000.00	21000.00	23000.00
TO	MWD/T	15000.00	17000.00	19000.00	21000.00	23000.00	25000.00
D_1		1.497841	1.503499	1.509384	1.515372	1.514069	1.509074
D_1		.360412	.360145	.359945	.359799	.359699	.359637
Σ_{a1}		.473861E-02	.459862E-02	.446247E-02	.433009E-02	.420192E-02	.407793E-02
Σ_{a2}		.104939	.101506	.097957	.094330	.090665	.086994
$v_1 \Sigma f_1$.278501E-01	.279943E-01	.281371E-01	.282746E-01	.284109E-01	.285474E-01
$v_2 \Sigma f_2$.754281E-01	.744237E-01	.733119E-01	.721206E-01	.708755E-01	.695992E-01
k_{∞}		1.091800	1.063656	1.036145	1.009119	.982488	.956182
P_F		.66276	.65966	.65691	.65448	.65234	.65048
Σf_1		.177887E-02	.171740E-02	.165788E-02	.160030E-02	.154481E-02	.149144E-02
Σf_2		.703823E-01	.683985E-01	.663558E-01	.642781E-01	.621877E-01	.601049E-01
MATERIAL	BUCKLING	.157680E-02	.109750E-02	.618770E-03	.154490E-03	.309160E-03	.774250E-03

BURNUP	INDEX	19	20	21	22	23	24
BURNUP	RANGE						
FROM	MWD/T	25000.00	27000.00	29000.00	31000.00	33000.00	35000.00
TO	MWD/T	27000.00	29000.00	31000.00	33000.00	35000.00	37000.00
D_1		1.504143	1.499300	1.494260	1.489446	1.484730	1.480145
D_2		.359607	.359603	.359621	.359659	.359711	.359775
Σ_{a1}		.395843E-02	.384377E-02	.373472E-02	.363120E-02	.353387E-02	.344309E-02
Σ_{a2}		.083351	.079768	.076277	.072905	.069682	.066636
$v_1 \Sigma f_1$.286839E-01	.288204E-01	.289633E-01	.291031E-01	.292432E-01	.293824E-01
$v_2 \Sigma f_2$.683123E-01	.670344E-01	.657837E-01	.645752E-01	.634249E-01	.623451E-01
k_{∞}		.930172	.904469	.879150	.854272	.829981	.806439
P_F		.64884	.64741	.64618	.64508	.64410	.64320
Σf_1		.144030E-02	.139151E-02	.134534E-02	.130177E-02	.126101E-02	.122318E-02
Σf_2		.580489E-01	.560380E-01	.540901E-01	.522206E-01	.504458E-01	.487794E-01
MATERIAL	BUCKLING	.123970E-02	.170390E-02	.219000E-02	.266440E-02	.313740E-02	.360660E-02

TABLE A-1 CONTINUED

BURNUP	INDEX	25	26	27	28	29	30
BURNUP	RANGE						
FROM	MWD/T	37000.00	39000.00	41000.00	43000.00	45000.00	47000.00
TO	MWD/T	39000.00	41000.00	43000.00	45000.00	47000.00	49000.00
D_1		1.476080	1.472077	1.468395	1.464800	1.461753	1.459101
D_2		.359849	.359930	.360016	.360106	.360198	.360290
Σa_1		.335888E-02	.328202E-02	.321237E-02	.315016E-02	.309475E-02	.304603E-02
Σa_2		.063788	.061161	.058765	.056607	.054684	.052993
$v_1 \Sigma f_1$.295113E-01	.296412E-01	.297653E-01	.298897E-01	.300019E-01	.301057E-01
$v_2 \Sigma f_2$.613461E-01	.604369E-01	.596196E-01	.588941E-01	.582544E-01	.576938E-01
k_∞		.783798	.762307	.742118	.723419	.706286	.690840
P_r		.64233	.64151	.64070	.63989	.63903	.63811
Σf_1		.118828E-02	.115656E-02	.112795E-02	.110246E-02	.107988E-02	.106011E-02
Σf_2		.472325E-01	.458157E-01	.445326E-01	.433845E-01	.423670E-01	.414751E-01
MATERIAL	BUCKLING	.403830E-02	.447120E-02	.488250E-02	.529230E-02	.565930E-02	.599550E-02

BURNUP	INDEX	31	32	33	34	35	36
BURNUP	RANGE						
FROM	MWD/T	49000.00	51000.00	53000.00	55000.00	57000.00	59000.00
TO	MWD/T	51000.00	53000.00	55000.00	57000.00	59000.00	61000.00
D_1		1.456861	1.455036	1.453634	1.452642	1.452056	1.451500
D_2		.360382	.360473	.360563	.360652	.360739	.360809
Σa_1		.300352E-02	.296667E-02	.293482E-02	.290728E-02	.288335E-02	.286235E-02
Σa_2		.051523	.050255	.049170	.048244	.047454	.046644
$v_1 \Sigma f_1$.302001E-01	.302848E-01	.303595E-01	.304238E-01	.304780E-01	.305322E-01
$v_2 \Sigma f_2$.572002E-01	.567583E-01	.563502E-01	.559559E-01	.555539E-01	.551534E-01
k_∞		.677127	.665149	.654875	.646254	.639221	.632111
P_r		.63713	.63607	.63492	.63367	.63233	.63103
Σf_1		.104295E-02	.102814E-02	.101542E-02	.100449E-02	.995086E-03	.986084E-03
Σf_2		.406985E-01	.400241E-01	.394365E-01	.389189E-01	.384536E-01	.379444E-01
MATERIAL	BUCKLING	.629870E-02	.656730E-02	.680030E-02	.699740E-02	.715850E-02	.730550E-02

TABLE A-2 Group Constants for Trojan Fuel of 17x17 Lattice
Design with 2% Enrichment

BURNUP	INDEX	1	2	3	4	5	6
BURNUP	RANGE						
FROM	MWD/T	0.00	20.00	60.00	100.00	500.00	1000.00
TO	MWD/T	20.00	60.00	100.00	500.00	1000.00	2000.00
D_1		1.398225	1.400718	1.402019	1.402278	1.403728	1.404847
D_2		.398630	.398665	.398620	.398540	.397762	.396883
Σ_{a1}		.559393E-02	.560195E-02	.560459E-02	.560347E-02	.558675E-02	.556118E-02
Σ_{a2}		.106348	.105817	.105663	.105765	.106948	.108306
$\nu_1 \Sigma f_1$.247691E-01	.249040E-01	.249720E-01	.249845E-01	.250497E-01	.250936E-01
$\nu_2 \Sigma f_2$.676148E-01	.694610E-01	.704737E-01	.707307E-01	.722909E-01	.735604E-01
k_{∞}		1.196189	1.166009	1.151157	1.148500	1.136372	1.128295
ρ_r		.61745	.61828	.61863	.61861	.61790	.61632
Σf_1		.214917E-02	.215241E-02	.215316E-02	.215234E-02	.214191E-02	.212724E-02
Σf_2		.776565E-01	.783304E-01	.787354E-01	.788742E-01	.798469E-01	.807050E-01
MATERIAL	BUCKLING	.316420E-02	.270310E-02	.247280E-02	.243150E-02	.222880E-02	.210530E-02

BURNUP	INDEX	7	8	9	10	11	12
BURNUP	RANGE						
FROM	MWD/T	2000.00	3000.00	5000.00	7000.00	9000.00	11000.00
TO	MWD/T	3000.00	5000.00	7000.00	9000.00	11000.00	13000.00
D_1		1.407265	1.409930	1.415438	1.420933	1.424306	1.420447
D_2		.395411	.394220	.392435	.391148	.390194	.389476
Σ_{a1}		.550493E-02	.544645E-02	.532726E-02	.521296E-02	.510490E-02	.500225E-02
Σ_{a2}		.110301	.111602	.112757	.112843	.112268	.111254
$\nu_1 \Sigma f_1$.251875E-01	.252906E-01	.254965E-01	.256913E-01	.258735E-01	.260359E-01
$\nu_2 \Sigma f_2$.755654E-01	.771744E-01	.794308E-01	.809631E-01	.819854E-01	.826436E-01
k_{∞}		1.111472	1.093264	1.057602	1.024508	.994562	.967322
ρ_r		.61221	.60753	.59815	.58964	.58217	.57560
Σf_1		.209669E-02	.206602E-02	.200542E-02	.194822E-02	.189467E-02	.184435E-02
Σf_2		.819396E-01	.827714E-01	.835417E-01	.836683E-01	.833847E-01	.828299E-01
MATERIAL	BUCKLING	.184260E-02	.155210E-02	.968860E-03	.414460E-03	.106590E-03	.569250E-03

TABLE A-2 CONTINUED

BURNUP	INDEX	13	14	15	16	17	18
BURNUP	RANGE						
FROM	MWD/T	13000.00	15000.00	17000.00	19000.00	21000.00	23000.00
TO	MWD/T	15000.00	17000.00	19000.00	21000.00	23000.00	25000.00
D1		1.416844	1.413577	1.410612	1.407610	1.404999	1.402578
D2		.388932	.388522	.388217	.387993	.387836	.387732
Σa_1		.490527E-02	.481349E-02	.472667E-02	.464508E-02	.456795E-02	.449551E-02
Σa_2		.109945	.108436	.106799	.105087	.103340	.101597
$v_1 \Sigma f_1$.261898E-01	.263332E-01	.264675E-01	.266015E-01	.267242E-01	.268410E-01
$v_2 \Sigma f_2$.830376E-01	.832361E-01	.832918E-01	.832464E-01	.831301E-01	.829718E-01
k_{∞}		.942410	.919456	.898177	.878391	.859867	.842503
P_r		.56985	.56477	.56027	.55630	.55273	.54953
Σf_1		.179730E-02	.175325E-02	.171206E-02	.167375E-02	.163799E-02	.160478E-02
Σf_2		.820961E-01	.812445E-01	.813210E-01	.793610E-01	.783890E-01	.774293E-01
MATERIAL	BUCKLING	.100960E-02	.142100E-02	.180640E-02	.219490E-02	.254960E-02	.288790E-02

BURNUP	INDEX	19	20	21	22	23	24
BURNUP	RANGE						
FROM	MWD/T	25000.00	27000.00	29000.00	31000.00	33000.00	35000.00
TO	MWD/T	27000.00	29000.00	31000.00	33000.00	35000.00	37000.00
D1		1.400335	1.398259	1.396600	1.394935	1.393444	1.392125
D2		.387669	.387641	.387640	.387660	.387697	.387746
Σa_1		.442775E-02	.436463E-02	.430582E-02	.425181E-02	.420224E-02	.415697E-02
Σa_2		.099885	.098228	.096645	.095155	.093765	.092482
$v_1 \Sigma f_1$.269524E-01	.270587E-01	.271532E-01	.272476E-01	.273372E-01	.274218E-01
$v_2 \Sigma f_2$.827932E-01	.826116E-01	.824404E-01	.822924E-01	.821720E-01	.820829E-01
k_{∞}		.826199	.810880	.796459	.782956	.770306	.758884
P_r		.54663	.54400	.54156	.53932	.53723	.53526
Σf_1		.157406E-02	.154574E-02	.151966E-02	.149590E-02	.147429E-02	.145471E-02
Σf_2		.764991E-01	.756123E-01	.747792E-01	.740104E-01	.733080E-01	.726743E-01
MATERIAL	BUCKLING	.321100E-02	.351970E-02	.379140E-02	.406420E-02	.432200E-02	.455730E-02

TABLE A-2 CONTINUED

BURNUP	INDEX	25	26	27	28	29	30
BURNUP	RANGE						
FROM	MWD/T	37000.00	39000.00	41000.00	43000.00	45000.00	47000.00
TO	MWD/T	39000.00	41000.00	43000.00	45000.00	47000.00	49000.00
D1		1.390979	1.390006	1.388959	1.388271	1.387750	1.387397
D2		.387806	.387872	.387945	.388022	.388104	.388188
λ_{a1}		.411581E-02	.407856E-02	.404520E-02	.401495E-02	.398776E-02	.396330E-02
λ_{a2}		.091309	.090247	.089294	.088441	.087686	.087020
$v_1 \Sigma f_1$.275017E-01	.275768E-01	.276544E-01	.277219E-01	.277849E-01	.278434E-01
$v_2 \Sigma f_2$.820259E-01	.819990E-01	.819977E-01	.820121E-01	.820361E-01	.820585E-01
k_{eff}		.747463	.737232	.727799	.719449	.711099	.703842
ρ_r		.53337	.53156	.52982	.52809	.52637	.52464
Σf_1		.143706E-02	.142120E-02	.140707E-02	.139436E-02	.138303E-02	.137291E-02
Σf_2		.721093E-01	.716106E-01	.711738E-01	.707896E-01	.704535E-01	.701564E-01
MATERIAL	BUCKLING	.479260E-02	.500520E-02	.522570E-02	.546825E-02	.558480E-02	.574530E-02

BURNUP	INDEX	31	32	33	34	35	36
BURNUP	RANGE						
FROM	MWD/T	49000.00	51000.00	53000.00	55000.00	57000.00	59000.00
TO	MWD/T	51000.00	53000.00	55000.00	57000.00	59000.00	61000.00
D1		1.387211	1.387196	1.387354	1.387689	1.388207	1.388917
D2		.388276	.388368	.388465	.388567	.388677	.388794
λ_{a1}		.394124E-02	.392123E-02	.390290E-02	.388591E-02	.386991E-02	.385453E-02
λ_{a2}		.086433	.085914	.085453	.085036	.084650	.084282
$v_1 \Sigma f_1$.278976E-01	.279472E-01	.279922E-01	.280327E-01	.280685E-01	.280992E-01
$v_2 \Sigma f_2$.820665E-01	.820456E-01	.819799E-01	.818520E-01	.816431E-01	.813335E-01
k_{eff}		.697295	.691450	.686304	.681857	.678119	.675108
ρ_r		.52289	.52112	.51930	.51742	.51549	.51347
Σf_1		.136385E-02	.135570E-02	.134832E-02	.134155E-02	.133527E-02	.132932E-02
Σf_2		.698681E-01	.696375E-01	.693924E-01	.691403E-01	.688676E-01	.685607E-01
MATERIAL	BUCKLING	.588890E-02	.601730E-02	.613040E-02	.622770E-02	.630860E-02	.637230E-02

TABLE A-3 Group Constants for Trojan Fuels of 17x17 Lattice
Design with 3% Enrichment

BURNUP	INDEX	1	2	3	4	5	6
BURNUP	RANGE						
FROM	MWD/T	0.00	20.00	60.00	100.00	500.00	1000.00
TO	MWD/T	20.00	60.00	100.00	500.00	1000.00	2000.00
D1		1.393948	1.396215	1.397544	1.397775	1.399100	1.400147
D2		.397780	.397772	.397718	.397650	.396979	.396204
Σa_1		.702113E-02	.703413E-02	.703953E-02	.703798E-02	.701551E-02	.698234E-02
Σa_2		.150337	.149391	.148903	.148925	.149533	.150398
$v_1 \Sigma f_1$.245424E-01	.246741E-01	.247490E-01	.247610E-01	.248247E-01	.248690E-01
$v_2 \Sigma f_2$.881506E-01	.902568E-01	.915647E-01	.918141E-01	.932820E-01	.943555E-01
k_∞		1.285573	1.256364	1.239346	1.236700	1.223228	1.214513
P_T		.58650	.58735	.58777	.58778	.58739	.58642
Σf_1		.273104E-02	.273642E-02	.273843E-02	.273751E-02	.272542E-02	.270836E-02
Σf_2		.104975E+00	.105587E+00	.105991E+00	.106096E+00	.106815E+00	.107407E+00
MATERIAL	BUCKLING	.466880E-02	.420960E-02	.395030E-02	.390980E-02	.370300E-02	.356830E-02

BURNUP	INDEX	7	8	9	10	11	12
BURNUP	RANGE						
FROM	MWD/T	2000.00	3000.00	5000.00	7000.00	9000.00	11000.00
TO	MWD/T	3000.00	5000.00	7000.00	9000.00	11000.00	13000.00
D1		1.402165	1.404324	1.408791	1.413353	1.417748	1.422207
D2		.394853	.393711	.391908	.390537	.389473	.388639
Σa_1		.691174E-02	.683928E-02	.669182E-02	.654645E-02	.640385E-02	.626514E-02
Σa_2		.151737	.152587	.153173	.152815	.151811	.150335
$v_1 \Sigma f_1$.249509E-01	.250373E-01	.252130E-01	.253853E-01	.255423E-01	.256899E-01
$v_2 \Sigma f_2$.959744E-01	.972958E-01	.991967E-01	.100464E+00	.101254E+00	.101680E+00
k_∞		1.198992	1.182760	1.150620	1.120086	1.091751	1.065493
P_T		.58378	.58063	.57388	.56738	.56142	.55608
Σf_1		.267300E-02	.263740E-02	.256632E-02	.249709E-02	.242977E-02	.236471E-02
Σf_2		.108226E+00	.108754E+00	.109128E+00	.108931E+00	.108333E+00	.107442E+00
MATERIAL	BUCKLING	.332530E-02	.306760E-02	.254810E-02	.203450E-02	.156660E-02	.112480E-02

TABLE A-3 CONTINUED

BURNUP	INDEX	13	14	15	16	17	18
BURNUP	RANGE						
FROM	MWD/T	13000.00	15000.00	17000.00	19000.00	21000.00	23000.00
TO	MWD/T	15000.00	17000.00	19000.00	21000.00	23000.00	25000.00
D ₁		1.426373	1.430547	1.433356	1.430486	1.427662	1.424976
D ₂		.387981	.387466	.387064	.386756	.386527	.386363
Σa_1		.613050E-02	.599941E-02	.587246E-02	.574856E-02	.562838E-02	.551166E-02
Σa_2		.148499	.146382	.144048	.141541	.138904	.136172
$v_1 \Sigma f_1$.258299E-01	.259588E-01	.260846E-01	.261993E-01	.263121E-01	.264207E-01
$v_2 \Sigma f_2$.101820E+00	.101731E+00	.101459E+00	.101039E+00	.100503E+00	.998756E-01
k _∞		1.041048	1.018125	.996522	.975997	.956429	.937677
P _r		.55132	.54707	.54330	.53992	.53691	.53422
Σf_1		.230194E-02	.224102E-02	.218286E-02	.212634E-02	.207193E-02	.201952E-02
Σf_2		.106330E+00	.105049E+00	.103640E+00	.102132E+00	.100554E+00	.989267E-01
MATERIAL	BUCKLING	.702400E-03	.312260E-03	.728710E-04	.424530E-03	.772550E-03	.110940E-02

BURNUP	INDEX	19	20	21	22	23	24
BURNUP	RANGE						
FROM	MWD/T	25000.00	27000.00	29000.00	31000.00	33000.00	35000.00
TO	MWD/T	27000.00	29000.00	31000.00	33000.00	35000.00	37000.00
D ₁		1.422417	1.419980	1.417395	1.415062	1.412815	1.410657
D ₂		.386254	.386192	.386170	.386181	.386221	.386286
Σa_1		.539845E-02	.528885E-02	.518344E-02	.508157E-02	.498374E-02	.489006E-02
Σa_2		.133373	.130537	.127688	.124846	.122036	.119277
$v_1 \Sigma f_1$.265257E-01	.266271E-01	.267323E-01	.268311E-01	.269278E-01	.270226E-01
$v_2 \Sigma f_2$.991784E-01	.984307E-01	.976491E-01	.968456E-01	.960339E-01	.952239E-01
k _∞		.919641	.902246	.885469	.869222	.853511	.838334
P _r		.53182	.52967	.52777	.52603	.52446	.52302
Σf_1		.196911E-02	.192070E-02	.187448E-02	.183020E-02	.178800E-02	.174791E-02
Σf_2		.972698E-01	.956007E-01	.939349E-01	.922837E-01	.906609E-01	.890772E-01
MATERIAL	BUCKLING	.143610E-02	.175310E-02	.208380E-02	.239400E-02	.269800E-02	.299570E-02

TABLE A-3 CONTINUED

BURNUP	INDEX	25	26	27	28	29	30
BURNUP	RANGE						
FROM	MWD/T	37000.00	39000.00	41000.00	43000.00	45000.00	47000.00
TO	MWD/T	39000.00	41000.00	43000.00	45000.00	47000.00	49000.00
D1		1.408592	1.406628	1.405042	1.403399	1.401907	1.400580
D2		.386370	.386471	.386587	.386714	.386850	.386994
Σ_{a1}		.480071E-02	.471576E-02	.463494E-02	.455899E-02	.448757E-02	.442063E-02
Σ_{a2}		.116598	.113983	.111476	.109084	.106810	.104660
$\nu_1 \Sigma f_1$.271154E-01	.272063E-01	.272871E-01	.273710E-01	.274515E-01	.275283E-01
$\nu_2 \Sigma f_2$.944234E-01	.936379E-01	.928708E-01	.921258E-01	.913993E-01	.906877E-01
k_{∞}		.823700	.809628	.796116	.783260	.771067	.759577
ρ_r		.52168	.52043	.51920	.51804	.51689	.51575
Σf_1		.170994E-02	.167411E-02	.164029E-02	.160869E-02	.157919E-02	.155171E-02
Σf_2		.875413E-01	.860603E-01	.846397E-01	.832858E-01	.819975E-01	.807745E-01
MATERIAL	BUCKLING	.328670E-02	.357060E-02	.382240E-02	.408110E-02	.432800E-02	.456200E-02

BURNUP	INDEX	31	32	33	34	35	36
BURNUP	RANGE						
FROM	MWD/T	49000.00	51000.00	53000.00	55000.00	57000.00	59000.00
TO	MWD/T	51000.00	53000.00	55000.00	57000.00	59000.00	61000.00
D1		1.399430	1.398471	1.397479	1.396873	1.396499	1.396362
D2		.387146	.387304	.387467	.387637	.387814	.387997
Σ_{a1}		.435807E-02	.429972E-02	.424565E-02	.419502E-02	.414781E-02	.410367E-02
Σ_{a2}		.102637	.100741	.098969	.097310	.095760	.094309
$\nu_1 \Sigma f_1$.276012E-01	.276700E-01	.277410E-01	.278018E-01	.278574E-01	.279073E-01
$\nu_2 \Sigma f_2$.899847E-01	.892817E-01	.885672E-01	.878250E-01	.870413E-01	.861975E-01
k_{∞}		.748832	.738872	.729764	.721482	.714098	.707653
ρ_r		.51455	.51333	.51209	.51076	.50934	.50782
Σf_1		.152621E-02	.150258E-02	.148082E-02	.146061E-02	.144192E-02	.142459E-02
Σf_2		.796140E-01	.785112E-01	.774592E-01	.764459E-01	.754632E-01	.744981E-01
MATERIAL	BUCKLING	.478170E-02	.498590E-02	.519590E-02	.537060E-02	.552650E-02	.566210E-02

TABLE A-4 Group Constants for Trojan Fuels of 18x18 Lattice
Design with 3% Enrichment

BURNUP FROM TO	INDEX RANGE MWD/T MWD/T	1	2	3	4	5	6
		0 20	20 60	60 100	100 500	500 1000	1000 2000
D ₁		1.360430	1.362210	1.363176	1.363557	1.364527	1.365520
D ₁		.417045	.416981	.416875	.416774	.415813	.414720
Σ _{a1}		.767491E-02	.768972E-02	.769565E-02	.769453E-02	.767649E-02	.764607E-02
Σ _{a2}		.165016	.163845	.163367	.163453	.164672	.166306
v ₁ Σf ₁		.234302E-01	.235556E-01	.236215E-01	.236325E-01	.236973E-01	.237447E-01
v ₂ Σf ₂		.958136E-01	.982677E-01	.996355E-01	.999315E-01	.101915E+00	.103512E+00
k _∞		1.239058	1.210271	1.195566	1.193222	1.180006	1.171201
P _F		.52990	.53080	.53121	.53119	.53057	.52925
Σf ₁		.298972E-02	.299586E-02	.299806E-02	.299724E-02	.298624E-02	.297024E-02
Σf ₂		.121015E+00	.121856E+00	.122373E+00	.122537E+00	.123804E+00	.124970E+00
MATERIAL	BUCKLING	.385760E-02	.342530E-02	.320020E-02	.316430E-02	.296110E-02	.282490E-02

BURNUP FROM TO	INDEX RANGE MWD/T MWD/T	7	8	9	10	11	12
		2000 3000	3000 5000	5000 7000	7000 9000	9000 11000	11000 13000
D ₁		1.367464	1.369601	1.373782	1.377934	1.382014	1.385825
D ₂		.412836	.411254	.408771	.406874	.405384	.404194
Σ _{a1}		.758583E-02	.752213E-02	.738980E-02	.726072E-02	.713640E-02	.701611E-02
Σ _{a2}		.169046	.171149	.173908	.175502	.176313	.176549
v ₁ Σf ₁		.238331E-01	.239310E-01	.241135E-01	.242871E-01	.244498E-01	.245944E-01
v ₂ Σf ₂		.106024E+00	.108157E+00	.111440E+00	.113958E+00	.116693E+00	.119738E+00
k _∞		1.155411	1.138929	1.106907	1.077166	1.050324	1.025947
P _F		.52578	.52181	.51356	.50584	.49890	.49267
Σf ₁		.293667E-02	.290312E-02	.283539E-02	.277012E-02	.270768E-02	.264769E-02
Σf ₂		.126781E+00	.128191E+00	.130051E+00	.131167E+00	.131759E+00	.131969E+00
MATERIAL	BUCKLING	.257770E-02	.230090E-02	.179110E-02	.130510E-02	.847540E-03	.443600E-03

TABLE A-4 CONTINUED

BURNUP	INDEX	13	14	15	16	17	18
BURNUP	RANGE						
FROM	MWD/T	13000.00	15000.00	17000.00	19000.00	21000.00	23000.00
TO	MWD/T	15000.00	17000.00	19000.00	21000.00	23000.00	25000.00
D ₁		1.389705	1.389225	1.385945	1.383877	1.381900	1.380254
D ₂		.403232	.402450	.401818	.401298	.400877	.400541
Σa_1		.690092E-02	.678941E-02	.668237E-02	.657860E-02	.647873E-02	.638199E-02
Σa_2		.176345	.175309	.174980	.173947	.172729	.171369
$v_1 \Sigma f_1$.247319E-01	.248564E-01	.249741E-01	.250845E-01	.251886E-01	.252869E-01
$v_2 \Sigma f_2$.118528E+00	.119393E+00	.120032E+00	.120485E+00	.120787E+00	.120965E+00
k _∞		1.003725	.983295	.964395	.946790	.930320	.914915
P _r		.48715	.48215	.47765	.47364	.47009	.46670
Σf_1		.259052E-02	.253567E-02	.248321E-02	.243296E-02	.238480E-02	.233867E-02
Σf_2		.131890E+00	.131586E+00	.131106E+00	.130489E+00	.129763E+00	.128952E+00
MATERIAL	BUCKLING	.562860E-03	.293500E-03	.626090E-03	.939390E-03	.123550E-02	.151630E-02

BURNUP	INDEX	19	20	21	22	23	24
BURNUP	RANGE						
FROM	MWD/T	25000.00	27000.00	29000.00	31000.00	33000.00	35000.00
TO	MWD/T	27000.00	29000.00	31000.00	33000.00	35000.00	37000.00
D ₁		1.379685	1.376980	1.375571	1.374253	1.373027	1.371891
D ₂		.400277	.400066	.399910	.399798	.399725	.399685
Σa_1		.628849E-02	.619878E-02	.611172E-02	.602777E-02	.594691E-02	.586913E-02
Σa_2		.169890	.168333	.166703	.165027	.163324	.161607
$v_1 \Sigma f_1$.253799E-01	.254753E-01	.255623E-01	.256458E-01	.257263E-01	.258041E-01
$v_2 \Sigma f_2$.121042E+00	.121036E+00	.120931E+00	.120831E+00	.120659E+00	.120450E+00
k _∞		.900165	.886301	.873091	.860476	.848489	.836974
P _r		.46375	.46100	.45852	.45623	.45412	.45216
Σf_1		.229448E-02	.225240E-02	.221197E-02	.217336E-02	.213657E-02	.210140E-02
Σf_2		.128078E+00	.127150E+00	.126202E+00	.125235E+00	.124238E+00	.123240E+00
MATERIAL	BUCKLING	.178310E-02	.206040E-02	.231220E-02	.255490E-02	.278920E-02	.301560E-02

TABLE A-4 CONTINUED

BURNUP	INDEX	25	26	27	28	29	30
BURNUP	RANGE						
FROM	MWD/T	37000.00	39000.00	41000.00	43000.00	45000.00	47000.00
TO	MWD/T	39000.00	41000.00	43000.00	45000.00	47000.00	49000.00
D_1		1.370343	1.369279	1.369221	1.368495	1.367863	1.367267
D_2		.399473	.399483	.399719	.399723	.399813	.399232
Σ_{a1}		.579411E-02	.572272E-02	.565362E-02	.558788E-02	.552503E-02	.546488E-02
Σ_{a2}		.159873	.158187	.156504	.154832	.153257	.151696
$\nu_1 \Sigma f_1$.258792E-01	.259519E-01	.260161E-01	.260885E-01	.261463E-01	.262076E-01
$\nu_2 \Sigma f_2$.120212E+00	.119948E+00	.119660E+00	.119350E+00	.119014E+00	.118646E+00
k_{∞}		.825981	.815430	.805423	.795838	.786787	.778183
P_T		.45033	.44859	.44690	.44529	.44373	.44220
Σf_1		.206794E-02	.203613E-02	.200577E-02	.197709E-02	.194991E-02	.192418E-02
Σf_2		.122263E+00	.121287E+00	.120325E+00	.119388E+00	.118452E+00	.117538E+00
MATERIAL	BUCKLING	-.323420E-02	-.344550E-02	-.362950E-02	-.382040E-02	-.400270E-02	-.417610E-02

BURNUP	INDEX	31	32	33	34	35	36
BURNUP	RANGE						
FROM	MWD/T	49000.00	51000.00	53000.00	55000.00	57000.00	59000.00
TO	MWD/T	51000.00	53000.00	55000.00	57000.00	59000.00	61000.00
D_1		1.366943	1.366653	1.366495	1.366463	1.366300	1.366338
D_2		.400043	.400167	.400310	.400460	.400645	.400842
Σ_{a1}		.540764E-02	.535283E-02	.530041E-02	.525018E-02	.520189E-02	.515569E-02
Σ_{a2}		.150181	.149713	.149297	.148924	.148591	.148291
$\nu_1 \Sigma f_1$.262662E-01	.263221E-01	.263751E-01	.264251E-01	.264719E-01	.265218E-01
$\nu_2 \Sigma f_2$.118240E+00	.117788E+00	.117279E+00	.116699E+00	.116035E+00	.115289E+00
k_{∞}		.770078	.762473	.755397	.748861	.742894	.737356
P_T		.44064	.43912	.43756	.43608	.43460	.43322
Σf_1		.189977E-02	.187667E-02	.185478E-02	.183399E-02	.181421E-02	.179542E-02
Σf_2		.116637E+00	.115743E+00	.114850E+00	.113951E+00	.113037E+00	.112098E+00
MATERIAL	BUCKLING	-.434010E-02	-.449410E-02	-.463760E-02	-.477000E-02	-.489050E-02	-.501760E-02

TABLE A-5 Group Constants for Oconee Fuels of 15x15 Lattice
Design with 3% Enrichment

BURNUP	INDEX	1	2	3	4	5	6
BURNUP	RANGE						
FROM	MWD/T	0.00	20.00	60.00	100.00	600.00	1000.00
TO	MWD/T	20.00	60.00	100.00	600.00	1000.00	2000.00
D ₁		1.442540	1.444910	1.446200	1.446400	1.447850	1.448580
D ₂		.387959	.387952	.387899	.387834	.387050	.386470
Σ_{a1}		.633317E-02	.634337E-02	.634723E-02	.634601E-02	.632414E-02	.630376E-02
Σ_{a2}		.134770	.134060	.133770	.133833	.134807	.135590
$\nu_1 \Sigma f_1$.249636E-01	.250817E-01	.251441E-01	.251533E-01	.252139E-01	.252415E-01
$\nu_2 \Sigma f_2$.797644E-01	.814723E-01	.824313E-01	.826208E-01	.841006E-01	.848781E-01
k _∞		1.331000	1.303070	1.288550	1.286470	1.273340	1.267710
P _r		.63781	.63850	.63881	.63881	.63831	.63763
Σf_1		.246100E-02	.246517E-02	.246652E-02	.246572E-02	.245319E-02	.244211E-02
Σf_2		.552622E-01	.549621E-01	.548215E-01	.548245E-01	.549709E-01	.551034E-01
MATERIAL	BUCKLING	.525547E-02	.484733E-02	.463286E-02	.460220E-02	.440858E-02	.432565E-02

BURNUP	INDEX	7	8	9	10	11	12
BURNUP	RANGE						
FROM	MWD/T	2000.00	2800.00	3000.00	5000.00	6600.00	8000.00
TO	MWD/T	2800.00	3000.00	5000.00	6600.00	8000.00	10000.00
D ₁		1.450500	1.452100	1.452500	1.456600	1.460000	1.462950
D ₂		.385207	.384330	.384130	.382430	.381360	.380590
Σ_{a1}		.624953E-02	.620408E-02	.619266E-02	.607367E-02	.597801E-02	.589467E-02
Σ_{a2}		.137170	.138080	.138270	.139330	.139480	.139240
$\nu_1 \Sigma f_1$.253133E-01	.25370E-01	.253859E-01	.255336E-01	.256511E-01	.257505E-01
$\nu_2 \Sigma f_2$.864535E-01	.875180E-01	.877656E-01	.896481E-01	.907228E-01	.914044E-01
k _∞		1.254390	1.243040	1.240120	1.211560	1.189160	1.170390
P _r		.63544	.63330	.63278	.62698	.62238	.61855
Σf_1		.241354E-02	.239024E-02	.238442E-02	.232535E-02	.227874E-02	.223857E-02
Σf_2		.553122E-01	.553708E-01	.553737E-01	.551452E-01	.547518E-01	.542967E-01
MATERIAL	BUCKLING	.411161E-02	.394151E-02	.389741E-02	.345980E-02	.310995E-02	.281283E-02

TABLE A-5 CONTINUED

BURNUP	INDEX	13	14	15	16	17	18
BURNUP	RANGE						
FROM	MWD/T	10000.00	12000.00	14000.00	16000.00	18000.00	20000.00
TO	MWD/T	12000.00	14000.00	16000.00	18000.00	20000.00	22000.00
D_1		1.467100	1.471270	1.475200	1.479230	1.483180	1.487150
D_2		.379707	.379000	.378440	.378000	.377652	.377380
Σa_1		.577728E-02	.566257E-02	.555018E-02	.544074E-02	.533440E-02	.523127E-02
Σa_2		.138390	.137130	.135540	.133710	.131689	.129525
$v_1 \Sigma f_1$.258861E-01	.260175E-01	.261374E-01	.262517E-01	.263611E-01	.264671E-01
$v_2 \Sigma f_2$.920356E-01	.923622E-01	.924485E-01	.923453E-01	.920914E-01	.917183E-01
k_{∞}		1.145000	1.121150	1.098640	1.077290	1.056980	1.037550
P_r		.61352	.60890	.60490	.60123	.59792	.59494
Σf_1		.218253E-02	.212825E-02	.207552E-02	.202458E-02	.197543E-02	.192810E-02
Σf_2		.535060E-01	.525999E-01	.516103E-01	.505619E-01	.494731E-01	.483589E-01
MATERIAL	BUCKLING	.240573E-02	.200725E-02	.164314E-02	.129321E-02	.956220E-03	.627030E-03

BURNUP	INDEX	19	20	21	22	23	24
BURNUP	RANGE						
FROM	MWD/T	22000.00	24000.00	26000.00	28000.00	30000.00	32000.00
TO	MWD/T	24000.00	26000.00	28000.00	30000.00	32000.00	34000.00
D_1		1.491000	1.495000	1.492490	1.489810	1.487250	1.484800
D_2		.377173	.377020	.376912	.376842	.376800	.376794
Σa_1		.513112E-02	.503454E-02	.494162E-02	.485099E-02	.476438E-02	.468135E-02
Σa_2		.127256	.124917	.122534	.120135	.117741	.115320
$v_1 \Sigma f_1$.265663E-01	.266645E-01	.267563E-01	.268467E-01	.269351E-01	.270208E-01
$v_2 \Sigma f_2$.912518E-01	.907147E-01	.901249E-01	.894991E-01	.888504E-01	.881900E-01
k_{∞}		1.018900	1.000970	.983674	.966985	.950862	.935301
P_r		.59224	.58980	.58758	.58557	.58374	.58206
Σf_1		.188252E-02	.183879E-02	.179679E-02	.175665E-02	.171832E-02	.168183E-02
Σf_2		.472315E-01	.461017E-01	.449783E-01	.438628E-01	.427628E-01	.416723E-01
MATERIAL	BUCKLING	.317167E-03	.799391E-05	.281370E-03	.568534E-03	.848270E-03	.112037E-02

TABLE A-5 CONTINUED

BURNUP	INDEX	25	26	27	28	29	30
BURNUP	RANGE						
FROM	MWD/T	34000.00	36000.00	38000.00	40000.00	42000.00	44000.00
TO	MWD/T	35000.00	38000.00	40000.00	42000.00	44000.00	45000.00
D ₁		1.482470	1.480260	1.477960	1.475935	1.474500	1.472560
D ₂		.376807	.376839	.376887	.376949	.377085	.377045
Σa_1		.460194E-02	.452626E-02	.445464E-02	.438652E-02	.432547E-02	.425656E-02
Σa_2		.113040	.110773	.108573	.106453	.104333	.102247
$v_1 \Sigma f_1$.271039E-01	.271844E-01	.272677E-01	.273448E-01	.274135E-01	.274876E-01
$v_2 \Sigma f_2$.875271E-01	.868692E-01	.862215E-01	.855861E-01	.848367E-01	.841955E-01
k_{∞}		.920295	.905854	.892013	.878756	.865111	.850667
ρ_r		.58052	.57908	.57777	.57651	.57526	.57396
Σf_1		.164718E-02	.161437E-02	.158351E-02	.155440E-02	.152947E-02	.150001E-02
Σf_2		.406974E-01	.397088E-01	.387617E-01	.378582E-01	.368754E-01	.359679E-01
MATERIAL	BUCKLING	.138433E-02	.163962E-02	.190408E-02	.214783E-02	.240132E-02	.267874E-02

BURNUP	INDEX	31	32	33	34	35	36
BURNUP	RANGE						
FROM	MWD/T	46000.00	48000.00	50000.00	52000.00	54000.00	56000.00
TO	MWD/T	48000.00	50000.00	52000.00	54000.00	56000.00	58000.00
D ₁		1.471580	1.470000	1.469103	1.468505	1.467911	1.468123
D ₂		.377100	.377135	.377170	.377200	.377240	.377280
Σa_1		.418619E-02	.411740E-02	.404250E-02	.397475E-02	.390766E-02	.383540E-02
Σa_2		.099911	.097845	.095633	.093517	.091389	.089275
$v_1 \Sigma f_1$.275688E-01	.276392E-01	.277256E-01	.277934E-01	.278657E-01	.279451E-01
$v_2 \Sigma f_2$.834567E-01	.827126E-01	.821988E-01	.813366E-01	.807396E-01	.800789E-01
k_{∞}		.837342	.822541	.808665	.795327	.781072	.767542
ρ_r		.57266	.57139	.57006	.56879	.56751	.56622
Σf_1		.146954E-02	.144232E-02	.141378E-02	.137898E-02	.134965E-02	.132486E-02
Σf_2		.350760E-01	.340987E-01	.331426E-01	.322753E-01	.312660E-01	.303345E-01
MATERIAL	BUCKLING	.290993E-02	.316392E-02	.342015E-02	.368774E-02	.391762E-02	.417431E-02

APPENDIX B

DESCRIPTION OF THE ONE-DIMENSION

CODE USED IN THIS STUDY

APPENDIX B

Description of the One-dimension

Code Used in This Study

B.I. BLOCK DIAGRAM

The block diagram on which the one-dimension code is established is shown in Figure (B-1). Block (1) is the initial loadings of the core for the very first cycle in searching for the equilibrium cycle. Based on the burnup levels of these initial loadings at each zone of the core, the corresponding group constants of each zone can be obtained from the local file in Block (4). The code will then begin the inner iterations starting from the initial flux guesses in Block (2). The routes A-B-C-A-B-C and A-B-D-E-C-A-B-D-E-C are the routes for inner iterations in which the fluxes solved in one loop of inner iteration are the initial flux guesses for the next loop of inner iteration, while the physical conditions of the core remain unchanged. The reason to have two passes A-B-C-A-B-C and A-B-D-E-C-A-B-E-C is that in the first pass when $L_2 < LLL$, the k eigenvalue is kept constant and so the possible irregularity of the initial flux guesses will die out without causing inconsistency to the k eigenvalue in the second pass when $LLL < L_2 < L_3$. After L iterations, block (5) will check whether the integrals of the fluxes in loop L_3-1 and L_3 are within a pre-set convergence limit (equation 3.15). If the fluxes do not converge, the physical conditions of the core will be changed. Here the thermal absorption cross sections of the fuels in the whole core (in whole core controlled case) or of the fuels in the central zone only (in the central zone controlled case) will be changed by adjusting

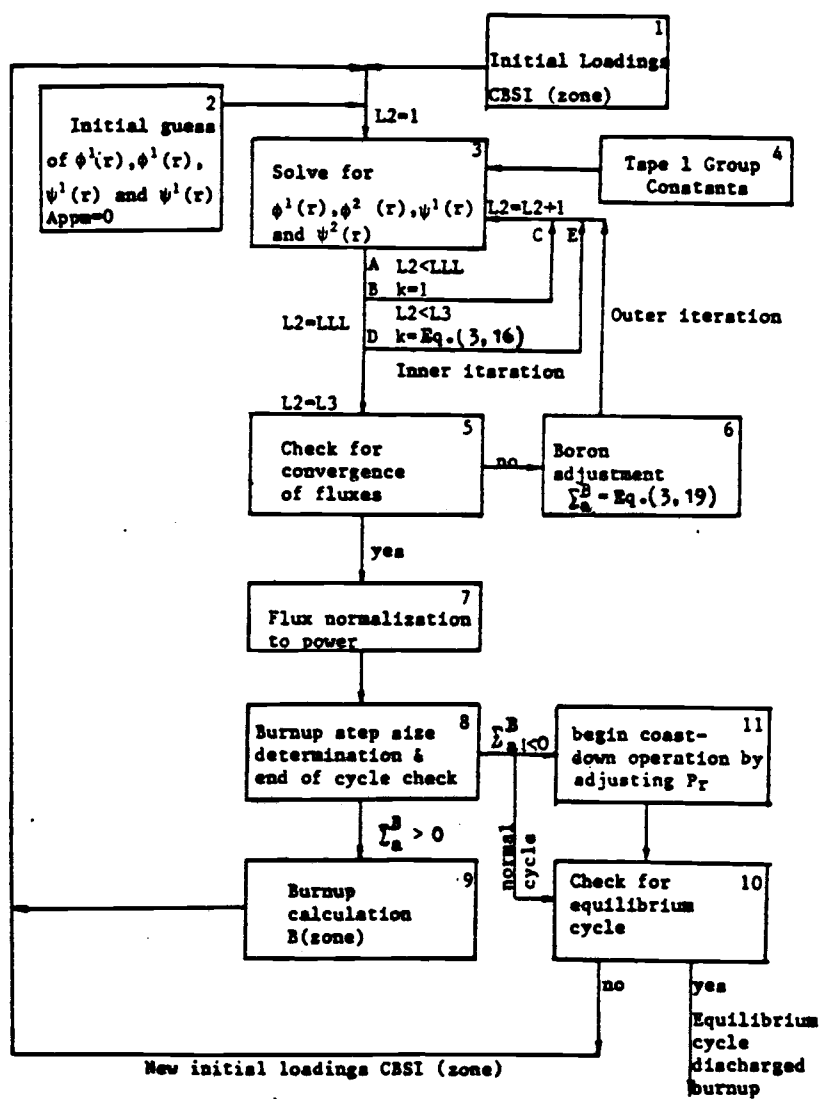


Figure G-12. Block diagram of the one-dimension code.

the boron content in the fuels. The amount of adjustment is proportional to the magnitude of the k eigenvalue after L3 inner iterations. After the physical conditions of the core have been changed, another series of inner iterations will start all over again. The pass D-Block (5)-Block (6) in which adjustment of the core physical condition is made is called the outer iteration. By repeating inner iterations and outer iterations several times, a proper critical core condition (critical boron concentration) can be found and the converged critical fluxes are obtained. These critical fluxes will be normalized to the power of the core in Block (7). Using the normalized critical fluxes, the individual zone average burnup, corresponding to a core average burnup step whose size is determined by input parameters described in the next section, can be calculated according to Equation (3.20). Block (8) and Block (9) will do these burnup calculations. The physical conditions of the core, namely, the group constants of each zone, will change due to this burning of fuels. The boron concentration required to keep the core critical will no longer be as much as before the burnup step. Another loop of inner and outer iterations has to be made to find another set of critical fluxes for the core with changed physical conditions. Once these critical fluxes are found, another burnup step follows. After several burnup steps, the core is considered to have reached the end of its cycle when the critical boron concentration needed no longer exceeds a small pre-fixed amount or the k eigenvalue without boron is less than 1 but greater than .9998. The end of cycle is guarded in Block (8). After the end of normal cycle, the cycle will be checked for whether it is the equilibrium

cycle or not in Block (10) by comparing the end-of-cycle zone average burnup distribution of the cycle with that of the previous cycle. If the end-of-cycle zone average burnup distributions for three consecutive cycles are nearly the same, it is considered that the equilibrium cycle has been reached. In case of coastdown operation, the cycle can be extended by changing the resonance escape probability according to Equation (3.27) after the end of its normal cycle. This is done in Block (11). As in a normal cycle, after the end of the coastdown cycle, an equilibrium check will be made in Block (10). If the cycle is not the equilibrium cycle, another cycle of search for equilibrium will begin with a new set of initial loadings.

B.2. INPUT FORM

This code is developed for CDC 3300 CYBER 70 computer through terminal mode 43 (Basic KSR). Input data are loaded through the terminal rather than through the paper card decks. Once the code is compiled and loaded for execution, the terminal will print out the following variables sequentially. Necessary values of these variables must be loaded to proceed with the calculation.

KB	:	The maximum number of burnup index of group constants in Tape 1.
P	:	The reactor rated power, in MWT.
T	:	The total weight of the uranium fuel in the core, in metric tonne.
CAL	:	The active reactor height, in cm.
CR	:	The reactor radius, in cm.

- N : The number of mesh divisions along the reactor radius.
- HR : The distance between the mesh points, in cm.
- NB : The number of zones, of either equal volume or equal pitch.
- NORE : ≤ 1 When NORE ≤ 1 , the code will stop at the end of Cycle 1, no equilibrium cycle search is attempted.
 < 1 When NORE < 1 , the code will continue to run after the end of the cycle until an equilibrium cycle is reached. The code will stop searching if L7 (defined later) reaches its maximum.
- NPTN : NPTN 1, the initial flux guesses are those in equations (3.13) and (3.14).
 NPTN 1, the initial flux guesses are constant.
- MORA : ≤ 1 When MORA ≤ 1 , the shuffle pattern and the initial loadings of the next new cycle can be adjusted manually in searching for an equilibrium cycle. The terminal will print out a series of variables (CBSI(I), I=1,15), the initial loadings. Proper values of these initial loadings must be loaded in order to proceed with the search of equilibrium cycle.
 : 1 When MORA 1, the initial loadings of the new cycle is adjusted automatically by the code according to Equation (3.11) in Section 3.5, Section B.

- L7 : 4 or 6 The maximum number of the reactor power generation cycles the code can run in searching for an equilibrium cycle. This is to limit the execution time of computer in case the equilibrium cycle cannot be
- L1 : 10 The maximum number of outer iterations in searching for critical boron concentration. L1 is set at 10 here. The number of actual outer iterations needed is usually less than 10. A convergence criterion will automatically terminate the outer iterations when the critical boron concentration is reached.
- L3 : 25 The maximum number of inner iterations for each outer iteration. L3 inner iterations are run before checking the convergence of the flux.
- LLL : 10 The number of inner iterations before checking the eigenvalue k . To have LLL inner iterations before beginning the calculation of the ratio k^{n+1}/k^n will avoid the disturbances that might be encountered in evaluating the ratio if the initial guesses of the fluxes are poor. LLL should always be less than L3.
- MDISB : ≤ 1 When MDISB ≤ 1 , the reactor is divided into regions of equal pitch.
- >1 When MDISB > 1 , the reactor is divided into regions of equal volume.
- ND1 : ND1=1 if the first central zone is controlled. ND1=2 if the first and second central zones are controlled, etc. In whole core controlled case, ND1=NB.

EBURN(J)

J=1,...NB,...15 The zone-wise burnup distribution at the end of the previous cycle. If the current cycle is the very first cycle in searching the equilibrium cycle, a zone wise end-of-cycle burnup distribution for a fictitious previous cycle is guessed. It is used as a reference to see if the current cycle will or will not lead to the equilibrium end-of-cycle burnup distribution by comparing total difference between $\sum_{J=1}^{NB} EBURN(J)$ of the previous cycle and $\sum_{J=1}^{NB} EBURN(J)$ of the current cycle. When the difference is less than DIB (defined later), the cycle is considered as converged to equilibrium. The maximum number of regions into which the core can be divided is 15.

CBSI(J)

J=1,...NB,...15 The initial loadings of the first cycle. A good guess will reduce the number of cycle iterations needed to reach an equilibrium cycle.

BW2,BPFM,BW3,
DIB ::

BW2, the core average burnup step size in MWD/MTU.

When the reactor is in the earlier stages of its cycle, large core average burnup step size is employed. BW2 is taken as 2500 MWD/MTU.

BPFM is a value (or the Boron concentration in ppm) corresponding to $\sum_a B$.

In whole core controlled in-out refueling case, when the boron concentration needed to keep the reactor critical is larger than BPFM (=400), the

core average burnup BW2 is taken; otherwise a ¹⁶²
smaller core average burnup step is taken.

In central zone controlled in-out refueling case,
BPFM is 800. In whole core controlled out-in
refueling case, BPFM is 200.

BW3 is a factor to determine the core average
burnup step sizes when the end of cycle is near.
BW3=.8 is used.

DIB , when the difference of the total sums of the
two consecutive cycle

DIB=3000 MWD/MTU. When the difference of the total
sums of the EOC burnups between two consecutive
cycles is less than DIB, the cycle is considered
as an equilibrium cycle.

KCD ; 1,2,3,4,5 When KCD=1, normal cycle without coastdown.

KDC=2, coastdown to 90% power level, corresponding
to coolant temperature 573.5°F.

KDC=3, coastdown to 80% power level, corresponding
to coolant temperature 561°F.

KCD=4, coastdown to 70% power level, corresponding
to coolant temperature 548.5°F.

KCD=5, coastdown to 60% power level, corresponding
to coolant temperature 536°F.

CTM(1),CTM(2),
CTM(3),CTM(4),
CTM(5):

CTM(1)=586°F, CTM(2)=573.5°F, CTM(3)=561°F, CTM(4)=
548.5°F, CTM(5)=536°F. They are the coolant

temperatures for 100%, 90%, 80%, 70% and 60% power correspondingly.

WW : 0.001666 The volume expansion coefficient of water. It is 0.001666/°F for coolant temperature between 586°F and 536°F under the reactor pressure of 2200 psia.

JA : ≥ 1 JA ≥ 1 , when trial functions (real fluxes) and adjoint fluxes are needed as input for two-dimension calculation. The fluxes used as trial functions are stored in local file TAPE 3.

<1 JA <1, when trial functions and adjoint fluxes are not needed.

ENIT, EIGN
EPPM, Q, Q1 : The fluxes are considered converged if CH1 in equation (3.15) is less than ENIT. The reactor is considered critical if the k eigenvalue in equation (3.16) after boron is added to the reactor is within a range such that $k-1$ is less than EIGN. The EOC is reached if the boron concentration in ppm needed to keep reactor critical is less than EPPM. Q is the overrelaxation factor in equations (3.5) and (3.6). Q1 is the convergence factor in equation (3.19). The values used are ENIT=0.00002, EIGN=0.0004, EPPM=10, Q=1.7 and Q1=.8

B.3. GROUP CONSTANTS LIBRARY

TAPE1 : A local file i.e., TAPE1, which contains the group constants, D_1 , D_2 , $\nu_1 \Sigma f_1$, $\nu_2 \Sigma f_2$, Σ_{a1} , Σ_{a2} , k_{∞} , P_T , Σf_1 and Σf_2 for the fuels loaded in the core at KB different burnup levels, has to be established. In this study 5 different types of fuel are under study, that is, fuels of Trojan type with 15x15 lattice 3% enrichment, 17x17 lattice 2% enrichment, 17x17 lattice 3% enrichment, 18x18 lattice 3% enrichment and Oconee type fuels 15x15 3% enrichment. Therefore, five group constant library files have to be established. The file is set up in the format as shown in Table (B-1).

TABLE B-1 . THE FORMATS FOR GROUP CONSTANTS STORED IN TAPE1.

Group Constants	D_1	D_2	$\nu_1 \Sigma f_1$	$\nu_2 \Sigma f_2$	Σ_{a1}	Σ_{a2}
Variable Name	BOY(I,1)	BOY(I,2)	BOY(I,3)	BOY(I,4)	BOY(I,5)	BOY(I,6)
Format	1x,F12.6	F12.6	E12.6	F12.6	E12.6	E12.6

Group Constants	k_{∞}	P_r	Σf_1	Σf_2	Burnup Level
Variable Name	BOY(I,7)	BOY(I,8)	BOY(I,9)	BOY(I,10)	BS(I)
Format	F12.6	F12.5	E12.6	E12.6	F8.2

(BS(I) is the burnup level,

I=1,45 for 45 different burnup levels in one-dimension code;

I=1,49 for 49 different burnup levels in two-dimension code)

The outputs from one-dimension calculations are divided into two groups. Outputs in the first group are interim calculation results which are useful in judging the correctness of the calculation and in making modifications on the input parameters to speed up the convergence of iterations. Data of this group are printed out on the terminal in the following sequences and forms. The sequence is somewhat different for normal cycle and coastdown cycle. Data in the second group are not printed out on the terminal but stored in a local file, Tape3.

A. First group output

A-1. Normal cycle

1. Information about cycle 1,2,....

2. Sequence number of outer iteration, m ; $\frac{\int (\phi_m^1 - \phi_{m-1}^1) dv}{\int \phi_m^1 dv}$;

$$\frac{\int (\phi_m^2 - \phi_{m-1}^2) dv}{\int \phi_m^2 dv} ; k_m = \frac{\int (\sum_{f_1} \phi_m^1 + \sum_{f_2} \phi_m^2) dv}{\int (\sum_{f_1} \phi_{m-1}^1 + \sum_{f_2} \phi_{m-1}^2) dv} ;$$

$$\int (\sum_{f_1} \phi_m^1 + \sum_{f_2} \phi_m^2) dv ; \int (\sum_{f_1} \phi_{m-1}^1 + \sum_{f_2} \phi_{m-1}^2) dv$$

3. Σ_a^B

4. Selected mesh point; oritical flux ϕ_m^1 ; ϕ_m^2 ; ϕ_{m-1}^1 ; ϕ_{m-1}^2

5. Flux peakings $\frac{\phi_m^1 \text{ (core centers)}}{\int \phi_m^1 dv / dv}$ and $\frac{\phi_m^2 \text{ (core center)}}{\int \phi_m^2 dv / dv}$

(In central zone controlled case, these ratios are not necessarily the peak values)

6. Flux normalization factor.

7-1 Bundle incremental and cumulative burnup corresponding to the core average burnup step, BUC.

7-2 Zone number; step increment; cycle increment; initial loading, final bundle burnup; burnup index and bundle power peaking factor.

8. Cumulative core average burnup, COREB.

(For every core average burnup step, outputs from step 2 through to step 8 are repeated. At the end of the cycle, the end-of-cycle outputs of step 2, 3 and 4 are printed out before step 9)

9. Equilibrium cycle convergence factors

Expected core average burnup, EXCB; Sum of current initial loadings over all zones, CIL; Sum of expected initial loadings over all zones;

$$\frac{NB.COREB + DxB}{2.DxB^{n-1}}, \text{ a ratio indicating}$$

the closeness of the current cycle to equilibrium cycle and the actual core average burnup of the current cycle, COREB.

10. Initial loadings of the next cycle suggested, and final burnups of the current cycle. Zone number I; initial loading for next cycle; final burnup of current cycle. (For every cycle, outputs from step 1 through to step 10 are repeated. When an

equilibrium cycle is reached, the final burnup of the outermost zone of the last cycle is the desired equilibrium discharge burnup)

A-2. Coastdown cycle

In the case of coastdown operation, additional outputs are printed out following the end of normal cycle and before the output in step 9 of A-1. These outputs are:

Information about coastdown operation

Power generation cycle number ; equilibrium cycle number ;

step of coastdown operation ; coolant temperature ;

Total cumulative core average burnup steps at beginning of this coast-down step.

B. Second group output

Outputs in this group are the fast flux, slow flux, fast adjoint and slow adjoint along all radial mesh points for three different reactor stages. They will serve as the trial functions and the weighting functions in two-dimension calculations. The one-dimension code will generate these outputs only when equilibrium cycle has been reached. They are stored in a local file Tape3.

```

PROGRAM YEN1DN(TAPE1,INPUT,OUTPUT,TAPE61=OUTPUT,
1 TAPE3)
CC A ONE DIMENSION TWO GROUP DIFFUSION CODE TO SIMULATE
CC THE CORE BURNUP WITH DIFFERENT ENRICHMENTS AND REFUELING
CC SCHEMES
REAL B1,X
INTEGER KB
DIMENSION AJ(15),G1(200),G2(200),HH1(200),HHH1(200)
DIMENSION HH2(200),HHH2(200)
DIMENSION E1(200),E2(200),EE1(200),EE2(200),F1(200),F2(200)
DIMENSION GOD(49),ULOVE(49)
DIMENSION P28(49),PT(49),CTM(5),BP(15)
DIMENSION FKK(15),DD(2,15),LZR(16),EBURN(15),CBSE(15),CBSE(15)
DIMENSION CCBE(15)
DIMENSION BUC(26),SIGMB1(15),SIGMB2(15),BS(49),NBS(15)
DIMENSION B(15),AA(2,15),BB(2,15),CC(2,15),SS(15),SH(15)
COMMON/SOURS/SIGH(2,49),SIGMF(2,49),SIGMA(2,49)
1 ,DIFC(2,49),FKAP(2,49)
COMMON/DAAD/AS1(15),AS2(15),AS3(15),AS4(15),AS5(15)
1 ,AS6(15),AS7(15),AS8(15),AS9(15)
PRINT*,"KB=",
READ*,KB
DO 910 I=1,KB
READ(1,911)DIFC(1,I),DIFC(2,I),SIGMF(1,I),SIGMF(2,I)
1 ,SIGH(1,I),SIGH(2,I),FKAP(1,I),FKAP(2,I),SIGMA(1,I)
2 ,SIGMA(2,I),BS(I)
911 FORMAT(1X,2F12.6,E12.6,F12.6,2E12.6,F12.6,F12.5,2E12.6,F8.2)
910 CONTINUE
PRINT*,"P=",
READ*,P
PRINT*,"T=",
READ*,T
PRINT*,"CAL=",
READ*,CAL
PRINT*,"CR=",
READ*,CR
PRINT*,"N=",
READ*,N
PRINT*,"HR=",
READ*,HR
PRINT*,"NB=",
READ*,NB
PRINT*,"NORE,NPTN=",
READ*,NORE,NPTN
PRINT*,"MORA=",
READ*,MORA
PRINT*,"L7=",
READ*,L7
PRINT*,"L1=",
READ*,L1

```

```

PRINT*, "L3=",
READ*, L3
PRINT*, "LLL=",
READ*, LLL
PRINT*, "NDISB=",
READ*, NDISB
PRINT*, "ND1=",
READ*, ND1
PRINT*, "EBURN(J)=",
READ*, EBURN(1), EBURN(2), EBURN(3), EBURN(4), EBURN(5),
1 EBURN(6), EBURN(7), EBURN(8), EBURN(9), EBURN(10),
2 EBURN(11), EBURN(12), EBURN(13), EBURN(14), EBURN(15)
888 PRINT*, "CBSI(J)=",
READ*, CBSI(1), CBSI(2), CBSI(3), CBSI(4), CBSI(5),
1 CBSI(6), CBSI(7), CBSI(8), CBSI(9), CBSI(10), CBSI(11)
2 CBSI(12), CBSI(13), CBSI(14), CBSI(15)
PRINT*, "BU2, BPPM, BU3, DIB=",
READ*, BU2, BPPM, BU3, DIB
PRINT*, "KCD=",
READ*, KCD
PRINT*, "CTM(1), CTM(2), CTM(3), CTM(4), CTM(5)=",
READ*, CTM(1), CTM(2), CTM(3), CTM(4), CTM(5)
PRINT*, "WU=",
READ*, WU
PRINT*, "JA=",
READ*, JA
PRINT*, "ENIT, EIGN, EPPM, Q, Q1=",
READ*, ENIT, EIGN, EPPM, Q, Q1
JB=2
CC NCB LARGER THAN 1 BORON IS ADDED TO 1ST ZONE ,ND1 NO OF ZONES WITH
CC BORON JA LARGER OR EQUAL TO 1, TRIAL AND WEIGHTING FUNCTIONS, JB=1
CC SUPERCRITICAL JB=0 CRITICAL
LS=N+1
DO 4002 I=1, KB
PT(I)=FKAP(2, I)
4002 CONTINUE
AF=0.05
A=(.738*P*1.0E+06*1.0E+13)/(CR**2*AF*CAL*200*1.602)
S=HR**2
IF(MDISB-1)132,132,134
134 ZR1=N/SQRT(FLOAT(NB))
DO 131 I=1, NB
JJ=I
LZR(JJ)=SQRT(FLOAT(I))*ZR1+0.5
131 CONTINUE
132 M=N/NB
KCK=0
KKK=0
CC L7 NO OF TOTAL CYCLE ITERATION, KCK NO OF EQUILIBRIUM CYCLE ITERATION
DO 4000 I7=1, L7
WRITE(61,5500)I7
5500 FORMAT(" INFORMATIONS ABOUT CYCLE ",I3)
IF(KKK.LT.1)GO TO 4003

```

```

CC      AFTER EVERY COASTDOWN OPERATION TO BEGIN A NEW CYCLE (KKK.GE.1)
CC      THE RESONANCE ESCAPE PROBABILITY, STEP OF COASTDOWN KC AND
CC      POWER LEVEL BU7 HAVE TO BE RESTORED TO 100% VALUE
CC      WHEN THERE IS NO COASTDOWN, KKK=0
      DO 4004 I=1,KB
      GOD(I)=PT(I)
      FKAP(2,I)=GOD(I)
4004    CONTINUE
4003    K=1
      COREB=0.
      KC=1
      BU7=1.
      STPS=0.
      KP=3
      APPM=0.
      APPM0=0.
      APPM1=0.
CC      BUNDLE BURNUP CATEGORY OF INITIAL LOADINGS
      DO 811 I=1,NB
      CBSE(I)=CBSI(I)
      CALL CATEG(CBSE,BS,NBS,I,KB)
      CCBE(I)=0.
      811    CONTINUE
      DO 7000 K=1,20
CC      AT THE END OF NORMAL CYCLE (APPM.LE.30) AND BEGINNING OF
CC      COASTDOWN OPERATION (KC.GT.1), ADJUST RESONANCE ESCAPE PROBABILITY
7001    IF (APPM.GT.30.) GO TO 508
      IF (KC.LE.1) GO TO 508
      DO 4001 I=1,KB
      FKAP(2,I)=0.
      WLOVE(I)=PT(I)
      FKAP(2,I)=(1.0+(1.0-WLOVE(I))*(CTH(1)-CTH(KC))*WU)*
      1 WLOVE(I)
4001    CONTINUE
      WRITE(61,*) " INFORMATIONS ABOUT COASTDOWN OPERATION"
      WRITE(61,4005) I7,KCK
4005    FORMAT(" POWER    GENERATION    CYCLE=",I3," ;EQUILIBRIUM CYCLE=",
      1 I3)
      IKC=KC-1
      WRITE(61,4006) IKC,CTH(KC)
4006    FORMAT(" STEP OF COASTDOWN OPERATION=",I3," ;COOLANT TEMPERATUR
      1 E=",F6.2)
      WRITE(61,4007) K
4007    FORMAT(" TOTAL BURNUP STEPS AT THE BEGINNING OF THIS COASTDOWN
      1 STEP=",I3)
508    APPM=0.
      APPM0=0.
CC      BUNDLE GROUP CROSS SECTION ASSIGNMENT
      DO 100 I=1,NB
      AA(1,I)=(AS1(I)-(1./1.))
      1 *AS3(I)/AS9(I))/AS7(I)

```

```

      AA(2,I)=AS2(I)/AS8(I)
      AJ(I)=AS7(I)/AS8(I)
      BB(1,I)=(1./1.)*
1    AS4(I)/AS7(I)
      BB(2,I)=AS1(I)/AS8(I)
      DD(1,I)=AS3(I)*1./1.
      DD(2,I)=AS4(I)*1./1.
      CC(1,I)=1/AS9(I)
100   CC(2,I)=FKAP(2,NBS(I))
      DO 50 J=1,L1
      DO 444 I=1,NB
      FK(I)=1.
      SIGMB1(I)=AS2(I)
444   CONTINUE
CC    FIRST L3 ITERATION
CC    INITIAL FLUX GUESS
      DO 10 I=1,LS
      IX=I-1
      X=(2.405*IX)/FLOAT(N)
      E1(I)=.8*A*BW7*(BESSEL(X))
      EE1(I)=E1(I)
      E2(I)=.2*E1(I)
10    EE2(I)=E2(I)
      L2=0
71    L2=L2+1
      IF(L2.EQ.1)GO TO 1206
      GO TO 1368
CC    AFTER LLL INNER ITERATIONS AND IN THE SECOND
CC    EQUILIBRIUM CYCLE (KCK.GE.1), IF TRIAL AND WEIGHTING
CC    FUNCTIONS ARE NEEDED (JA.GE.1), INITIAL GUESSES OF
CC    ADJOINT ARE SET EQUAL TO NEUTRON FLUXES
1206  IF(KCK.LT.1)GO TO 1368
      IF(JA.LT.1)GO TO 1368
      DO 1227 I=1,LS
      HH1(I)=E2(I)
      HHH1(I)=EE2(I)
      HH2(I)=E1(I)
      HHH2(I)=EE1(I)
1227  CONTINUE
1368  R=HR*(N-1)
      MB=1
      ZF1=0.
      ZF2=0.
      MBB=NB
      DO 40 I=1,N
      L=N+1-I
      IF(MDISB-1)137,137,138
138   IF(L-LZR(MBB-1))135,135,136
135   MBB=MBB-1
      GO TO 136
137   B1=(FLOAT(I)-1)/FLOAT(N)
      IF(B1-MB)70,80,80
80    MB=MB+1

```



```

70  MBB=MB-MB+1
136 IF(L.GT.1)GO TO 1468
    F1(L)=((E1(L+1)+EE1(L+1))*S+.25*CC(1,MBB)*BB(1,MBB)
1   *.5*(E2(L)+EE2(L)))/(1.+S*.25*AA(1,MBB))
    GO TO 1469
1468 F1(L)=-((1.+S*AA(1,MBB))*(.5*(E1(L)+EE1(L)))+.5*((1.-HR/(2.*R))
1   *(E1(L+1)+EE1(L+1))+(1.+HR/(2.*R))*(E1(L-1)+EE1(L-1))))+
2   S*CC(1,MBB)*BB(1,MBB)*(.5*(E2(L)+EE2(L)))
1469 EE1(L)=E1(L)
    E1(L)=F1(L)
    IF(L.GT.1)GO TO 1470
    F2(L)=((E2(L+1)+EE2(L+1))*S+.25*S*CC(2,MBB)*BB(2,MBB)
1   *.5*(E1(L)+EE1(L)))/(1.+S*.25*AA(2,MBB))
    GO TO 1471
1470 F2(L)=-((1.+S*AA(2,MBB))*(.5*(E2(L)+EE2(L)))+.5*((1.-HR/(2.*R))
1   *(E2(L+1)+EE2(L+1))+(1.+HR/(2.*R))*(E2(L-1)+EE2(L-1))))+S*
2   CC(2,MBB)*BB(2,MBB)*(.5*(E1(L)+EE1(L)))
1471 EE2(L)=E2(L)
    E2(L)=F2(L)
    IF(KCK.LT.1)GO TO 6006
    IF(JA.LT.1)GO TO 6006
    IF(L.GT.1)GO TO 1472
    G2(L)=((HH2(L+1)+HHH2(L+1))*S+.25*S*CC(1,MBB)
1   *BB(1,MBB)*AJ(MBB)*.5*(HH1(L)+HHH1(L)))/
2   (1.+S*.25*AA(2,MBB))
    GO TO 1473
1472 G2(L)=-((1.+S*AA(2,MBB))*(.5*(HH2(L)+HHH2(L))
1   +.5*((1.-HR/(2.*R))*(HH2(L+1)+HHH2(L+1))
2   +(1.+HR/(2.*R))*(HH2(L-1)+HHH2(L-1))))+S*
3   CC(1,MBB)*BB(1,MBB)*AJ(MBB)*(.5*(HH1(L)
4   +HHH1(L)))
1473 HHH2(L)=HH2(L)
    HH2(L)=G2(L)
    IF(L.GT.1)GO TO 1474
    G1(L)=((HH1(L+1)+HHH1(L+1))*S+.25*S*CC(2,MBB)
1   *BB(2,MBB)*.5*(HH2(L)+HHH2(L))/AJ(MBB))/
2   (1.+S*.25*AA(1,MBB))
    GO TO 1475
1474 G1(L)=-((1.+S*AA(1,MBB))*(.5*(HH1(L)+HHH1(L))
1   +.5*((1.-HR/(2.*R))*(HH1(L+1)+HHH1(L+1))
2   +(1.+HR/(2.*R))*(HH1(L-1)+HHH1(L-1))))+
3   S*CC(2,MBB)*BB(2,MBB)*(.5*(HH2(L)+HHH2(L)))
4   /AJ(MBB)
1475 HHH1(L)=HH1(L)
    HH1(L)=G1(L)
6006 ZF1=ZF1+(DD(1,MBB)*E1(L)+DD(2,MBB)*E2(L))*HR*R
    ZF2=ZF2+(DD(1,MBB)*EE1(L)+DD(2,MBB)*EE2(L))*HR*R
    R=R-HR
40  CONTINUE
    EE1(1)=E1(1)
    EE2(1)=E2(1)

```

```

      EE1(N+1)=E1(N+1)
      EE2(N+1)=E2(N+1)
      E1(N+1)=E1(N)/(1.+(HR/2.8))
      E2(N+1)=E2(N)/(1.+(HR/0.666))
      IF(KCK.LT.1)GO TO 3131
      IF(JA.LT.1)GO TO 3131
      HH2(1)=HH2(1)
      HH1(1)=HH1(1)
      HH2(N+1)=HH2(N+1)
      HH1(N+1)=HH1(N+1)
      HH2(N+1)=HH2(N)/(1.+(HR/0.666))
      HH1(N+1)=HH1(N)/(1.+(HR/2.8))
3131 IF(E1(1).LE.0.10E+7)GO TO 34
      DO 234 I=1,NB
      IF(L2-LLL)77,77,78
78 FK(I)=FK(I)+ZF1/ZF2
77 AA(1,I)=(AS1(I)-(1./1.)
1 *AS3(I)/FK(I))/AS7(I)
      CC(1,I)=1/FK(I)
234 CONTINUE
      IF(L2-L3)71,72,72
72 H1=0.
      H2=0.
      Z1=0.
      Z2=0.
      R=HR
      DO 180 I=2,LS
      Z1=Z1+HR*((EE1(I)+EE1(I-1))/2.)*R
      Z2=Z2+HR*((EE2(I)+EE2(I-1))/2.)*R
      H1=H1+HR*((E1(I)+E1(I-1))/2.)*R
      H2=H2+HR*((E2(I)+E2(I-1))/2.)*R
      R=R+HR
180 CONTINUE
      CH=H1-Z1
      CH1=(H1-Z1)/H1
      CH2=(H2-Z2)/H2
      WRITE(61,1100)J,CH1,CH2,FK(1),ZF1,ZF2
1100 FORMAT(1X,I3,5E10.3)
      IF(KCK.LT.1)GO TO 75
      IF(JA.LT.1)GO TO 75
      IF(JB.LT.1)GO TO 75
      JB=0
      WRITE(3,*)" SUP FAST FLUX SLOW FLUX FAST ADJOINT SLOW A
1DJOINT"
      WRITE(3,510)PF1,PF2
510 FORMAT(" FAST FLUX PEAKING FACTOR=",E10.3," SLOW FLUX PEAKING
1 FACTOR=",E10.3)
CC THE TRIAL AND WEIGHTING FUNCTIOS FOR 2-D CALCULATION
      DO 6005 I=1,LS
      WRITE(3,6003)I,E1(I),E2(I),HH1(I),HH2(I)
6003 FORMAT(1X,I3,2X,E12.5,2X,E12.5,2X,E12.5,2X,E12.5)
6005 CONTINUE

```

```

75 IF(ABS(CH1)-0.00004)1,1,2
2 IF(ABS(CH1)-0.0001)3,3,4
4 IF(ABS(CH1)-0.001)5,5,6
6 IF(CH)9,1,7
5 IF(CH)9,1,7
3 IF(CH)9,1,7
7 IF(J.GT.1)GO TO 3133
  PPH=CH1*BU1*100.*3650.*COS((0.38-CH1*100.)*BU0)
  CH0=CH1
  GO TO 3000
3133 APPH=APPH*CH0/(CH0-CH1)
  GO TO 3003
9 IF(K.GT.1)GO TO 3422
  IF(J.LE.1)GO TO 34
3422 PPH=(APPH-APPH0)*CH3/(CH3-CH1)
  APPH2=APPH
  APPH=APPH0+PPH
  APPH0=APPH2
  GO TO 3003
3000 APPH=APPH+PPH
3003 WRITE(61,999)APPH
  CH3=CH1
999 FORMAT(1X,F10.3)
  IF(APPH-1.)6666,6666,321
6666 IF(APPH+30.)666,666,1
321 DO 201 I=1,NB
  SIGMB2(I)=SIGMB1(I)+APPH*1.8738E-05
  IF(NCB.LE.1)GO TO 606
  IF(I.GT.NB1)SIGMB2(I)=SIGMB1(I)
606 AA(2,I)=SIGMB2(I)/ASB(I)
201 CONTINUE
50 CONTINUE
1 WRITE(61,1111)J,APPH,CH1,CH2,CH
1111 FORMAT(1X,I3,2X,F10.3,3E10.3)
  DO 1201 I=1,NB
  II=I*20-10
  WRITE(61,1101)E1(II),E2(II),EE1(II),EE2(II)
1101 FORMAT(1X,4E10.3)
1201 CONTINUE
  IF(KCX.LT.1)GO TO 505
  IF(JA.LT.1)GO TO 505
  IF(KP.GE.2)GO TO 506
  IF(APPH.GE.30.)GO TO 505
  WRITE(3,*)" EOC FAST FLUX SLOW FLUX FAST ADJOINT SLOW A
1BJOINT"
  GO TO 504
506 WRITE(3,*)" BGC FAST FLUX SLOW FLUX FAST ADJOINT SLOW A
1BJOINT"
504 WRITE(3,510)PF1,PF2
  DO 1302 I=1,LS
  WRITE(3,6003)I,E1(I),E2(I),HH1(I),HH2(I)
1302 CONTINUE

```

```

      KP=1
505 PF1=E1(1)*(CR**2.)/(H1*2.)
      PF2=E2(1)*(CR**2.)/(H2*2.)
      WRITE(61,608)PF1,PF2
608 FORMAT(1X,2F10.3)
      IF(ABS(APPM)-30)403,403,404
404 BUC(K)=BW2
      IF(APPM.LE.BPPH)BUC(K)=BW3+BUC(K-1)*APPM/(APPM1-APPM)
      APPM1=APPM
      STPS=STPS+BUC(K)
      GO TO 401
CC   KCD NO OF COASTDOWN STEPS KC=KCD=1 NORMAL NO COASTDOWN
403 IF(KC.GE.KCD)GO TO 507
      KC=KC+1
      GO TO 7001
CC   EQUILIBRIUM CYCLE INITIAL LOADING AND LENGTH
507 IF(NORE-1)34,34,829
CC   IF NORE.LE.1 END OF NORMAL CYCLE
CC   IF NORE.GT.1 SEARCH FOR EQUILIBRIUM CYCLE
829 DXB=0.
      CFR=(COREB*NB+EBURN(NB))/(2.*EBURN(NB))
      EIL=0.
      EXCB=0.
      DO 408 I=1,NB
      DXB=DXB+ABS(EBURN(I)-CBSE(I))
      EIL=EIL+CCBE(I)
      EXCB=EXCB+(CBSI(I)+I*CCBE(I))/(NB**2.)
408 CONTINUE
      EIL=EIL-CCBE(NB)
      CIL=CBSI(NB)
      WRITE(61,*)" EQUILIBRIUM CYCLE CONVERGENCE FACTORS"
      WRITE(61,*)"  EXCB      CIL      EIL      CFR      DXB
1  COREB"
      WRITE(61,67)EXCB,CIL,EIL,CFR,DXB,STPS
67  FORMAT(1X,F10.3,1X,F10.3,1X,F10.3,1X,F8.3,1X,F10.3,1X,F10.3)
      IF(NORA.GT.1)GO TO 812
CC   MANUALLY ADJUST THE SHUFFLE PATTERN AND INITIAL LOADINGS
CC   OF NEW CYCLE IN SEARCHING FOR EQUILIBRIUM DISCHARGE BURNUP
      DO 814 I=1,NB
      WRITE(61,813)CBSI(I),CBSE(I)
813 FORMAT(1X,E10.3,1X,E10.3)
814 CONTINUE
      PRINT*,"CBSI(J)="
      READ*,CBSI(1),CBSI(2),CBSI(3),CBSI(4),CBSI(5),CBSI(6),
1 CBSI(7),CBSI(8),CBSI(9),CBSI(10),CBSI(11),CBSI(12),
2 CBSI(13),CBSI(14),CBSI(15)

```

```

      GO TO 816
812  NC=ND1+1
      BENNY=0.
      RATO=.5*(CBSE(1)+CBSI(2))/CBSE(1)
      DO 605 I=NC,NB
      BENNY=BENNY+CCBE(I-1)
      CBSI(I)=.25*(BENNY*(CIL/EIL+2.*RATO)+CBSI(I)*(COREB/EXCB))
605  CONTINUE
      DO 616 I=1,NB1
      CBSI(I)=0.
616  CONTINUE
CC   BUNDLE BURNUP DISTRIBUTION OF PRECEEDING CYCLE
816  DO 409 I=1,NB
      EBURN(I)=CBSE(I)
409  CONTINUE
      COREB=0.
      KKK=KKK+1
      BU7=BU7-0.1
      WRITE(61,*)" INITIAL LOADINGS OF NEXT CYCLE AND FINAL BURNUPS OF
1CURRENT CYCLE"
      WRITE(61,*)" I    INITIAL FOR NEXT    FINAL FOR CURRENT"
      DO 703 I=1,NB
      WRITE(61,705)I,CBSI(I),CBSE(I)
705  FORMAT(1X,I3,3X,E12.5,6X,E12.5)
703  CONTINUE
      IF(DXB.LE.DIB)GO TO 704
      GO TO 4000
CC   KCK NO OF CYCLES REACH EQUILIBRIUM CONDITION
704  KCK=KCK+1
      IF(KCK.GE.2)GO TO 666
      GO TO 4000
CC   BUNDLE BURNUP
401  DO 4444 I=1,NB
      SS(I)=0.
      SN(I)=0.
4444  CONTINUE
      TN=0.
      NB=1
      VZ=0.
      DO 2203 I=1,N
      IF(NDISB-1)139,139,140
140  IF(I-LZR(NB))90,90,91
139  B1=FLOAT(I)/FLOAT(N)
      IF(B1-NB)90,90,91
91   NB=NB+1
90   SS(NB)=I*.2.-VZ+SS(NB)
      FS=(I*.2.-VZ)*ASS(NB)*E1(I+1)+(I*.2.-VZ)
1   *AS6(NB)*E2(I+1)
      SN(NB)=SN(NB)+FS
      TN=TN+FS
      VZ=I*.2.

```

```

2203 CONTINUE
CC FLUX NORMALIZATION FACTOR FNOR
   FNOR=(P*1.0E+06*1.0E+13)/(3.1416*(HR**2.)*TM*CAL
1   *1.602*200.)
   WRITE(61,2337)FNOR
2337 FORMAT(" NORMALIZATION FACTOR=",F12.5)
CC PRINT OUT OF STEP INCREMENT TOTAL INCREMENT INITIAL BURNUP FINAL
CC BURNUP AND BURNUP CATAGORY
   WRITE(61,235)BUC(K)
235  FORMAT(" BUNDLE INCREMENTAL AND CUNULATIVE BURNUP CORRESPONDING
1     ",/, " TO INCREMENTAL CORE AVERAGE BURNUP BUC=",F10.3)
   WRITE(61,*)" ZONE NO STEP INCREMENT CYCLE INCREMENT INITIAL
1     FINAL CATEGORY BUNDLE PUR PEAKING"
   DO 1203 I=1,NB
   BP(I)=SN(I)*NB/TM
   B(I)=((N**2)*BUC(K)+SN(I)/(SS(I)*TM))
   CBSE(I)=CBSE(I)+B(I)
   CCBE(I)=CCBE(I)+B(I)
   CALL CATEG(CBSE,BS,NBS,I,KB)
   WRITE(61,1301)I,B(I),CCBE(I),CBSI(I),CBSE(I),NBS(I),BP(I)
1301 FORMAT(3X,I3,4X,F12.3,4X,F12.3,4X,F12.3,4X,F12.3,4X,I3,4X,F12.3)
1203 CONTINUE
   COREB=COREB+BUC(K)
   WRITE(61,1204)COREB
1204 FORMAT(" CUNULATIVE CORE AVERAGE BURNUP COREB=",F10.3)
7000 CONTINUE
4000 CONTINUE
34  WRITE(61,1205)K
1205 FORMAT(1X,I3,14H"END OF CYCLE")
666 PRINT*,"KKK=",
   READ*,KKK
   IF(KKK-1)777,888,888
777 STOP
   END
   SUBROUTINE CATEG(CBSE,BS,NBS,I,KB)
   DIMENSION CBSE(15),BS(49),NBS(49)
   COMMON/DAAD/AS1(15),AS2(15),AS3(15),AS4(15),AS5(15)
1,AS6(15),AS7(15),AS8(15),AS9(15)
   COMMON/SOURS/SIGN(2,49),SIGNF(2,49),SIGMA(2,49),DIFC(2,49)
1,FKAP(2,49)
   DO 501 KI=1,KB
   IKK=KI
   IF(CBSE(I)-BS(IKK))502,501,501
501 CONTINUE
502 NBS(I)=IKK
   IF(NBS(I).GT.1)60 TO 927
   RB=1.
   NAO=NBS(I)
   NA1=1
   GO TO 929
927 NAO=NBS(I)
   NA1=NBS(I)-1

```

```

RB=(CBSE(I)-BS(NA1))/(BS(NA0)-BS(NA1))
929 AS1(I)=(1.-RB)*SIGN(1,NA1)+RB*SIGN(1,NA0)
AS2(I)=(1.-RB)*SIGN(2,NA1)+RB*SIGN(2,NA0)
AS3(I)=(1.-RB)*SIGNF(1,NA1)+RB*SIGNF(1,NA0)
AS4(I)=(1.-RB)*SIGNF(2,NA1)+RB*SIGNF(2,NA0)
AS5(I)=(1.-RB)*SIGNA(1,NA1)+RB*SIGNA(1,NA0)
AS6(I)=(1.-RB)*SIGNA(2,NA1)+RB*SIGNA(2,NA0)
AS7(I)=(1.-RB)*DIFC(1,NA1)+RB*DIFC(1,NA0)
AS8(I)=(1.-RB)*DIFC(2,NA1)+RB*DIFC(2,NA0)
AS9(I)=(1.-RB)*FKAP(1,NA1)+RB*FKAP(1,NA0)
RETURN
END
FUNCTION BESSEL(X)
BESSEL=1.-(X**2)/4+((X**2)**2)/64-
1 (((X**2)**2)*(X**2))/2304+(((X**2)**2)**2)/
2 147456
RETURN
END

```

APPENDIX C

Description of the Two-Dimension
Code Used in the Study

APPENDIX C

Description of the Two-Dimension Code

C.1 BLOCK DIAGRAM

Figure (C-1) is the block diagram of two-dimension code. It differs from the one-dimension code in several ways. In Block (4), in addition to the group constants, the trial and weighting functions, serving as input, have to be included in the two-dimension calculations. Block (4-1), which Figure (B-1) does not have, is the place where the elements of the matrix $\overline{AF} = \overline{C}$, Equation (4.14), are prepared. Since, there is no coastdown option in the two-dimension code, therefore there is no need for Block (11). Blocks performing the same functions as those in the one-dimension code are numbered the same as their counterparts in the one-dimension code.

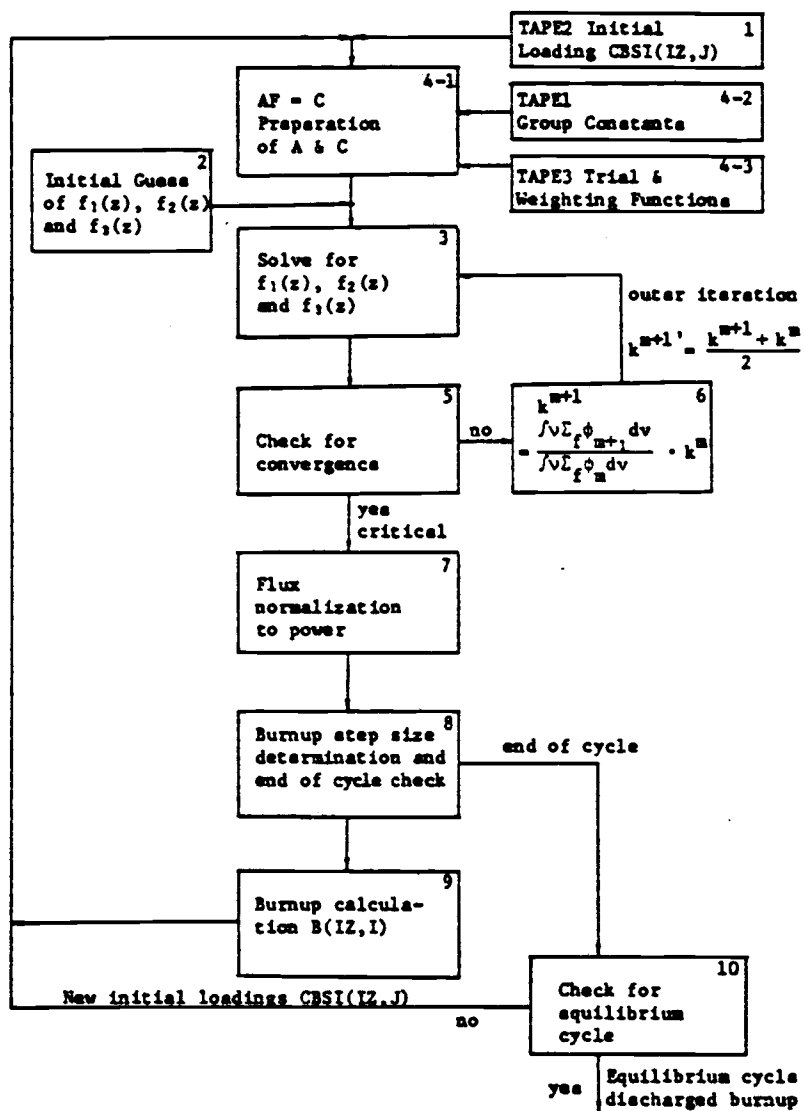


Figure (C-1). Computer Block Diagram of the Two-Dimension Code.

C.1 DATA LIBRARY

- TAPE1 : TAPE1 is a local file which contains the group constants D_1 , D_2 , $\nu_1 \Sigma_{f1}$, $\nu_2 \Sigma_{f2}$, Σ_{a1} , Σ_{a2} , k_∞ , P_T , Σ_{f1} and Σ_{f2} of the fuels under study for different burnup levels. It has a format as shown in Table (B-1). TAPE1 can be used in both the one-dimension and the two-dimension code.
- TAPE2 : In searching for the equilibrium cycle, the initial loadings for every element of the first cycle have to be identified. A good guess of the initial loadings will significantly reduce the number of cycles needed to reach an equilibrium cycle. The guess of the element initial loadings, CBSI(IZ,IR), is stored in TAPE2 in a format as shown in Table (C-1).
- TAPE3 : For different study cases, either whole core controlled or central zone controlled, different sets of trial functions and weighting functions are needed in the two-dimension code. TAPE3 is the local file that contains these trial functions and the weighting functions generated by the one-dimension code. Its format is shown in Table (C-2).

C.2 INPUT FORM

Like the one-dimension code, the input data are loaded through the terminal rather than through card decks. A conversion of the code has to be made if card deck input is to be used. Free format is used for real number variables and I-format for integer number variables.

KB	:	The maximum number of burnup index in TAPE1.
P	:	The reactor rated power, in MWD/MTU.
T	:	The total weight of uranium fuels in the core, in metric tonne.
CAL	:	The reactor active height, in cm.
CR	:	The reactor radius, in cm.
N	:	The number of mesh divisions in radial direction.
HR	:	The distance between the radial mesh points, in cm. It is equal to CR/N.
NB	:	The number of zones radial-wise, either equal volume or equal pitch.
NZZ	:	The number of equal distance divisions in z-direction for half reactor height.
DR ₁ , DR ₂ , DR ₃	:	Initial guesses of $f_1(z)$, $f_2(z)$ and $f_3(z)$ are correspondingly DR ₁ , DR ₂ and DR ₃ multiplied by $\cos(z/CAL)$.
L7,L8	:	L7 is the maximum number of power generation cycles for searching an equilibrium cycle. L8

is the maximum number of core burnup steps in one cycle. Both L7 and L8 are used to limit the computer time in case a poor run is made. L7 and L8 are taken as 4 and 7 respectively here.

ENIT : The convergence criterion of the inner iteration. The flux is considered as convergent if

$$\frac{\int (v_1 \Sigma_{f1} \phi_{m+1}^1 + v_2 \Sigma_{f2} \phi_{m+1}^2) dv - \int (v_1 \Sigma_{f1} \phi_m^1 + v_2 \Sigma_{f2} \phi_m^2) dv}{\int (v_1 \Sigma_{f1} \phi_{m+1}^1 + v_2 \Sigma_{f2} \phi_{m+1}^2) dv} < \text{ENIT}$$

for outer iteration loop $m+1$ and m .

NEB,NFB,NOR1,
NOR2 : Factors used in routing the loop of iteration.
NEB=1,NFB=1,NOR1=2,NOR2=0.

FRX : Overrelation factor.

SB1,BW3,BW1,
DFEQ : SB1 is the first core average burnup step size desired. A large first core average burnup step size is used in order to reduce the number of core average burnup steps in a cycle in the code simulation of reactor power generation. SB1=4000 MWD/T. Smaller core average burnup step sizes are automatically taken by the code for the following burnup steps. BW3 is the factor used to adjust the smaller core average

burnup step size taken automatically by the code. The end of cycle is defined as when the k eigenvalue is in the range of BW1 to .9994.

BW1 is set to a value between 1 and 1.0004.

If the core average burnup step sizes taken are too large so that the k eigenvalue of core after the last burnup step is less than .9994, a smaller BW3 is then used to reduce the core average burnup step size so that the k eigenvalue will fall into the range of BW1 to .9994.

BW3 is taken as .95 in this study. When the overall difference of the end of cycle element burnups of two consecutive cycles is less than DFEQ twice continually, the cycles are considered having reached equilibrium. DFEQ is taken as 5000 MWD/MTU.

- MDISB : <1 When MDISB <1, the reactor is divided into regions of equal pitch.
- >1 When MDISB >1, the reactor is divided into regions of equal volume.
- IDGT : Factor needed for the subroutine LEQTIF in solving Equation (4-14). IDGT = 4 is used to control accuracy.
- IOP : 7 The maximum number of outer iterations in every

core average burnup step. This is set to prevent the number of outer iterations from going too high. Convergence of outer iterations is expected to be reached before the number of outer iterations reaches IOP.

PHO,FPO,SBO : Factors in editing the output. PHO >1, if the axial functions $f_1(z)$, $f_2(z)$, and $f_3(z)$ for each inner iteration are desired to be displayed in the terminal.

SBO >1, if the element burnups after each core average burnup step are desired to be displayed in the terminal. The element burnups at the end of equilibrium cycle are always available in local file TAPE6 no matter what value of SBO is.

FPO >1, if the fluxes, flux peaking factors, element powers and power peaking factors for each core average burnup step are desired. Data are stored in local file TAPE7.

Variable Name	CBSI(IZ,1)	CBSI(IZ,2)	CBSI(IZ,3)	CBSI(IZ,4)	CBSI(IZ,5)
Format	//,20x,E12.5	E12.5	E12.5	E12.5	E12.5

CBSI(IZ,6)	CBSI(IZ,7)	CBSI(IZ,8)	CBSI(IZ,9)
E12.5	E12.5	E12.5	E12.5

Table C-1 . The formata for the initial loadings of the first core element (IZ,IR) (IZ=1,20; IR=1,6 for 6 zonea case and IR=1,9 for 9 zones case)

Variable Name	AT(I,1,J)	AT(I,2,J)	RT(I,1,J)	RT(I,2,J)
Format	6x,E12.5	2x,E12.5	2x,E12.5	2x,E12.5

Table C-2 . The formats for the trial functiona AT and the weighting functions RT stored in Tape3.
(I=1,3 for three different reactor conditiona ;
J=1, 180 for different radial positiona)

C.4 OUTPUT FORM OF 2-D CODE

Outputs in two-dimension calculations are also divided into two sets. First set outputs are those displayed on the terminal. Second set outputs are those stored in local files--TAPE6 and TAPE7.

A. First Set Outputs :

When input parameters PHO=1 and SBO=1, the outputs appear on the terminal in sequential order are:

- (1) Z-location from the top of the reactor; f_1 ; f_2 ; f_3 ; $f_1+f_2+f_3$.
- (2) Loop number m of outer iteration: k^m eigenvalue

$$= \frac{\int (\nu_1 \Sigma_{f_1} \phi_m^1 + \nu_2 \Sigma_{f_2} \phi_m^2) dv}{\int (\nu_1 \Sigma_{f_1} \phi_{m-1}^1 + \nu_2 \Sigma_{f_2} \phi_{m-1}^2) dv} k^{m-1}; \text{ neutrons at loop } m,$$

$$\int (\nu_1 \Sigma_{f_1} \phi_m^1 + \nu_2 \Sigma_{f_2} \phi_m^2) dv; \text{ neutrons at loop } m-1,$$

$$\int (\nu_1 \Sigma_{f_1} \phi_{m-1}^1 + \nu_2 \Sigma_{f_2} \phi_{m-1}^2) dv.$$

- (3) Flux normalization factor; core average fast flux; core average slow flux; core average power.
- (4) Section (element) burnup information:: Section location
Z(axial), R(radial); step increment; cycle increment;
initial loading; final burnup; burnup index.

- (5) Bundle burnup informations: Bundle (zone number); step increment; cycle increment; initial loading; final burnup.
- (6) Cumulative core average burnup.

B. Second set outputs

- (1) At the end of cycle, the element burnup at the beginning and end of the cycle are stored in TAPE6.
- (2) The critical element fluxes, flux peaking factors, element power, and element power peaking factors are stored in local file TAPE7.

```

      PROGRAM YEN2D(TAPE1,TAPE2,TAPE3,INPUT,OUTPUT,
1 TAPE61=OUTPUT,TAPE6,TAPE7)
CC      A TWO DIMENSION TWO GROUP DIFFUSION CODE TO SIMULATE
CC      THE CORE BURNUP FOR DIFFERENT CORE ENRICHMENT AND
CC      REFUELING SCHEMES,R DIRECTION DIFFUSION , Z DIRECTION
CC      SYNTHESIS
      REAL A(3,3),C(3,1),WKAREA(9)
      INTEGER M,ND,IA,IDGT,IER
      DIMENSION BOY(10,49),AT(3,2,182),BPPK(10)
      DIMENSION RT(3,2,182),AE(22,3,3),BETA(22,3,3),RHWA(22,3,3)
      DIMENSION PHI(10,3,22),A(3,3),GEU(10),BUC(12),SS(10)
      DIMENSION SM(22,10),EGV(7),BBD(10),BBI(10),BBF(10)
      DIMENSION B(22,10),C(3,1),LZR(10),FLX1(182,22)
      DIMENSION FLX2(182,22),FV1(10,22),FV2(10,22)
      DIMENSION FT1(10,22),FT2(10,22),PSS(10,22),BSI(10)
      DIMENSION PPFK(10),PFKK1(10),PFKK2(10),EQB(5,22,10)
      DIMENSION CBSI(22,10),CCBE(22,10)
      COMMON/THANK/CBSE(22,10),BS(49),NBST(22,10)
      PRINT*,"KB=",
      READ*,KB
      PRINT*,"P=",
      READ*,P
      PRINT*,"T=",
      READ*,T
      PRINT*,"CAL=",
      READ*,CAL
      PRINT*,"CR=",
      READ*,CR
      PRINT*,"N=",
      READ*,N
      PRINT*,"HR=",
      READ*,HR
      PRINT*,"NB=",
      READ*,NB
      PRINT*,"NZZ=",
      READ*,NZZ
      PRINT*,"DR1,DR2,DR3=",
      READ*,DR1,DR2,DR3
      PRINT*,"BU1,BU3=",
      READ*,BU1,BU3
      PRINT*,"L7,L8=",
      READ*,L7,L8
      PRINT*,"ENIT=",
      READ*,ENIT
      PRINT*,"NEB,NFB,NOR1,NOR2=",
      READ*,NEB,NFB,NOR1,NOR2
      PRINT*,"FRX1=",
      READ*,FRX1
      PRINT*,"MDSB=",
      READ*,MDSB

```

```

      PRINT*, "IDGT=",
      READ*, IDGT
      PRINT*, "IOP=",
      READ*, IOP
      PRINT*, "SB1,DFEQ=",
      READ*, SB1,DFEQ
      PRINT*, "PHO,FPO,SBO=",
      READ*, PHO,FPO,SBO
      N1=1
      ND=3
      IA=3
      INT=3
CC  CROSS SECTIONS ASSOCIATED WITH HERMITIAN OPERATOR
      DO 201 J=1,NB
        READ(1,202)(BOY(I,J),I=1,10),BS(J)
202  FORMAT(1X,2F12.6,E12.6,F12.6,2E12.6,F12.6,F12.5,2E12.6,F8.2)
201  CONTINUE
CC  EQUAL VOLUME OR EQUAL PITCH ZONE DIVISION
      IF(MDISB-1)132,132,134
134  ZR1=N/SQRT(FLOAT(NB))
      DO 131 I=1,NB
        LZR(I)=SQRT(FLOAT(I))*ZR1+0.5
131  CONTINUE
CC  INITIAL SEGMENT BURNUP
132  DZ=CAL/(2.*FLOAT(NZZ))
      N=N/NB
      AT(1,1,N+1)=0.
      AT(2,1,N+1)=0.
      AT(3,1,N+1)=0.
      AT(1,2,N+1)=0.
      AT(2,2,N+1)=0.
      AT(3,2,N+1)=0.
      RT(1,1,N+1)=0.
      RT(2,1,N+1)=0.
      RT(3,1,N+1)=0.
      RT(1,2,N+1)=0.
      RT(2,2,N+1)=0.
      RT(3,2,N+1)=0.
CC  TRIAL AND WEIGHTING FUNCTION INPUT
      DO 205 I=1,INT
        READ(3,430)
430  FORMAT(//)
        DO 206 J=1,N
          READ(3,207)AT(I,1,J),AT(I,2,J),RT(I,1,J),RT(I,2,J)
207  FORMAT(6X,E12.5,2X,E12.5,2X,E12.5,2X,E12.5)
206  CONTINUE
205  CONTINUE
        DO 203 IZ=1,NZZ
          IF(NEB.EQ.1)GO TO 772
          DO 771 J=1,NB

```

```

      CBSI(IZ,J)=0.0
771  CONTINUE
      GO TO 203
772  READ(2,4002)(CBSI(IZ,JJ),JJ=1,NB)
203  CONTINUE
4002  FORMAT(/,20X,9E12.5)
      DO 3995 KE=1,L7
      WRITE(61,5133)KE
5133  FORMAT(" INFORMATIONS ABOUT CYCLE ",I3)
CC   ZEROING THE SEGMENT BURNUP CATEG
      WRITE(61,*)" INITIAL LOADING PATTERN"
      WRITE(61,663)(I,I=1,NB)
663  FORMAT("  Z  R=",15I3)
      DO 211 IZ=1,NZZ
      DO 212 I=1,NB
      NBST(IZ,I)=1
      CCBE(IZ,I)=0.
      CBSE(IZ,I)=CBSI(IZ,I)
CC   WHOLE CORE ELEMENT BURNUP CATEG
      CALL CATEG(I,IZ,NB,KB)
212  CONTINUE
      WRITE(61,767)IZ,(NBST(IZ,I),I=1,NB)
767  FORMAT(1X,I3,4X,15I3)
211  CONTINUE
      COREB=0.
      IHH=1
      LZ=NZZ+1
      DO 2222 IZ=2,LZ
      SCS=COS(3.141592*(IZ-2)/(NZZ*2.))
      PHI(1,1,IZ)=DR1*SCS
      PHI(1,2,IZ)=DR2*SCS
      PHI(1,3,IZ)=DR3*SCS
2222  CONTINUE
      DO 404 K=1,L8
      APPH=0.
      NOR=NOR1
      IHH=0
      DO 2121 I=1,NB
      BBD(I)=0.
      BBI(I)=0.
      BBF(I)=0.
      BSI(I)=0.
2121  CONTINUE
CC   SCALAR PRODUCTS FORMING THE MATRIX ELEMENTS
      DO 172 IZ=1,NZZ
      DO 173 I=1,INT
      DO 174 J=1,INT
CC   ZEROING SCALAR PRODUCTS
      AE(IZ,I,J)=0.
      RHUA(IZ,I,J)=0.

```

```

      BETA(IZ,I,J)=0.
      MB=1
      BU7=1.
      DO 175 IR=1,N
      IRR=IR-1
      IF(IR.EQ.1)IRR=IR
      IF(MDISB-1)339,339,340
340  IF(IR-LZR(MB))390,390,391
339  B1=FLOAT(IR)/FLOAT(M)
      IF(B1-MB)390,390,391
391  MB=MB+1
390  AE(IZ,I,J)=AE(IZ,I,J)+(BOY(1,NBST(IZ,MB))*AT(I,1,IR)*RT(J,1,IR)+
1  BOY(2,NBST(IZ,MB))*AT(I,2,IR)*RT(J,2,IR))*IR*(HR**2.)
      RHUA(IZ,I,J)=RHUA(IZ,I,J)+(AT(I,1,IR)*((BOY(3,NBST(IZ,MB))
1  /1.)*RT(J,1,IR))+AT(I,2,IR)*((BOY(4,NBST(IZ,MB))
2  /1.)*RT(J,1,IR)))*IR*(HR**2.)
      BETA(IZ,I,J)=BETA(IZ,I,J)-AT(I,1,IR)*(BOY(5,NBST(IZ,MB)))
1  *RT(J,1,IR)*IR*(HR**2.)-AT(I,2,IR)*(BOY(6,NBST(IZ,MB)))*
2  RT(J,2,IR)*IR*(HR**2.)+AT(I,1,IR)*(BOY(5,NBST(IZ,MB)))*
3  BOY(8,NBST(IZ,MB))*RT(J,2,IR)*IR*(HR**2.)+
4  BOY(1,NBST(IZ,MB))*RT(J,1,IR)*((AT(I,1,IRR)-2.*AT(I,1,IR)+
5  AT(I,1,IR+1))*IR+(AT(I,1,IR+1)-AT(I,1,IRR))*HR/2.)+
6  BOY(2,NBST(IZ,MB))*RT(J,2,IR)*((AT(I,2,IRR)-2.*AT(I,2,IR)+
7  AT(I,2,IR+1))*IR+(AT(I,2,IR+1)-AT(I,2,IRR))*HR/2.)
175  CONTINUE
174  CONTINUE
173  CONTINUE
172  CONTINUE
777  FORMAT(1X,3E10.3)
CC  INITIAL CONDITIONS OF PHI FUNCTIONS
      DO 176 I=1,INT
      DO 1761 J=1,INT
      AE(NZZ+1,I,J)=AE(NZZ,I,J)
      RHUA(NZZ+1,I,J)=RHUA(NZZ,I,J)
      BETA(NZZ+1,I,J)=BETA(NZZ,I,J)
1761  CONTINUE
      DO 1762 I1=1,10
      PHI(I1,I,NZZ+2)=0.
1762  CONTINUE
176  CONTINUE
CC  MATRIX ELEMENTS AX=C GENERATION
      IS=0
      FKT=1.
      NK1=2
      HWU=1.
      DO 505 IH=1,IOP
      IF(IH.LE.NFB)GO TO 9999
9998  NOR=NOR2
9999  IHH=IHH+1
      IS=IS+1

```

```

      IF(NK1.GT.1)FKT=1.
      LS=NZZ
      DO 180 IZ=2,LZ
      IZ2=IZ
      IZ1=IZ2-1
      CENTER=1.
      IF(IZ2.GT.2)GO TO 1777
      IZ1=IZ2+1
1777 DO 181 J=1,INT
      C(J,1)=0.
      DO 182 J8=1,INT
      A(J,J8)=(-2.*AE(IZ2-1,J8,J)+(BETA(IZ2-1,J8,J)
1 +RHW(IZ2-1,J8,J)/FKT)*(DZ**2.)*1.)
      C(J,1)=C(J,1)-AE(IZ2,J8,J)*PHI(IHH,J8,IZ2+1)-
1 AE(IZ1-1,J8,J)*PHI(IHH,J8,IZ1)
182 CONTINUE
181 CONTINUE
CC SOLVE AX=C BY LINEAR EQUATION SUBROUTINE
   CALL LEQ1F(A,N1,ND,IA,C,IDGT,WKAREA,IER)
   TEMPP=0.
   RLX1=1.
   IF(IHH.LE.2)GO TO 989
   RLX1=FRX1
989 DO 183 KI=1,INT
   PHI(IHH,KI,IZ2)=PHI(IHH,KI,IZ2)+RLX1*
1 (C(KI,1)-PHI(IHH,KI,IZ2))
   TEMPP=TEMPP+PHI(IHH,KI,IZ2)
   PHI(IHH+1,KI,IZ2)=PHI(IHH,KI,IZ2)
183 CONTINUE
   IF(PHO.LT.1)GO TO 180
   WRITE(61,184)IZ,(PHI(IHH,KI,IZ2),KI=1,INT),TEMPP
184 FORMAT(3X,I3,3X,E12.5,3X,E12.5,3X,E12.5,3X,E12.5)
180 CONTINUE
   GEU(IHH)=0.
CC EIGENVALUE K ITERATION BY COMPAREING NEUTRON
CC GENERATIONS IN TWO CONSECUTIVE TIME STEPS
   DO 191 IZ=1,NZZ
   ISS=1
   DO 192 IR=1,N
   IF(IR.GT.LZR(ISS))ISS=ISS+1
   DO 193 J=1,INT
   GEU(IHH)=GEU(IHH)+(BOY(3,NBST(IZ,ISS))*AT(J,1,IR)
1 *PHI(IHH,J,IZ+1)+BOY(4,NBST(IZ,ISS))*AT(J,2,IR)*
2 PHI(IHH,J,IZ+1))*IR*(HR**2.)*DZ
193 CONTINUE
192 CONTINUE
191 CONTINUE
   IF(IHH.EQ.1)GO TO 9999
   IF(IS.LT.NOR)GO TO 9999
   IS=0

```

```

      FKT1=FKT
      FKT=(GEU(IHH)/GEU(IHH-1))*FKT1
      FKT=(FKT+FKT1)*.5
      NK1=0
      WRITE(61,5500)
      WRITE(61,*)" LOOP N; K=(M)/(M-1); NEUTRON AT M ; NEUTRON AT M-1"
      WRITE(61,184)IHH,FKT,GEU(IHH),GEU(IHH-1)
      WRITE(61,5500)
      IF(IHH.LE.4)GO TO 3551
      IF(FKT.LE.BW1)GO TO 44
3551 IF(ABS((GEU(IHH)-GEU(IHH-1))/GEU(IHH)).LE.ENIT)GO TO 301
505  CONTINUE
301  EGV(K)=FKT
      DEN=EGV(K)-1.
CC   CRITICAL FLUX AT EACH SEGMENT , FLUX NORMALIZATION
CC   PEAKING FACTORS
      TFV1=0.
      TFV2=0.
      TFVS=0.
      BUC(K)=SB1
      IF(K.GT.1)BUC(K)=BUC(K-1)*BW3*(DEN)/(EGV(K-1)-EGV(K))
      IF(FKT.LT.BW1)GO TO 44
      DO 403 IZ=1,NZZ
      VF1=0.
      VF2=0.
      PPS=0.
      VOL=0.
      MB=1
      DO 4031 I=1,INT
      PHI(1,I,IZ)=PHI(IHH,I,IZ)
4031 CONTINUE
      VZ=0.
      DO 402 IR=1,N
      IF(IR.EQ.(LZR(MB)+1))GO TO 4021
      GO TO 3091
4021 VF1=0.
      VF2=0.
      PPS=0.
      VOL=0.
3091 FLX1(IR,IZ)=0.
      FLX2(IR,IZ)=0.
      DO 309 J=1,INT
      FLX1(IR,IZ)=FLX1(IR,IZ)+AT(J,1,IR)*PHI(IHH,J,IZ+1)
      FLX2(IR,IZ)=FLX2(IR,IZ)+AT(J,2,IR)*PHI(IHH,J,IZ+1)
309  CONTINUE
      IF(MDISB-1)405,405,406
406  IF(IR-LZR(MB))407,407,408
405  B1=FLGAT(IR)/FLOAT(M)
      IF(B1-MB)407,407,408
408  MB=MB+1

```



```

407 VS=3.14159*((IR*HR)**2.)*DZ-VZ
    VOL=VOL+VS
    VF1=VF1+VS*FLX1(IR,IZ)
    VF2=VF2+VS*FLX2(IR,IZ)
    PPS=PPS+VS*(FLX1(IR,IZ)*BOY(9,NBST(IZ,NB))+
1 FLX2(IR,IZ)*BOY(10,NBST(IZ,NB)))
    TFV1=TFV1+VS*FLX1(IR,IZ)
    TFV2=TFV2+VS*FLX2(IR,IZ)
    TFVS=TFVS+VS*(FLX1(IR,IZ)*BOY(9,NBST(IZ,NB))
1 +FLX2(IR,IZ)*BOY(10,NBST(IZ,NB)))
    FV1(NB,IZ)=VF1/VOL
    FV2(NB,IZ)=VF2/VOL
    PSS(NB,IZ)=PPS/VOL
    VZ=3.14159*((IR*HR)**2.)*DZ
402 CONTINUE
403 CONTINUE
    FNOR=(P*.5*1.0E+6*1.0E+13)/(TFVS*200.*1.602)
    TVOL=3.14159*(CR**2.)*CAL*.5
    CAF1=FNOR*TFV1/TVOL
    CAF2=FNOR*TFV2/TVOL
    CAPR=FNOR*TFVS/TVOL
    WRITE(61,5500)
    WRITE(61,*)" NORMALIZATION; CORE AVG F FLUX; CORE AVG S FLUX; COR
1E AVG POWER"
    WRITE(61,420)FNOR,CAF1,CAF2,CAPR
420 FORMAT(5X,E10.4,6X,E10.4,6X,E10.4,6X,E10.4)
    PRINT(7,*)" FLUX AND PEAKING FACTOR MAP"
    DO 1442 J=1,NB
    BPPK(J)=0.
1442 CONTINUE
    DO 1234 IZ=1,NZZ
    DO 1235 J=1,NB
    FT1(J,IZ)=FV1(J,IZ)*FNOR
    PFKK1(J)=FT1(J,IZ)/CAF1
    FT2(J,IZ)=FV2(J,IZ)*FNOR
    PFKK2(J)=FT2(J,IZ)/CAF2
    PSS(J,IZ)=PSS(J,IZ)*FNOR
    PPFK(J)=PSS(J,IZ)/CAPR
    BPPK(J)=BPPK(J)+PPFK(J)
1235 CONTINUE
    IF(KE.LE.1)GO TO 1234
    IF(FPO.LT.1)GO TO 1234
    WRITE(7,1433)IZ,(J,J=1,NB)
    WRITE(7,1434)(FT1(JS,IZ),JS=1,NB)
    WRITE(7,1435)(PFKK1(JS),JS=1,NB)
    WRITE(7,1436)(FT2(JS,IZ),JS=1,NB)
    WRITE(7,1435)(PFKK2(JS),JS=1,NB)
    WRITE(7,1437)(PSS(JS,IZ),JS=1,NB)
    WRITE(7,1438)(PPFK(JS),JS=1,NB)
1433 FORMAT(" Z=",I3,"; R= ",10I12)

```

```

1434 FORMAT("      FAST      FLUX",10E12.5)
1435 FORMAT("      PEAKING FACTOR",10E12.5)
1436 FORMAT("      THERMAL  FLUX",10E12.5)
1437 FORMAT("      SECTOR   POWER",10E12.5)
1438 FORMAT("      POWER PEAKING",10E12.5)
1234 CONTINUE
      TBP=0.
      DO 1440 J=1,NB
        TBP=TBP+BPPK(J)
1440 CONTINUE
      DO 1441 J=1,NB
        BPPK(J)=BPPK(J)*NB/TBP
1441 CONTINUE
      WRITE(7,1439)(BPPK(JS),JS=1,NB)
1439 FORMAT("  BUNDLE PWR PEAKING",10E12.5)
CC  BUNDLE BURNUP CALCULATION -SEGMENT-WISE
300  TTM=0.
      DO 4445 IZ=1,NZZ
        DO 4444 I=1,NB
          SS(I)=0.
          SM(IZ,I)=0.
4444 CONTINUE
          TM=0.
          NB=1
          VZ=0.
          DO 2203 I=1,N
            IF(MDISB-1)139,139,140
140    IF(I-LZR(NB))90,90,91
139    B1=FLOAT(I)/FLOAT(N)
            IF(B1-NB)90,90,91
91    NB=NB+1
90    SS(NB)=(FLOAT(I))*2.-VZ+SS(NB)
            FS=((FLOAT(I))*2.-VZ)*FNOR*(BOY(9,NBST(IZ,NB))
1    *FLX1(I,IZ)+BOY(10,NBST(IZ,NB))*FLX2(I,IZ))
            SM(IZ,NB)=SM(IZ,NB)+FS
            TM=TM+FS
            VZ=(FLOAT(I))*2.
2203 CONTINUE
          TTM=TM+DI+TTM
4445 CONTINUE
          WRITE(61,5500)
          WRITE(61,*)" SECTION BURNUP INFORMATIONS"
5500 FORMAT(/)
          WRITE(61,*)" SECTION Z  R ; STEP INCRE ; CYCLE INCRE ; INITIAL B
1  URNUP; FINAL BURNUP; CATEGORY"
          IF(SBO.GE.1)GO TO 5013
          WRITE(61,*)" CHOOSE NOT TO PRINT OUT ,SECTOR BURNUPS AVAILABLE IN
1  TAPE6 "
5013 DO 1223 IZ=1,NZZ
      DO 1203 I=1,NB

```

```

      B(IZ,I)=((N**2.)*BUC(K)*SN(IZ,I)*CAL/(SS(I)
1    *ITM*2.))
      CBSE(IZ,I)=CBSE(IZ,I)+B(IZ,I)
      CCBE(IZ,I)=CCBE(IZ,I)+B(IZ,I)
      CALL CATEG(I,IZ,NB,KB)
1203  CONTINUE
      DO 501 I=1,NB
      IF(SBD.LT.1)GO TO 5012
      WRITE(61,1301)IZ,I,B(IZ,I),CCBE(IZ,I),CBSI(IZ,I),CBSE(IZ,I),
1    NBST(IZ,I)
1301  FORMAT(9X,I3,1X,I3,1X,E12.5,1X,E12.5,2X,E12.5,3X,E12.5,3X,I3)
5012  BBD(I)=BBD(I)+CCBE(IZ,I)
      BBI(I)=BBI(I)+CBSI(IZ,I)
      BBF(I)=BBF(I)+CBSE(IZ,I)
      BSI(I)=BSI(I)+B(IZ,I)
501  CONTINUE
1223  CONTINUE
      WRITE(61,5500)
      WRITE(61,*)" BUNDLE BURNUP INFORMATIONS"
      WRITE(61,*)" BUNDLE;STEP INCRE;POWER PEAK;CYCLE INCRE; INITIAL ;
1    FINAL "
      TZSI=0.
      DO 1224 I=1,NB
      ZBD=BBD(I)/(FLOAT(NZZ))
      ZBI=BBI(I)/(FLOAT(NZZ))
      ZBF=BBF(I)/(FLOAT(NZZ))
      ZSI=BSI(I)/(FLOAT(NZZ))
      BPF=ZSI/BUC(K)
      TZSI=TZSI+ZSI
      WRITE(61,1225)I,ZSI,BPF,ZBD,ZBI,ZBF
1225  FORMAT(3X,I3,3X,F9.3,3X,F9.3,3X,F9.3,3X,F9.3,3X,F9.3)
1224  CONTINUE
      TZSI=TZSI/NB
      WRITE(61,1111)TZSI
1111  FORMAT(1X,"AVERAGE STEP INCREMENT BURN",1X,F10.2)
      COREB=COREB+BUC(K)
      WRITE(61,1204)COREB
1204  FORMAT(1X,"CORE BURNUP",1X,F10.2)
404  CONTINUE
44  WRITE(61,1222)COREB
1222  FORMAT(1X," TOTAL CYCLE CORE BURNUP ",1X,F10.2)
      WRITE(6,*)" EQUILIBRIUM CYCLE SECTOR AVERAGE INITIAL LOADINGS AND
1    FINAL BURNUPS"
      SMEG=0.
      DO 4000 IZ=1,NZZ
      CBSI(IZ,1)=0.
      WRITE(6,4008)IZ,(J,J=1,NB)
4008  FORMAT(" Z=",I3,"; R= ",10I12)
      WRITE(6,4012)(CBSI(IZ,J),J=1,NB)
      WRITE(6,4022)(CBSE(IZ,J),J=1,NB)

```

```

4012 FORMAT(" INITIAL   LOADING=" ,10E12.5)
4022 FORMAT(" DISCHARGE  BURNUP=" ,10E12.5)
      EQB(KE,IZ,1)=CBSE(IZ,1)
      ADT=.5*(CBSE(IZ,1)+CBSI(IZ,2))/CBSE(IZ,1)
      DO 3999 JK=2,NB
      CBSI(IZ,JK)=CBSI(IZ,JK-1)+ADT*CCBE(IZ,JK-1)
      EQB(KE,IZ,JK)=CBSE(IZ,JK)
3997  CONTINUE
      IF(KE.LT.2)GO TO 4000
      DO 3997 JH=1,NB
      SREQ=SREQ+ABS(EQB(KE,IZ,JH)-EQB(KE-1,IZ,JH))
3997  CONTINUE
4000  CONTINUE
      IF(KE.EQ.1)GO TO 3995
      WRITE(61,3777)SREQ
3777  FORMAT(" SUM OF BUNDLE BURNUP DIFFERENCE BETWEEN
1     PREVIOUS AND CURRENT CYCLES=" ,E12.5)
      IF(SREQ.LT.DFEQ)GO TO 3996
3995  CONTINUE
3996  STOP
      END
      SUBROUTINE CATEG(I,IZ,NB,NB)
      COMMON/THANK/CBSE(22,10),BS(49),NBST(22,10)
      DO 82 KI=1,NB
      K2=KI
      IF(CBSE(IZ,I)-BS(KI))31,62,82
82    CONTINUE
81    NBST(IZ,I)=K2
      RETURN
      END

```